An Efficiency Comparison of Liquid Hydrogen, Ammonia, and Liquid Organic Hydrogen Carriers for Maritime Use

ANDERS VANGSNES BØE

DANIEL OLAUSEN GULLBRÅ

TOMMY ARNE REINERTSEN

Bachelor's thesis in Energy Technology
Bergen, Norway 2021

Høgskulen på Vestlandet

An efficiency comparison of liquid hydrogen, ammonia, and liquid organic hydrogen carriers for maritime use

Anders Vangsnes Bøe

Daniel Olausen Gullbrå

Tommy Arne Reinertsen

Department of Mechanical and Marine Engineering

Western Norway University of Applied Sciences

NO-5063 Bergen, Norway

IMM 2021 - M60

Høgskulen på Vestlandet

Fakultet for Ingeniør- og Naturvitskap

Institutt for maskin- og marinfag

Inndalsveien 28

NO-5063 Bergen, Norge

Cover and backside images © Norbert Lümmen

Norsk tittel:	*Sammenligning av virkningsgraden til flytende hydrogen, ammoniakk, og flytende organiske hydrogenbærere for maritim bruk*
Author(s), student number:	Anders Vangsnes Bøe, 580836
	Daniel Olausen Gullbrå, 580843
	Tommy Arne Reinertsen, 580841
Study program:	Energy Technology
Date:	June 2021
Report number:	IMM 2021-M60
Supervisor at HVL:	Jonathan Torstensen
Assigned by:	Ocean Hyway Cluster
Contact person:	Mark Purkis
Antall filer levert digitalt:	6

Preface

This thesis was written by students from the Department of Mechanical and Marine Engineering at the Western Norway University of Applied Sciences (*Høgskulen på Vestlandet, HVL*), as part of a Bachelor of Science degree in the field of Energy Technology. The objective of the thesis was given by Ocean Hyway Cluster, who also provided us with our external industry supervisor, Mark Purkis, M.Sc. Our internal academic supervisor is associate professor Jonathan Torstensen. We were recommended for the assignment by assistant head of department Velaug Myrseth Oltedal, as we have written several project reports on hydrogen technologies in the past. The subject is incredibly interesting, and we have gained valuable new insight into the maritime sector.

The ongoing COVID-19 pandemic has made the process of writing this thesis challenging, because communication has, for the most part, been limited to a digital presence. It was also impossible to see the cargo ship MV Rubin in person. Observing the scale of the vessel, and possible limiting factors regarding conversion to hydrogen propulsion would have been beneficial. Luckily, there is a plethora of pictures, video, and articles about cargo vessels. The sheer amount of literature absorbed during the writing of this thesis would perhaps not have been possible to process *without* social isolation. In this regard, the pandemic turned out to be advantageous.

We would like to thank our supervisors Mark and Jonathan for their guidance throughout this project, as well as Velaug and associate professor Norbert Lümmen for their insight and expertise in hydrogen technology and thermodynamics. Further thanks are due to all aforementioned, in addition to Per Jørgen Silden, M.Sc. (Skipskompetanse AS), for their help in revealing the potential of an idea that emerged during this project. The crew of MV Rubin also deserves our gratitude for providing the necessary technical data on the vessel.

A very special thanks to Kristina Heggland Skutlaberg for her support, patience and understanding during this project (as well as the entire bachelor's degree). Without her, this thesis would be a mere shadow of its current form.

Hopefully, the result is a useful and interesting read.

- Anders, Daniel and Tommy.

Arena Ocean
Hyway Cluster

Keywords: green hydrogen, energy supply, energy efficiency, hydrogen carriers, maritime sector

Abstract

Likely responsible for approximately 2.5 % of the global greenhouse gas emissions, the maritime sector is highly motivated to find alternative, sustainable methods of propulsion. Hydrogen produced from renewable energy is often suggested as the best possible solution.

However, being the *least* dense material in the universe, gaseous hydrogen is not favourable on ships because of the immense volume required. Storing and transporting hydrogen in liquid form, or bound in other molecules, may be a viable solution. This thesis aims to answer *which* hydrogen carrier technology is best suited depending on several criteria (efficiency, energy density, safety, emissions, and cost), as well as to answer which one of these criteria is ultimately the most important. The technologies explored are cryogenically liquefied hydrogen, stored at -253 °C, ammonia stored at -33.33 °C, and dibenzyltoluene (as well as toluene) stored at >15 °C.

The comparison between the hydrogen carriers is done in two steps: First, a general comparison is made using conservative efficiency estimates (and *not* utilising available waste heat), where a reference amount of hydrogen, 3 tons, is transported a set distance of 1000 km. The second comparison is a threefold case where the fish-feed carrier *MV Rubin* is hypothetically retrofitted with alternative, zero-emissions powertrains, one for each carrier technology. In this case higher efficiency estimates are used, and heat recovery is incorporated into the design. By analysing tracking data, the longest route travelled by MV Rubin is set as a benchmark for the hydrogen carriers.

The general comparison estimates a total supply chain efficiency of 20, 15, and 15 % (while the case suggests 30, 27, and 25 %) for liquid hydrogen, ammonia, and dibenzyltoluene, respectively. Both comparisons show that either carrier, based on *green* hydrogen, reduce the total carbon emissions by *well* over 80 % compared to the traditional fossil fuels. A significant reduction is also achieved compared to the emissions associated with hydrogen production from fossil sources.

Toluene and ammonia have the lower total specific cost, including production and transportation, estimated at 3.7 to 5.5 €/kg_{H_2}, while liquid hydrogen and dibenzyltoluene is considerably more expensive, at 5 to 6.7 €/kg_{H_2}. Hydrogen produced from steam methane reformation costs about 2.4 to 4 €/kg_{H_2}, for comparison. [a]

Ammonia has the highest energy density among the carriers, both volumetric as well as gravimetric, including the storage system. Dibenzyltoluene has the lowest *gravimetric* energy density at 1.7 kWh/kg_{H_2}, and liquid hydrogen has the lowest *volumetric* energy density at 1200 kWh/m^3. The ease of handling leads to greater possibilities for storage of dibenzyltoluene compared to the other two, which potentially reduces the cost of a retrofit system. The low health and safety risk associated with dibenzyltoluene compared to liquid hydrogen and ammonia is also a significant advantage.

[a] At the time of writing, 1 € is equal to approximately 10 NOK.

Nøkkelord: grønt hydrogen, energiforsyning, energieffektivisering, hydrogenbærere, maritim sektor

Sammendrag

Den maritime bransjen er svært motivert til å finne alternative, bærekraftige metoder for fremdrift, ettersom de trolig er ansvarlig for omtrent 2.5 % av verdens drivhusgassutslipp. Hydrogen produsert med fornybar energi er ofte foreslått som den beste mulige løsningen.

Hydrogen er det letteste materialet i universet, som medfører at anvendelse av hydrogengass på båt er ugunstig på grunn av enorme krav til lagringsareal. En mulig løsning er å lagre og transportere hydrogenet i flytende form, eller bundet i andre molekyler. Denne bacheloroppgaven forsøker å besvare hvilken hydrogenbærer som er best egnet, avhengig av forskjellige kriterier (virkningsgrad, energitetthet, sikkerhet, utslipp, og kostnad), i tillegg til å forsøke å bestemme hvilket av kriteriene som er viktigst. Lagringsmetodene som utforskes er kryogenisk flytendegjort hydrogen, lagret ved -253 °C, ammoniakk lagret ved -33.33 °C, og dibenzyltoluen (og toluen) lagret ved temperaturer over 15 $°C$.

Sammenligningene mellom hydrogenbærerne blir gjort i to steg: Først blir en generell sammenligning gjort med svært konservative estimater (og uten utnyttelse av spillvarme) hvor en referansemengde hydrogen, 3 tonn, fraktes en bestemt avstand, 1000 km. Den andre sammenligningen omhandler en tredelt spesifikk case, der fiskefôrsfrakteren *MS Rubin*, blir hypotetisk ombygd til en alternativ, nullutslippsløsning, en for hver hydrogenbærer. Mer optimistiske estimater benyttes, og alle løsningene utnytter spillvarme i den grad det lar seg gjøre. Den lengste ruten til båten, som ble utledet ved analyse av sporingsdata, setter målet hydrogenbærerne skal nå.

Den generelle sammenligningen anslår en totalvirkningsgrad på 20, 15 og 15 % (mens casen anslår 30, 27 og 25 %) for henholdsvis flytende hydrogen, ammoniakk og dibenzyltoluen. Begge sammenligningene viser at enhver *grønn* hydrogenbærer vil redusere de totale utslippene med godt *godt* over 80 %, sammenlignet med de fossile løsningene. Utslipp med hensyn på produksjon blir også betydelig reduserte, sammenlignet med hydrogen produsert fra fossile kilder.

Toluen og ammoniakk har lavest totalkostnad, inkludert produksjon og transport, anslått til rundt 3.7 til 5.5 €/kg_{H_2}, mens flytende hydrogen og dibenzyltoluen er betraktelig mer kostbare, anslått til rundt 5 til 6.7 €/kg_{H_2}. Hydrogen produsert fra fossile kilder koster, til sammenligning, rundt 2.4 til 4 €/kg_{H_2}. [b]

Ammoniakk har den høyeste energitettheten av bærerene, være det seg både volumetrisk og gravimetrisk, inkludert lagringstank. Dibenzyltoluen har lavest *gravimetrisk* energitetthet, med 1.7 kWh/kg_{H_2}, og flytende hydrogen har lavest *volumetrisk* energitetthet ved 1200 kWh/m^3. Dibenzyltoluen er mye enklere å håndtere og lagre, noe som trolig fører til en lavere installasjonskostnad. I tillegg er helse- og sikkerhetsrisikoen for dibenzyltoluen veldig lav sammenlignet med flytende hydrogen og ammoniakk.

[b] I skrivende stund er 1 € tilnærmet lik 10 NOK

Table of contents

Preface V

Abstract VII

Sammendrag IX

Nomenclature XV

1. Introduction 1

1.1 Background 1

1.2 Ocean Hyway Cluster 2

1.3 Objective 2

2. Theory 3

2.1 Hydrogen as an energy carrier 4

2.1.1 Production of hydrogen 4

2.1.2 Green hydrogen from electrolysis 6

2.1.3 Energy densities 10

2.2 Liquid hydrogen 10

2.2.1 Production of liquid hydrogen 10

2.2.2 Industrial scale production and use of L-H_2 12

2.2.3 Storage and transportation of L-H_2 12

2.3 Ammonia 13

2.3.1 Production and industrial use of ammonia 14

2.3.2 Storage and transportation of ammonia 16

2.3.3 Application of ammonia as a hydrogen carrier 17

2.4 Liquid Organic Hydrogen Carriers 18

2.4.1 Synthetic fuels 18

2.4.2 Reusable hydrocarbons 19

2.4.3 Carriers, challenges, and combinations 20

2.4.4 DBT production 22

2.4.5 Hydrogen cycle and longevity 23
2.5 Applications 27
2.5.1 A summary of fuels and hydrogen carriers 27
2.5.2 Fuel cells 28
2.5.3 Electric motors and batteries 33
2.5.4 Heat engines 34
2.6 Large carrier MV Rubin 41
2.6.1 Engines and machinery of *MV Rubin* 42
2.6.2 Operating profile and shipping route of *MV Rubin* 42
3. Analysis 45
3.1 Methods 45
3.2 Comparison of hydrogen carriers and their supply chains 45
3.2.1 Energy densities including storage tanks 45
3.2.2 Supply chain efficiencies 48
3.2.3 Cost of fuels 52
3.2.4 Transportation and emissions 56
3.2.5 Safety and handling 61
3.3 Case: MV Rubin 69
3.3.1 Analysing the shipping route 69
3.3.2 Average energy and power requirements 71
3.3.3 Liquid hydrogen system 74
3.3.4 Ammonia system 76
3.3.5 LOHC system 78
4. Discussion 81
4.1 Renewable hydrogen 81
4.2 Sustainable technology 82

4.3 Water to water efficiency 83

4.4 Determining factors for the maritime use of hydrogen 84

5. Conclusion 87

6. Suggested further work 87

7. References 89

List of equations 109

List of figures 110

List of tables 112

List of reaction equations 113

Attachments 114

Attachment 1. Calculations 114

Attachment 2. E-mail correspondence with MV Rubin 114

Attachment 3. E-mail correspondence with Prototech 114

Attachment 4. AIS - Automated calculations 115

Attachment 5. Python script 116

Attachment 6. AIS CSV-file for use with python script 116

Nomenclature

Abbreviation	Description
AC	Alternating Current
ACGIH	American Conference of Governmental Industrial Hygienists
AEA	Ammonia Energy Association
AEGL	Acute Exposure Guideline Levels
AFC	Alkaline Fuel Cell
Ag	Silver
CCS	Carbon Capture and Storage
CCU	Carbon Capture and Utilisation
CG-H_2	Compressed gaseous hydrogen
CH_3OH	Methanol
CHP	Combined Heat and Power
CO	Carbon monoxide
CO_2	Carbon dioxide
CSIRO	Commonwealth Scientific and Industrial Research Organisation
CSV	Comma Separated Value
DBT	Dibenzyltoluene
DMFC	Direct Methanol Fuel Cell
DOE	Department of Energy
DP	Dynamic Positioning
DPM	Diphenylmethane
DR	Dry Reforming
DWT	Deadweight Tonnage
EGR	Exhaust gas recirculation
EPA	Environmental Protection Agency

GHG	Greenhouse Gases
GWP	Global Warming Potential
H0-DBT	Dehydrogenated Dibenzyltoluene
H18-DBT	Hydrogenated Dibenzyltoluene
H_2	Hydrogen
HBP	Haber-Bosch Process
HDSAM	Hydrogen Delivery Scenario Analysis Model
HHV	Higher Heating Value
HISC	Hydrogen induced stress cracking
HTPEMFC	High Temperature Polymer Electrolyte Membrane Fuel Cell
HTSE	High Temperature Steam Electrolysis
HV	Heating value
HVL	Høgskulen på Vestlandet
ICE	Internal Combustion Engine
IMO	International Maritime Organization
Ir	Iridium
KOH	Potassium Hydroxide
LCA	Life Cycle Analysis
LGC	Large Gas Carriers
L-H_2	Liquid Hydrogen
L-He	Liquid Helium
LHL	Large-scale Hydrogen Liquefaction
LHV	Lower Heating Value
L-N_2	Liquid Nitrogen
LNG	Liquid Natural Gas
L-NH_3	Liquid Ammonia

LOA	Length Overall (marine vessels)
LOHC	Liquid Organic Hydrogen Carrier
LSM	Strontium doped Lanthanum Manganite
MCM	Methylcyclohexane (Toluene)
MEA	Membrane Electrode Assembly
MGO	Marine Gasoil (ISO 8217)
MR	Mixed Refrigerants
NaCl	Sodium Chloride
NaOH	Sodium Hydroxide
NASA	National Aeronautics and Space Administration
NEC	N-ethylcarbazole
NH_3	Ammonia
Ni	Nickel
NOX	Nitrogen Oxides
OCH	Organic Chemical Hydrides
OH^-	Hydroxide
OHC	Ocean Hyway Cluster
PBI	Polybenzimidazole
PdAg	Palladium-Silver
PEMFC	Polymer Electrolyte Membrane Fuel Cell
PPE	Personal Protective Equipment
ppm	Parts Per Million
Pt	Platinum
PTI	Power Take In
PTO	Power Take Out
rpm	Revolutions Per Minute

SMR	Steam Methane Reforming
SOFC	Solid Oxide Fuel Cell
SOH	Potassium Hydroxide
SOLAS	Safety of Life at Sea
STP	Standard Temperature and Pressure (20 °C and 1 atm)
SWL	Safe Working Load
tpd	Tons per day
USAF	United States Air Force
WGSR	Water-Gas Shift Reaction
WtW	Water to Water
YSZ	Yttria Stabilized Zirconia

Variable	Description
atm	Atmospheric pressure [1 atm = 101,325 kPa ≈ 1 bar]
$\boldsymbol{avaliability}$	Percentage of the time available [decimal or %]
BSFC	Brake Specific Fuel Consumption [g/kWh]
$\mathbf{Cost}_{\boldsymbol{annual}}$	Annual expenditure [€/year]
$\boldsymbol{Cost}_{\boldsymbol{hyd,total}}$	CAPEX hydrogenation reactor-system [€]
$\mathbf{Currency}_{\mathbf{year}}$	Currency in a given year
$\boldsymbol{D_v}$	Summary of OPEX [€/year]
$\mathbf{Dist}_{12}$	Distance between two coordinates [m]
E	Energy [J or kWh]
$\boldsymbol{E_{Florø-Tromsø}}$	Work done on voyage Florø – Tromsø [kWh]
$\mathbf{E}_{\mathbf{in}}$	Energy in [kWh or kJ]
$\mathbf{E}_{\mathbf{loss}}$	Energy loss [kWh or kJ]
$\mathbf{E}_{\mathbf{out}}$	Energy out [kWh or kJ]
$\boldsymbol{e_{SOFC,th}}$	Specific thermal waste heat available [kWh/kg]
$\boldsymbol{f}$	Discount rate/100
$\boldsymbol{g}$	Gibbs free energy
$\boldsymbol{h_{H18-DBT}}$	Gravimetric energy density of H18-DBT [kWh/kg]
$\boldsymbol{h_{H18-DBT+tank}}$	Gravimetric energy density of H18-DBT including tank [kWh/kg]
$\boldsymbol{h_{H_2}}$	Gravimetric energy density, hydrogen LHV [kWh/kg]
$\boldsymbol{h_n}$	Lower heating value [MJ/kg or kWh/kg]
$\boldsymbol{h_{n,ISO\ 8217}}$	Lower heating value for ISO 8217 F-RMK 700 [MJ/kg or kWh/kg]
$\boldsymbol{h_{NH3}}$	Gravimetric energy density, ammonia LHV [kWh/kg]
$\boldsymbol{I_0}$	Capital investment [€/year]
$\mathbf{L}_{\mathbf{1\ or\ 2}}$	Longitude points [decimal degree]

m_{CO2}	Amount of CO_2 [kg]
$m_{H_2,annual}$	Annual hydrogen production [kg/year]
$m_{H_2,daily}$	Daily hydrogen demand [kg/day]
$m_{H_2,trailer}$	Hydrogen capacity of trailer [kg/day]
$m_{specific,storage,L-H_2}$	Mass including storage for liquid hydrogen [kg]
$m_{specific,storage}$	Mass including storage [kg]
m_{tank}	Mass of a tank [kg]
$n_{deliveries,daily}$	Number of deliveries daily
$n_{truck,trip,daily}$	Number of daily trips per truck
P	Pressure [unit Pa or bar]
$P_{hyd,max}$	Maximum power rating of hydrogenation reactor [kW]
$\mathbf{P_{installed,HPB}}$	Installed power rating for Haber-Bosch plant [kW]
SFOC	Specific Fuel-Oil Consumption [g/kWh]
T	Temperature [unit °C or K]
$t_{Florø-Tromsø}$	Voyage time Florø-Tromsø [h]
$t_{operatingtime}$	Operating time [h]
Ts	Entropy times temperature
$u_{H18-DBT+tank}$	Volumetric energy density of H18-DBT including tank [kWh/m^3]
u_{L-H_2}	Volumetric energy density, hydrogen at -273 °C and 1 atm [kWh/m^3]
u_{NH_3}	Volumetric energy density, ammonia at-33.33 °C and 1 atm) [kWh/m^3]
$V_{tank,inner}$	Inner volume of a tank [m^3]
$V_{tank,outer}$	Outer volume of a tank [m^3]
$\mathbf{W_a}$	Weight percentage ash

$\mathbf{W_s}$	Weight percentage sulphur
wt%	Weight percent [%]
$\mathbf{W_{task,net}}$	Average work done with regard to the task at hand [kWh]
$\mathbf{W_w}$	Weight percentage water
$\boldsymbol{\eta}$	Efficiency / degree of utilisation [decimal or %]
$\boldsymbol{\eta_{AEC,el}}$	Electrical efficiency, AEC [decimal or %]
$\boldsymbol{\eta_{AFC,el}}$	Electrical efficiency, AFC [decimal or %]
$\boldsymbol{\eta_{fuelcell,general}}$	Efficiency of hypothetical fuel cell [decimal or %]
$\boldsymbol{\eta_{HBP}}$	Efficiency, Haber-Bosch process
$\boldsymbol{\eta_{hyd}}$	Efficiency of hydrogenation-system [decimal or %]
$\boldsymbol{\eta_{ICE}}$	Efficiency of internal combustion engine [decimal or %]
$\boldsymbol{\eta_{liquefaction}}$	Efficiency of liquefaction [decimal or %]
$\boldsymbol{\eta_{liquefaction}}$	Efficiency of liquefaction plant [decimal or %]
$\boldsymbol{\eta_{NH_3,cracking}}$	Efficiency, cracking of ammonia
$\boldsymbol{\eta_{PEMEC,el}}$	Electrical efficiency, PEMEC [decimal or %]
$\boldsymbol{\eta_{PEMFC,el}}$	Electrical efficiency, PEMFC [decimal or %]
$\boldsymbol{\eta_{SOEC,ut}}$	Degree of utilisation, SOEC [decimal or %]
$\boldsymbol{\eta_{SOEC+HBP,ut}}$	Degree of utilisation, SOEC + HBP [decimal or %]
$\boldsymbol{\eta_{SOFC,el}}$	Electrical efficiency, SOFC [decimal or %]
$\boldsymbol{\eta_{SOFC,th}}$	Thermal efficiency, SOFC [decimal or %]
$\boldsymbol{\eta_{SOFC,ut}}$	Degree of utilisation, SOFC [decimal or %]
$\boldsymbol{\eta_{WtW}}$	Water-to-Water efficiency [decimal or %]
$\boldsymbol{\lambda_{1\ or\ 2}}$	Latitude points [decimal degree]
$\boldsymbol{\mu}$	Viscosity [cP or mPa∗s]
$\boldsymbol{\rho}$	Density [kg/m^3]
$\boldsymbol{\rho_{15}}$	Density, I*SO 8217* fuel at 15 °C and 1 atm [kg/m^3]

$\boldsymbol{\rho_{H18-DBT}}$	Density, dibenzyltoluene at 20 °C and 1 atm [kg/m^3]
$\boldsymbol{\rho_{L-H_2}}$	Density, hydrogen at -273 °C and 1 atm [kg/m^3]
$\boldsymbol{\rho_{NH_3}}$	Density, ammonia at -33.33 °C and 1 atm) [kWh/m^3]
$\boldsymbol{\Pi(\eta)}$	Product of multiple efficiencies
$\boldsymbol{q_{consumption}}$	Specific energy consumption with regard to distance [kWh/km]
Ϙ	Ratio [decimal]
$Ϙ_{\boldsymbol{loaded}}$	Ratio between hydrogen+tank and fuel transported+tank
$Ϙ_{\boldsymbol{loaded}}$	Ratio between hydrogen+tank and fuel/tank returned

1. Introduction

1.1 Background

The sustainable future requires a robust and safe supply of renewable energy. Hydrogen is often proposed as an energy carrier but transporting large volumes of pure gaseous H_2 comes with great risks, low *volumetric* energy density and substantial energy losses [1]. Alternatives include liquifying or compressing the gas, embedding it in metallic crystalline structures, or bonding it chemically to carrier molecules, to mention a few [2]. The global shipping industry is responsible for roughly 2.5 % of annual *greenhouse gas* (**GHG**) emissions but is dedicated to reduce this by implementing various hydrogen technologies [1], [3]. The *International Maritime Organization* (**IMO**) has set a goal of 70 % reduction of GHGs by 2050 (compared to 2008) [4]. The question of which solutions are most suitable for the maritime sector remains an open one, but one that must be answered soon. Researcher *Tjalve Magnusson Svendsen* at *CMR Prototech* put it this way:

"Given that large ships have a lifetime of 30 to 50 years, the shipping industry needs to choose a direction today if they are to reach the IMO targets before 2050 and comply with the Paris Agreement" [5].

The properties of the energy carrier itself is one thing, and technological maturity quite another. It may be the latter which primarily limits the options for ships being built in the near future. *Royal Dutch Shell* has recently become an advocate for *liquid hydrogen* (**L-H_2**) as the main energy carrier across sectors, but L-H_2 systems are generally *very* expensive due to their cryogenic nature, and only one ship, built in late 2020, currently exists for liquid hydrogen transportation [6], [7]. The recently completed *Sustainable Energy Catapult Centre* in *Stord* (western Norway) is scheduled to test engines from *Wärtsilä* and fuel cells from *Prototech* in the near future, both running on *ammonia* (**NH_3**) [8]. The intention is to deliver ship-ready technology within 2-3 years, and ammonia is already transported worldwide in large quantities despite the danger of it being a highly toxic substance [9]. Meanwhile, *Hydrogenious* aim to start testing their *liquid organic hydrogen carrier* (**LOHC**) technology at maritime scale (200 kW_{el}) as early as 2022 [10]. This solution is safer but may be difficult to implement, and the carrier itself has significantly lower gravimetric energy density than the other two fuels [11].

Alternatively, the fuel or carrier may not be available in sufficient quantities to warrant implementation. Liquid hydrogen is mostly produced in North America for spacecraft, ammonia is widely used as an ingredient in artificial fertilisers, and the most viable LOHCs being produced are currently intended for use as industrial heat transfer oils [12], [13]. The size of these markets varies, and the production methods may not necessarily scale well. Production of all three hydrogen carriers is planned in Norway in the near future [14]–[16].

Finally, increased safety risks associated with cryogenic storage or toxic chemicals may also bring additional complexities (and therefore expenses) to the daily operation of the ship. All the aforementioned problems are being solved by industry and academia the world over. Among these are *Ocean Hyway Cluster* (**OHC**), who aim to connect them and inspire collaboration.

1.2 Ocean Hyway Cluster

OHC is, in their own words, Norway's leading network for maritime hydrogen. More specifically it is an arena program, run by *Hub for Ocean* and supported by *Norwegian Innovation Clusters* [17]. Their objective is to make Norway a leading nation in the development and use of hydrogen technology for the maritime sector. In 2021 they are collaborating with HVL students on 8 bachelors and 3 master projects, which benefits both the students and OHC team members [18]. This thesis is one of those projects, with an objective supplied by OHC, and reformulated by the students.

1.3 Objective

There are far too many factors regarding maritime hydrogen use to consider in one bachelor's thesis. The intention is therefore to answer the following question:

Which hydrogen carrier technology is best suited for maritime supply chains, with regard to energy density and efficiency, safety, emissions, and fuel cost?

Three main hydrogen carrier technologies are presented, with a case study showing how these can work on a specific ship sailing along the western coast of Norway. Additionally, a general comparison is made with the aim to determine which hydrogen "form" is most efficiently transported.

Similar comparisons have been done in the past. Gretz, et.al. (1990) envisioned a Canadian energy export program by producing green hydrogen through hydropower and transporting it as either liquid hydrogen, ammonia, or bound in a specific LOHC [19]. However, only liquid hydrogen technologies were tested [20]. More recently, Wijayanta, et.al. (2019) compared the exact same substances and found that using ammonia gave the highest total energy efficiency and also the lowest cost [21]. Van Hoecke, et.al. (2021) went even further in their analysis of hydrogen for maritime applications and included synthetic fuels and metal hydrides in the comparison as well. They showed that the energy requirements for storage and release were very similar for ammonia and liquid hydrogen, while LOHC requires roughly 10% more energy, but conclude that no single solution satisfies all requirements [22]. Moradi and Growth (2019) performed a risk and reliability analysis of several hydrogen storage technologies and concluded that compressed and liquified hydrogen technologies are clearly more mature, but LOHC shows potential and needs time to develop further [23].

The source of the hydrogen itself is not considered in this thesis, other than the assumption that it is produced in a sufficiently sustainable manner. Technical evaluations begin at the carrier production stage and consider the energy requirements for production, storage, transport, and use aboard a given vessel. For the specific case, the fish feed carrier *MV Rubin* was selected by Mark Purkis at OHC.

In the following chapters the carriers are presented in sequence. Energy calculations for the case are done "in reverse", which is necessary when starting with operating data, and the remaining analysis follows the supply chain, from hydrogen production to fuel expenditure - from water to water.

2. Theory

All preliminary data in this study has been gathered from textbooks, scientific studies, and industry reports. The textbooks are primarily chosen from the curriculums of relevant courses at *Høgskulen på Vestlandet* (**HVL**), and where several are available the newest is generally considered to provide the most accurate data. The scientific studies and industry reports, however, are mainly sourced from literary searches in libraries such as *Science Direct* and the *Ocean Hyway Cluster Members' Area*.

Figures, molecule models and graphs are created in Adobe Illustrator, Arguslab, and Microsoft Excel, respectively. Molecule- and atom models are illustrated using the CPK-colour scheme, developed by *Corey*, *Pauling* and *Koltun*, from whom the name stems [24].

Units used by the industry are converted to SI, with a few exceptions where the unit is in a power of the SI-unit (bar and cP, for example). When densities of materials are presented, they are usually referring to a set of practical *storage conditions* (**SC**) which are separately defined for each fuel and hydrogen carrier in their respective chapters. Unless otherwise stated, *Standard Temperature and Pressure* (**STP**)-conditions are used, which are defined at 0 °C and 1 atm (or 101.325 kPa) [25]**.** Masses are sometimes given in tons, which always refers to the metric tonne and not the imperial definition.

The *heating value* (**HV**) of a fuel is often utilised when referring to the efficiency of power conversion equipment. The HV is defined as the amount of thermal energy released from a given amount of fuel at a reference temperature when the fuel is completely burned up and the combustion products are cooled back down to reference. Most fuels contain hydrogen - which forms water when burned – and the heating value is therefore categorised in two sections: The *lower heating value* (**LHV**) is used when the water leaves the system as vapour, while the *higher heating value* (**HHV**) is used when the water vapour is completely condensed, and the heat of vaporisation is recovered [26]. *All heating values are LHV unless otherwise stated*.

In order to distinguish between variables, specific properties (divided by mass, volume or mol) are written with a lowercase letter, while the corresponding extensive property is written with a capital letter. LHV and/or HHV are sometimes also referred to as *gravimetric energy density* which, if multiplied with the density of the fuel in question, yields the *volumetric energy density* as presented in **equation (1)** …

$$u = e * \rho \tag{1}$$

… where u is volumetric energy density, e is gravimetric energy density, and ρ is density. When efficiencies are described, it is sometimes referred to "Gibbs free energy" which is the "available energy" in a system, defined as the entropy subtracted from the enthalpy of a system, as described in **equation (2)** [26, p. 661] …

$$g = h - Ts \tag{2}$$

… where g is the Gibbs free energy, h is the enthalpy and Ts is the entropy multiplied by temperature (in kelvin). Reaction equations in this thesis is at reference 25 $°C$.

2.1 Hydrogen as an energy carrier

Being the simplest and most abundant element in the universe, hydrogen is quite plentiful on Earth as well, though mainly bound with oxygen as water or with carbon as hydrocarbons, because of its highly reactive nature [27]. It may also be found as a single molecule consisting of two hydrogen atoms in natural hydrogen deposits, although this is an extremely rare occurrence [28].

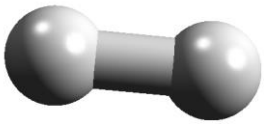

Figure 1: Molecular model (ball and stick) of hydrogen.

As stated in **chapter 1.1** the world needs a zero-emission energy carrier, which is the primary motivation for considering hydrogen as an alternative for today's fossil fuelled energy and transportation industries [29]. As illustrated in **Figure 1**, hydrogen molecules consist of only hydrogen atoms, which means that consumption of hydrogen through a fuel cell has no GHG-emission; and if produced correctly, has little *if any* GHG-emission associated with production as well. *Combustion* of hydrogen, however, may lead to emissions of NO_x and N_2O, further elaborated in **chapter 2.5.4**.

2.1.1 Production of hydrogen

There are several ways of producing hydrogen, either as a targeted product or as a by-product. The production method, as well as the energy source used for production, determines the categorisation of the hydrogen, divided into colours, as presented in **Table 1**.

Table 1: Colours of hydrogen [30]

Brown	Grey	Blue	Turquoise	Pink	Yellow	Green
Produced by gasification of organic or fossil-based materials	Produced by steam reforming natural gas *without* CCS	Produced by steam reforming natural gas *with* CCS	Produced by methane pyrolysis with solid carbon as a by-product	Produced by electrolysis from nuclear energy sources	Produced by electrolysis from mixed sources	Produced by electrolysis from renewable sources

These seven categorisations are the ones mostly used by the scientific community, although there are more. In the industry, however, only *blue*, *grey,* and *green* is used. The most common production method to date is *steam methane reforming* (**SMR**) of natural gas, which is either categorised as *grey hydrogen,* without *carbon capture and storage* (**CCS**), or as *blue hydrogen,* with CCS (although blue hydrogen is not yet commercially available). At present, approximately 96% of the world's hydrogen is produced from fossil sources, as shown in **Figure 2** [7], [31], [32].

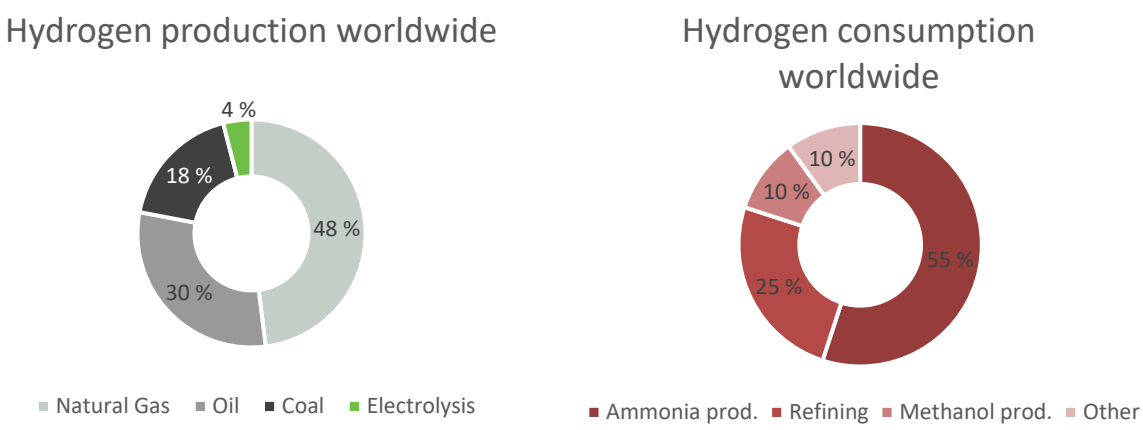

Figure 2: Hydrogen worldwide production and consumption by source and application [7], [31], [32]

The least common production method is *green hydrogen*, produced using renewable energy sources through *electrolysis* – a process where electric current is passed through an *electrolyte*, a substance which efficiently transmits electrons or ions [33]. The cost of hydrogen varies, depending on production method [31].

The *European union* (**EU**) has initiated a wide guarantee of origin system, called *CertifHy*, where an upper limit threshold of 36.4 g_{CO_2} / MJ_{H_2} (or 3.9 kg_{CO2} / kg_{H_2}) defines the maximum amount of the carbon intensity present in the hydrogen in order to class it as "low carbon-hydrogen", where both green and blue resides [34].

Besides electrical power, electrolyte, and catalyser, only clean water is needed in this chemical reaction, producing hydrogen and oxygen at a ratio of 2:1 by molecules, or 1:8 by mass [35]. This contrasts with the non-renewable ways of producing hydrogen by the use of hydrocarbons, which also yields carbon bound in different molecules, such as carbon monoxide or carbon dioxide [36]. Production of green hydrogen is generally more expensive than grey/blue, which is why petroleum derived hydrogen still will be used for some time into the future [37], [38]. Although there are multiple, complex, parallel, and intertwined processes taking place during steam methane reforming, it is generally simplified in **reaction equations** (**i**) through (**iii**) [39], [40]**.**

$$\mathrm{CH_4}\ (g) + \mathrm{H_2O}\ (g) \rightleftharpoons \mathrm{CO}\ (g) + 3H_2\ (g) \qquad \Delta h = 206\,\frac{kJ}{mol} \qquad \textbf{(i)}$$

$$\mathrm{CO}\ (g) + \mathrm{H_2O}\ (g) \rightleftharpoons \mathrm{CO_2}\ (g) + \mathrm{H_2}\ (g) \qquad \Delta h = -41\,\frac{kJ}{mol} \qquad \textbf{(ii)}$$

$$\mathrm{CH_4}\ (g) + \mathrm{CO_2}\ (g) \rightleftharpoons 2\mathrm{CO}\ (g) + \mathrm{H_2}\ (g) \qquad \Delta h = 248\,\frac{kJ}{mol} \qquad \textbf{(iii)}$$

Commonly when illustrating the SMR-process, equations (**i**) and (**ii**) are the only ones used, where the first is the regular steam methane reforming (which is quite endothermic, requiring a lot of heat), and the second reaction is known as the *water-gas shift reaction* (**WGSR**). WGSR is an exothermic reaction, and is favourable in steam methane reforming, as it reduces the overall need for thermal energy [39], [41]. Finally, the third equation (**iii**), is known as *dry reforming* (**DR**), usually present during SMR-processes, though not as a planned reaction. Unreacted methane will react with the newly formed CO_2 present,

which forms CO-gas and more H_2. This is an endothermal process, increasing the total heat requirements. The CO-gas produced from the DR may also take part in the WGSR [2], [42].

Production methods from non-renewable sources include partial oxidation, auto thermal reforming, pyrolysis, as well as the aforementioned SMR. Gasification of coal or biomass is also possible. Most of the hydrogen available today is already in high demand by industries using hydrogen in chemical processes or refining of other materials, such as ammonia for the fertilizer industry [43]. There are some benefits to producing hydrogen from steam methane reforming, some of which are the ease of handling, hydrogen yield per molecule of methane, and the abundance of natural gas, as well global availability. The demand for hydrogen is on the rise, and natural gas will continue to provide hydrogen for some time, until renewable production methods catch up in terms of scale and price [27]. As per 2021, only a fraction of the global hydrogen production is available for the commercial market. Therefore, to be able to utilise hydrogen in new areas, such as the energy and transport sectors, new infrastructure will have to be developed [31].

2.1.2 Green hydrogen from electrolysis

The most common and commercially available method of producing renewable hydrogen is electrolysis using alkaline or *polymer electrolyte membrane* (**PEM**) electrolysers. A third type is *solid oxide electrolysers* (**SOEC**) which is not yet commercially available, although manufacturers claim it soon will be [44]. Electrolysis being an endothermal process, requires input of electricity and the use of a catalyst to lower the activation energy, and each technology has different requirements. It should be noted that the efficiencies presented in the following chapters refer to the system-wide efficiency, not the efficiency of a single cell.

Alkaline Electrolyser Cell

Alkaline electrolyser cell (**AEC**) was the first large scale commercial electrolysers, based on an alkaline electrolyte, generally 30 % *calcium hydroxide* (**KOH**) or 25 % *sodium hydroxide* (**NaOH**) in order to increase conductivity, while the ion used to drive the process is hydroxides (**OH^-**) [45]. The reaction of AEC is presented in **reaction equations** (**iv**) through (**vi**):

$$Anode: 4OH^- \ (aq) \rightarrow O_2 \ (g) + 2H_2O \ (l) + 4e^- \qquad \textbf{(iv)}$$

$$Cathode: 4H_2O \ (l) + 4e^- \rightarrow 2H_2 \ (g) + 4OH^- \ (aq) \qquad \textbf{(v)}$$

$$Overall: 2H_2O \ (l) \rightarrow 2H_2 \ (g) + O_2 \ (g) \qquad \textbf{(vi)}$$

The catalysers used are NaOH and *sodium chloride* (**NaCl**), while an often-used electrode is nickel (**Ni**) [46]. A basic sketch of an AEC is presented in **Figure 3**.

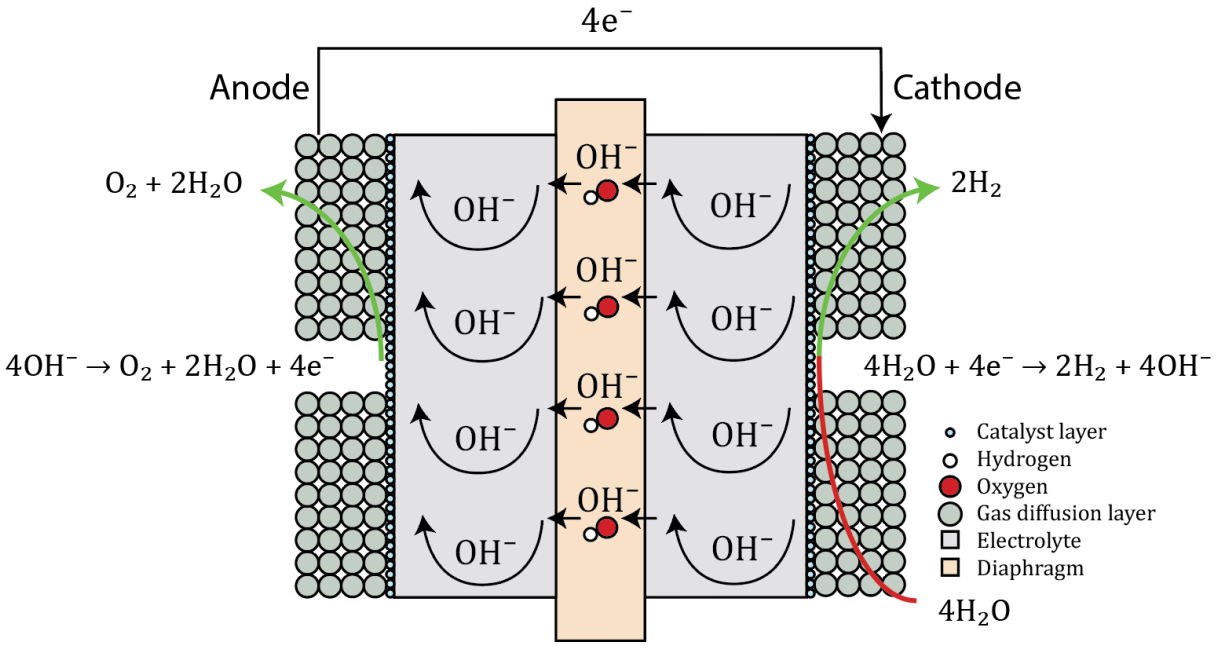

Figure 3: Basic principle of an alkaline electrolyser cell, inspired by Keçebaş [47]

AEC produces hydrogen of high purity of 99.999% and 99.99 % purity with and without purification, respectively. The electrical efficiency, $\eta_{AEC,el}$, of AEC is about 60-70 %, operating at 60 – 80 ° C [48]. These numbers may increase as new research is being done to be able to develop AEC with higher efficiencies [7]. As with most electrolyser- and fuel cells, stack-ability is a huge benefit in reducing the physical footprint, as well as increasing the voltage of the modules. AEC are capable of producing hydrogen with 99.999% and 99.99 % purity with and without purification respectively [49].

Polymer electrolyte membrane electrolyser cell

Polymer electrolyte membrane electrolyser cells (**PEMEC**, also referred to as proton exchange membrane electrolyser cells) were developed in the 1960's as a response to the shortcomings of the current alkaline electrolyser cells [50]. PEMEC at a conceptual level consists of a porous polymer membrane, typically Nafion, which also transports the electrons between the electrodes, all of which form the *membrane electrode assembly* (**MEA**) [51]. This is presented in **Figure 4**. *Bipolar plates* conduct electricity, hydrogen (and water) which makes it possible to stack multiple cells together. This is further elaborated in **chapter 2.5.2**. The proton exchange process is presented in **reaction equation** (**vii**) to (**ix**):

$$Anode: 2H_2O\ (l) \rightarrow\ O_2\ (g) + 2H^+\ (g) + 4e^- \qquad \textbf{(vii)}$$

$$Cathode: 4H^+\ (g) + 4e^- \rightarrow 2H_2\ (g) \qquad \textbf{(viii)}$$

$$Overall: 2H_2O\ (l) \rightarrow 2H_2\ (g) + O_2\ (g) \qquad \textbf{(ix)}$$

The membrane in a PEMEC has several advantages, such as allowing for a high variation in temperature and pressure, resilience, and corrosive resistance [52]. The latter is due to the electrodes usually being made of platinum **(Pt)** and iridium **(Ir)** (which are relatively rare and quite expensive materials) [53], [54]. A PEMEC is illustrated in **Figure 4.**

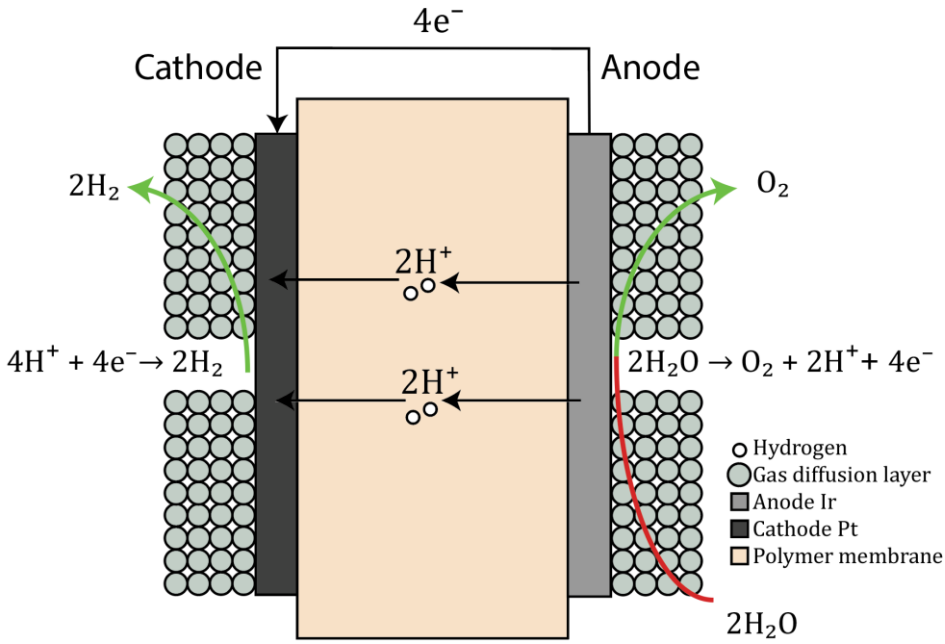

Figure 4: Basic principle of a PEM electrolyser cell.

The efficiency of a PEMEC is traditionally stated to range from 35 to 70 %, but most (if not all) new PEM electrolyser cells achieve an electrical efficiency, $\eta_{PEMEC,el}$, in the 60 to 70 % range, and operates at around 50 – 80 °C [48]. PEMECs are capable of producing hydrogen with a purity of 99.9998 % [55].

Solid Oxide Electrolyser Cell

Operating at temperatures above 700 °C [56], a *solid oxide electrolyser cell* (**SOEC**) is theoretically a lot more efficient than its contemporaries, mainly because the high temperatures allow for *high-temperature steam electrolysis* (**HTSE**). This not only increases the reaction rate, but also leads to less electricity required for the electrolysis process itself [56]–[58]. Presented in **reaction equation** (**x**) through (**xii**):

$$Anode: 2O^{2-}\ (g) \rightarrow O_2\ (g) + 4e^- \qquad \textbf{(x)}$$

$$Cathode: 2H_2O\ (g) + 4e^- \rightarrow 2H_2\ (g) + 2O^{2-}\ (g) \qquad \textbf{(xi)}$$

$$Overall: 2H_2O\ (g) \rightarrow 2H_2\ (g) + O_2\ (g) \qquad \textbf{(xii)}$$

SOECs are more similar to PEMEC than AFC, featuring a solid electrolyte in the form of an oxygen-conducting ceramic material, which allows for oxygen-diffusion in place of hydrogen-diffusion. Steam splits into hydrogen and oxygen at the cathode side, where the oxygen ions are drawn through the ceramic electrolyte and recombined with the electrons at the anode. The anode is typically a composite of *yttria stabilized zirconia* (**YSZ**) and *strontium-doped lanthanum manganite* (**LSM**), and the cathode is typically a Ni/YSZ cermet with 30 % porosity [56], [59]. A SOEC is illustrated in **Figure 5.**

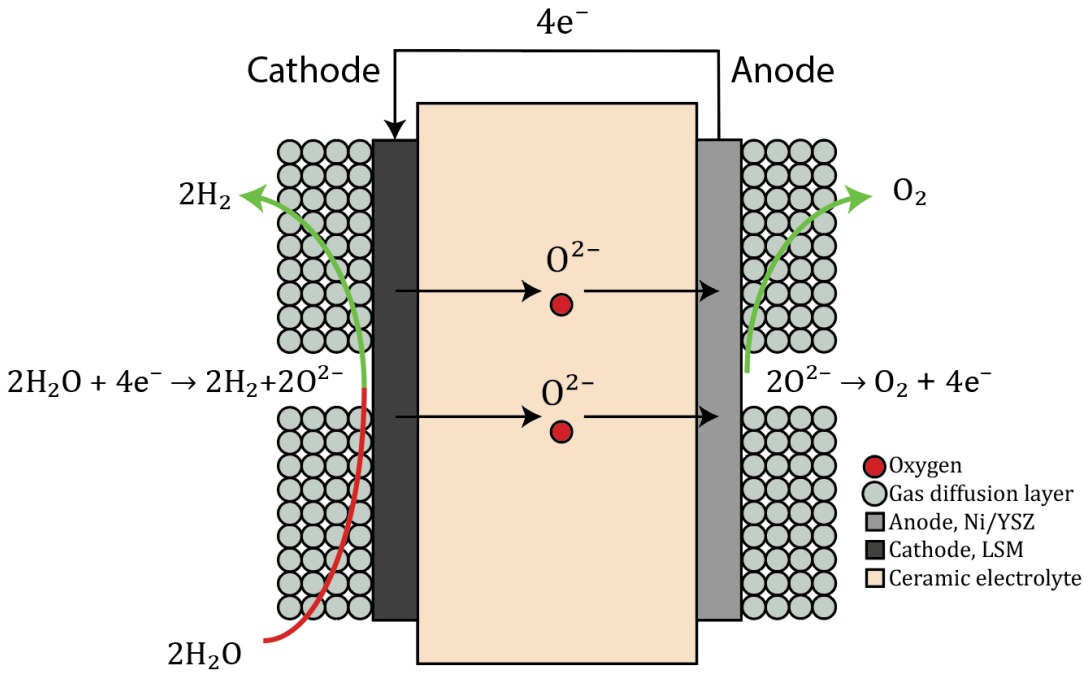

Figure 5: Basic principle of a solid oxide electrolyser cell.

Even though fuel cells based on this technology are wide-spread, electrolysis has proven difficult for years. *Haldor Topsøe* recently made an announcement stating that a facility based on SOEC will be functional in 2023, with degree of utilisation, $\eta_{SOEC,ut}$, reaching 90 % [44].

A comparison of different methods of hydrogen production is presented in **Table 2**.

Table 2: Comparison of different hydrogen production technologies

Fuel cell type	AEC	PEMEC	HTPEMEC	SOEC	SMR
Purity	low	medium	low	high	low
Efficiency	moderate	moderate	moderate	high	high
Degree of utilisation	low	low	moderate	high	high
Responsiveness	high	high	moderate	low	low
Catalyst cost	low	high	moderate	moderate	low
Life expectancy	moderate/high	moderate/high	moderate/high	high	high
Handling and complications	low	low	high	medium	high

= bad = good = moderate/medium

2.1.3 Energy densities

At standard temperature and pressure, hydrogen has almost three times the gravimetric energy density of low sulphur-diesel, but only a miniscule fraction of its volumetric energy density on account of the hydrogen density at ambient conditions being approximately 0.08 kg/m^3 [60]. **Table 3** compares the energy densities, and it is clear that the density of hydrogen must be increased dramatically if it is to be considered a serious contender in the use as a fuel.

Table 3: Gravimetric- and volumetric density comparison – hydrogen and diesel [27], [60], [61]

	Gravimetric density	**Volumetric density**
Hydrogen @ ambient	120.2 [MJ/kg] or 33.33 [kWh/kg]	9.98 [MJ/m^3] or 2.8 [kWh/m^3]
Low-sulfur diesel	42.6 [MJ/kg] or 11.83 [kWh/kg]	36 046 [MJ/m^3] or 10 012.78 [kWh/m^3]

There are several options for increasing the density, either by compressing the hydrogen (**CG-H_2**) to 350 – 700 bars, liquefaction by cooling, by converting it to *Ammonia* (**NH_3**), or by storing it *Liquid Organic Hydrogen Carriers* (**LOHC**)-molecules. The common factor for the last three is that they are stored at temperatures and pressures in which they are in a liquid state, hereby referred to as *storage conditions.* These conditions are defined more precisely for each carrier in the following **chapters 2.2**, **2.3**, and **2.4**.

2.2 Liquid hydrogen

Liquid hydrogen, abbreviated **L-H_2,** is pure hydrogen that is cryogenically cooled below its boiling point (where cryogenics is defined as "science and technologies applied at temperatures below -150 °C") [62]. This process is called *liquefaction* and can be done in various ways, ultimately cooling gaseous hydrogen to -253 °C (20 K) at atmospheric pressure. Doing so condenses the hydrogen, forcing it to go from a gas phase to a liquid phase, thereby increasing its density, ρ_{L-H_2}, to approximately 71 kg/m^3. This corresponds to a volumetric energy density, u_{L-H_2}, of approximately 2360 kWh/m^3 [63]. The process is both energy and time consuming, and various production methods can be utilised to alleviate both of these demands, for example by increasing the pressure, or cooling in several stages. The energy needed for liquefaction usually makes up a significant portion of the energy stored in the hydrogen (25-30 %), but new technologies can potentially reduce this to 20 % or below [7], [11]. Liquid hydrogen is used in a variety of applications and a multitude of ways, from experimental physics, medical applications, and food processing, to power plants and use as rocket fuel [64]. In this thesis however, the application of liquid hydrogen will be limited to use as a fuel, either in fuel cell or in combustion engine powertrains, further elaborated in **chapter 2.5**.

2.2.1 Production of liquid hydrogen

There are currently no production facilities in Norway making liquid hydrogen, although this is due to change in the next few years with projects like *Aurora* at *Mongstad* on the west coast of Norway [14]. Though there are a few facilities elsewhere in Europe, the cost (both economic and environmental) of transporting the L-H_2 to the Norwegian west coast is substantial [65], and is further elaborated on in **chapter 2.2.3**. Another point to note is

that almost all hydrogen produced, and therefore almost all L-H_2 produced, is grey (or brown) hydrogen as previously stated in **chapter 2.1.1**.

The basic concept of liquefaction can be summarized by the following stages, as visualized in **Figure 6**:

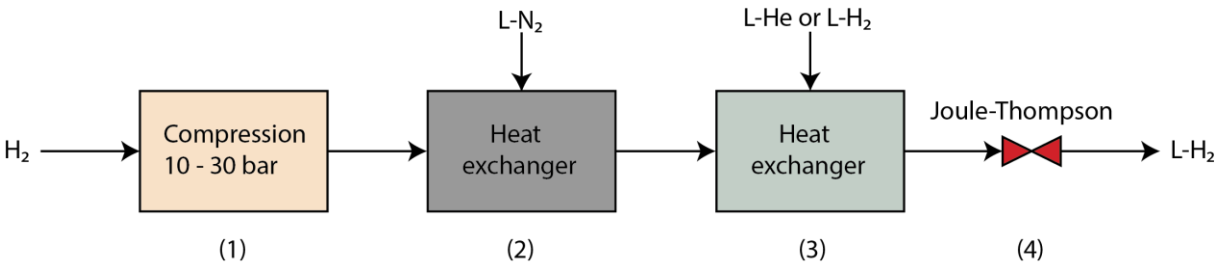

Figure 6: Extremely simplified liquification diagram.

(1): Pre-compressing hydrogen at ambient conditions, usually referring to ambient temperature (20 °C) and the pressure supplied by the hydrogen production method (10-30 bar). This stage varies by source of hydrogen, and affects the exergy needed in further stages, with exception to pre-cooling as described by *Walnum et al.* [66].

(2): Pre-cooling the hydrogen to about -200 °C using *liquid nitrogen* (**L-N_2**), as well as purifying the hydrogen to reduce the amount of contamination. Liquefaction of hydrogen requires no more than one part per million impurity (**ppm**) [27].

(3): Cryogenic cooling to about -240 °C. Materials for cooling are elaborated on below.

(4): Liquefaction by utilising Joule-Thompson valves or expansion valves, leaving the hydrogen at atmospheric pressure and -253 °C [66].

The basic process of liquefaction of hydrogen is usually done using a reversed *Brayton*- or *Claude* cycle, at both the pre-cooling (nitrogen) and cryo-cooling stages (helium or hydrogen). Research is being done regarding the use of mixed refrigerants (**MR**) to enable a more dynamic temperature transfer during the pre-cooling [67]. This process is common in liquefaction of natural gas (**LNG**), but is more difficult for **L-H_2** as the temperatures are much lower [68], [69].

Liquefaction of hydrogen is done using one of two compression cycles, each with their own benefits. Common for both cycles is a precooling stage using liquid nitrogen (**L-N_2**), purification of the hydrogen using an adsorption system, and a *Joule-Thompson valve* as the final stage bringing the hydrogen to –253 °C at about atmospheric pressure. The *Helium Brayton Cycle* is used for small-scale liquefaction, and benefits from having a lower cost of investment where the hydrogen can be injected at low pressure. However, this process suffers from low efficiency, hence practically only being viable for small-scale production of **L-H_2**. The *Claude Cycle* uses self-recycled H_2 for cooling instead of helium, demands hydrogen injected at slightly higher pressures than in the Helium Brayton Cycle, and is more efficient. It is therefore better for *large-scale hydrogen liquefaction* (**LHL**) with a production scale above 1700 kg_{H_2}/day, according to one of the largest and most well-known manufacturers of hydrogen tanks, *Linde* [70].

Other promising production methods

The Brayton- and Claude cycles are only a few of the different production methods available. There are several promising studies being conducted [71], including a method for using a sterling engine for cryogenic cooling, developed by *Lümmen et. al. (HVL*) [72].

2.2.2 Industrial scale production and use of L-H_2

Today one of the largest production- and storage facilities for liquid hydrogen is owned and used by *The National Aeronautics and Space Administration* (**NASA**) and *The United States Air Force* (**USAF**) for use as liquid rocket fuel in combination with liquefied oxygen [73], [74]. Liquid hydrogen has previously been desirable as a fuel because of its greater volumetric energy density compared to gaseous hydrogen, but challenges with both production and storage of L-H_2 have put a stop to the vision of using it as a fuel in large-scale supply chains. The energy economy in recent years as well as the growing threat of global warming has sped up the process of innovation and investment in hydrogen technologies, L-H_2 included [29], [64].

2.2.3 Storage and transportation of L-H_2

For hydrogen storage of any form, the level of hydrogen purity is of utmost importance. This is to ensure that no unforeseen reactions can happen while the hydrogen is in storage or transit, either spontaneously, because of handling, or due to temperature or pressure changes [27], [75], [76]. The hydrogen purity in liquefaction is critical, as no element, *besides helium*, has a melting point below the boiling point of hydrogen [69]. Therefore, any element (except helium) present during the liquefaction of hydrogen will be solid and can potentially clog essential components in the equipment [27], [66]. The purity required is generally $\geq$1 ppm [27], [76]. This purification can be done through several different methods such as ad- or absorption, distillation, partial condensation or separation by permeation [27].

The storage tanks used for L-H_2 consist of an inner tank containing the hydrogen, with an outer tank lined with thermally insulating materials. The input of ambient heat causes the cryogenic fluid to boil (as it is kept at constant volume and pressure) and venting of the vapour is called *boil-off* [77]. For long term storage, a high-quality insulated tank must be used to limit the rate of this boil-off. Double walled cryogenic storage tanks are most common, being specifically built to hinder heat transfer, but they are both expensive and heavy [78]. To further prevent boil-off, active cooling may be utilised by a cooled radiation shield, not unlike the ones used for storing liquid helium (**L-He**) at CERN [79], [80]. Linde states that as a "rule of thumb" the physical footprint of a CG-H_2 tank is about 4 times greater than that of an L-H_2 tank containing the same amount of hydrogen [81], despite only 90 % of the tank volume being usable (due to the aforementioned boil-off *and* the need for the liquid and gas to remain in a quasi-equilibrium) [81], [82]. Various companies design and manufacture tanks used for cryogenic storage with a wide range of specifications. *Linde* supplies tanks for both small-scale and large-scale applications (both transport and stationary storage). Most of the tanks produced by Linde are rated for 12 bar pressure, which leaves some headroom for boil-off before the hydrogen must be vented into the atmosphere. Up until now, venting hydrogen has been considered neither a health hazard nor impactful on the environment. Recent studies, however, suggest that

large quantities of hydrogen in the atmosphere may deplete the ozone-layer, something *Cicero* is currently researching [83], [84].

Determining a general, average boil-off rate is not trivial, as it is influenced by a number of factors such as insulation material, ambient temperature, volume, and the geometric shape of the tank – to name a few [82]. It is, however, usually regarded to be somewhere around 0.2 to 0.5 % loss of volume per day, and losses from unloading can reach upwards of 5 % [79], [81], [82].

LHL methods vary, and proposals for facilities with a higher efficiency are underway [85]. *Asadnia* and *Mehrpooya* [85] have proposed a facility with an energy consumption of 7,7 MWh per tonne L-H_2 produced, while current facilities consume between 12.5 and 15 MWh per tonne [23], [85]. When the travel distance from the production site to the application site is great, its recommended to transport the hydrogen as liquid rather than compressed gas, even in cases where the hydrogen is vapourised and used in its gaseous phase (for example in hydrogen powered cars and trucks) [86]. *Compressed gaseous hydrogen* (**CG-H_2**) for hydrogen cars is stored at 350 or 700 bar, and has a density of approximately 16 or 27 kg/m^3, respectively, when including the necessary supporting systems [87], [88]. Since L-H_2 has almost twice the energy density of CG-H_2, transport vehicles can carry almost twice the amount of fuel. L-H_2 is widely regarded to be better suited than CG-H_2 for use as a fuel over long distances as well. The specific distance required for L-H_2 to be more efficient is debatable and involves multiple variables. Regardless, *more than* 250 km has become the consensus [81], [86].

2.3 Ammonia

Naturally occurring in air, dirt, water, plants, and animals, ammonia is produced and renewed through the nitrogen cycle. It is an inorganic and extremely toxic, colourless gas with a characteristically pungent odour [89]. Pure ammonia is *hygroscopic* (easily absorbs water) in its *anhydrous* state (waterless), and is a relatively simple molecule being made up of one nitrogen and three hydrogen atoms, hence the formula: **NH_3** [25], [90] . A simplified ball and stick molecular model of ammonia is presented in **Figure 7**.

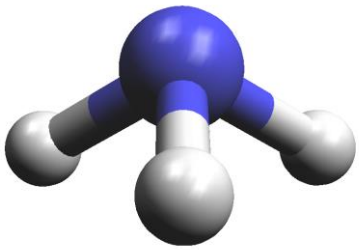

Figure 7: Molecular model (ball and stick) of ammonia.

Storing ammonia at temperatures *below* -33.33 °C or at pressures *above* 18 bar, ensures a liquified state [91], both of which should, according to the A*mmonia as a marine fuel safety handbook* [9], comply with the *IGC Code* for fuel tanks. This is further elaborated on in **chapter 3.2.5. Table 4** presents the energy densities and hydrogen content of ammonia at -33.33 °C and 1 atm, hereby referred to as *storage conditions* for ammonia.

Table 4: Energy density and hydrogen content of ammonia [92], [93]

Density, ρ_{NH_3}	[682 kg/m³]
Gravimetric energy density (LHV), h_{NH_3}	18.8 [MJ/kg] *or* 5.22 [kWh/kg]
Volumetric energy density, u_{NH_3}	12821 [MJ/m³] *or* 3560 [kWh/m³]
Hydrogen ratio	17.8 [wt%$_{H_2}$]
Hydrogen content	121.4 [$kg_{H_2}/m^3_{NH_3}$]

As is the case for hydrogen, ammonia is also categorised by colour according to production methods, and follows the same convention as in **chapter 2.1.1** [94], [95].

2.3.1 Production and industrial use of ammonia

Ammonia is considered one of the most commonly produced inorganic chemicals in the world, being the chief ingredient in synthetic fertilizers [43], with an annual worldwide production estimated to be about 180 million tons [96]. Ammonia is also used as the base material in other production processes, like the production of plastics and other polymers because of its physiochemical properties [97]. Solutions of ammonia are also used in the reduction of nitrogen oxide gasses (NOx) in diesel engines [98]. Production is mainly done through a process known as the Haber-Bosch process (**HBP**), developed by *Frits Haber*, and industrially upscaled by *Carl Bosch* in 1913, utilising nitrogen (from the atmosphere) and hydrogen (*traditionally* from SMR) at high temperatures and pressures to synthesize ammonia [99].

As nitrogen is a relatively inert substance, it requires a catalyst for the reaction to occur at reasonable temperatures [100]. By utilising simple iron oxide catalysts, the reaction is usually operated at 300-500 °C and 100-150 bar [101]. This process is highly inefficient, and one cycle converts only 10-15 % of the hydrogen, which necessitates recycling of unreacted gas back into the stream in order to produce an acceptable yield of 98 %, as illustrated in **Figure 8** [102]. The process is a spontaneous, reversable, and exothermic process [91], [103], presented in **reaction equation (xiii).**

$$N_2\,(g) + 3H_2\,(g) \rightleftharpoons 2NH_3\,(g) \qquad \Delta h = -91.8\,\frac{kJ}{mol} \qquad \textbf{(xiii)}$$

By removing the ammonia as soon as possible, one ensures that the equilibrium favours the creation of products, and even though the reaction favours creation of ammonia at low temperatures, it is necessary to keep the reaction at a higher temperature to get a better rate of yield [100]. The ammonia is then cooled and liquified for storage [104].

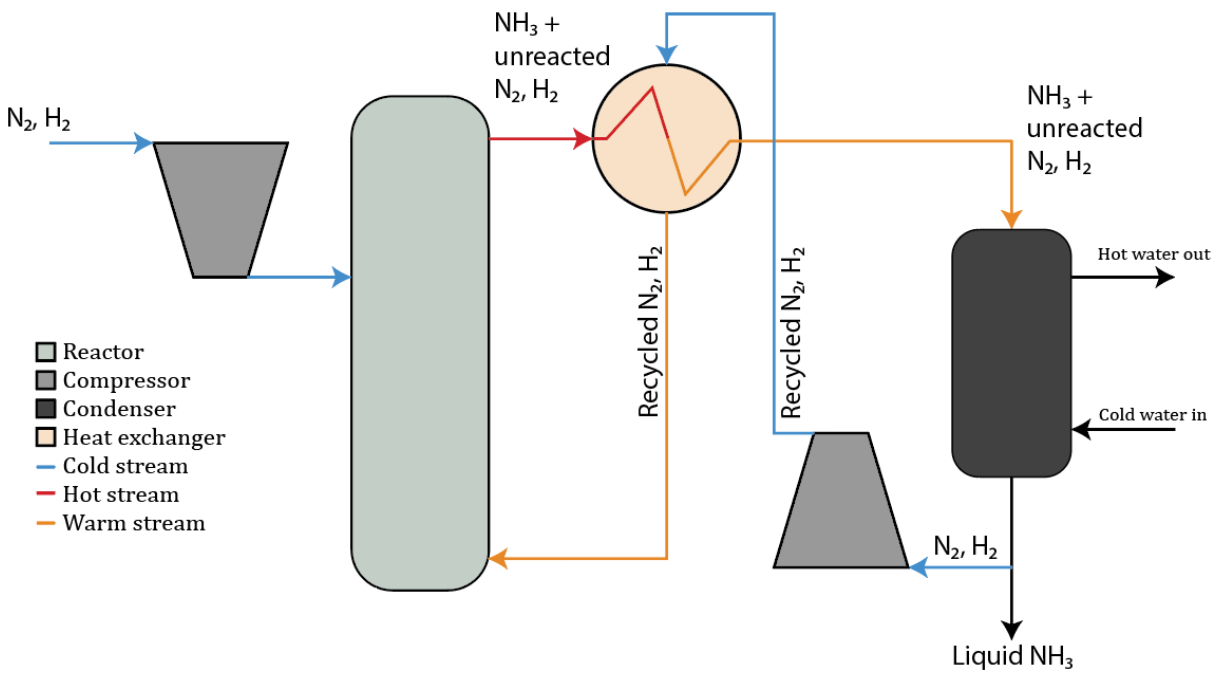

Figure 8: Haber-Bosch process, inspired by esru.strath.ac.uk [105]

Even though the process has been improved upon for over a hundred years, it still requires approximately 2 % of the world's total energy supply, and is responsible for approximately 1.6 % of the total global CO_2 emissions [101]. The Norwegian ammonia producer Yara recently announced plans to start production of green ammonia on the plant at *Herøya* in *Porsgrunn,* utilising hydrogen from electrolysis and HBP, both with energy from renewable sources [15].

The efficiency of HBP is typically around 66 %, even though it is exothermic, it needs energy for compression work, as well as the need to keep the process at operating temperature and energy loss during the cooling of the product. The exothermic nature makes it possible to reach a much higher *degree of utilisation* if combined with processes requiring heat, in particular the previously mentioned *solid oxide electrolyser cells* (SOEC) from **chapter 2.1.2** [106]. According to *Amon Maritime* an AEC and HBP-system should reach efficiencies, η_{HBP}, of 56 %, while a combination with SOEC could potentially reach a degree of utilisation, $\eta_{SOEC+HBP,ut}$, as high as 73 % in the future [107].

Possible alternative production methods

The high energy demand for production of ammonia through HBP has motivated scientists to pursue other production methods. A very promising alternative involves producing the ammonia directly from water and air, in ceramic membrane electrolysers, at substantially higher efficiencies than that of HBP. The main challenge lies in the low production rate [108]–[110]. A concept illustration is presented in **Figure 9**.

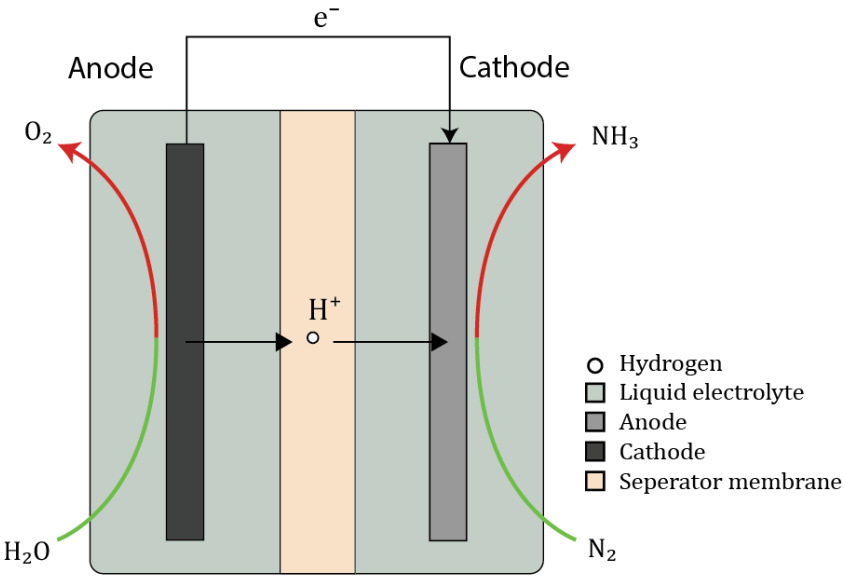

Figure 9: Concept illustration of direct ammonia electrolyser [110]

2.3.2 Storage and transportation of ammonia

Storing ammonia in a liquified state is achieved by lowering the temperature, increasing the pressure, or both, as stated at the beginning of **chapter 2.3**. Storing ammonia at -33.33 °C requires a continuous liquefaction cycle through compressors and heat exchangers as the toxicity of ammonia makes venting the boil-off unacceptable. By capturing the boil-off and compressing it, the temperature increases, and the ammonia is then fed through a heat exchanger which lowers the temperature. The pressure is then released, cooling the liquid below the original temperature, and the ammonia is reintroduced into the storage tank, as illustrated in **Figure 10** [105], [107]. As a safety feature, the refrigerated tanks have a built in containment barriers in case of leaks, typically conceived as an inner- and outer tank structure [107].

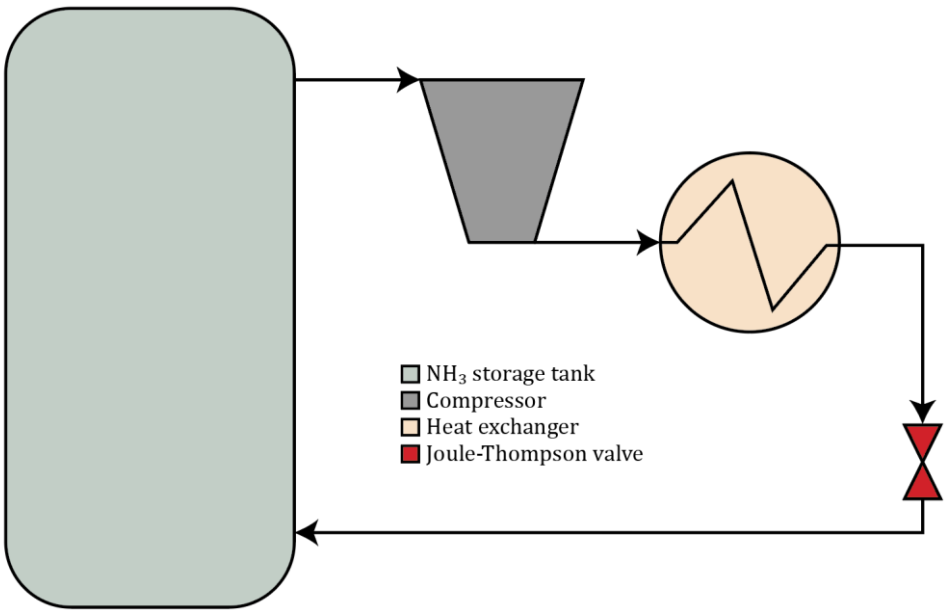

Figure 10: Active cooling system for liquid ammonia storage.

The other storage option is ammonia pressurised to 18 bar, which corresponds to the vapour pressure at 45 °C. While this requires compression work when loading, there are minimal energy losses during storage, unlike the refrigerant tanks [107]. Information about energy requirements and efficiencies for storage has proven difficult to acquire.

A unique challenge associated with ammonia is its corrosive properties, which makes material choices a crucial step in designing ammonia systems. Anhydrous ammonia may form cracks in steel, especially if it is polluted by air or CO_2, a phenomenon known as *ammonia stress corrosion cracking*. It is common to add a small amount of water (0.2 %) to overcome this [111]. The additives used in stainless steel influences the rate of corrosion when interacting with ammonia [112], [113].

The transport of ammonia is a well-established industry, ranging from road and rail transportation in the 40-60 m^3-scale, to large fully refrigerated *Large Gas Carriers* (**LGC**) with a capacity in the 60 000 m^3-scale [107].

Although there is no existing bunkering network for ammonia as a fuel, the existing infrastructure and storage- and distribution technology may be rebuilt into a bunkering network. Ammonia bunkering stations should be fairly similar to LNG bunkering stations, but with less requirements related to temperature and pressures. The toxicity of ammonia, however, will likely necessitate extensive use of *Personal Protective Equipment* (**PPE**) and no-walk safety zones before and during flow of fuel [107].

2.3.3 Application of ammonia as a hydrogen carrier

Ammonia is usable both in fuel cells and combustion engines, either as a fuel itself, or by decomposing it and releasing the hydrogen [114]. Direct use of ammonia is further elaborated on in **chapter 2.5.4**. Ammonia decomposition, or cracking, is simply the synthesis process, the Haber-Bosch process (HBP) from **chapter 2.3.1**, in reverse, as described in **reaction equation** (**xiv**) [91], [103]:

$$2NH_3\ (g) \rightleftharpoons N_2\ (g) + 3H_2\ (g) \qquad \Delta h = 91.8\ \frac{kJ}{mol} \qquad \textbf{(xiv)}$$

Note that this process in endothermic, in contrast to the HBP. The operating temperature is 850 °C and the reaction takes place on a Nickel catalyst [91], [115]. *The Ammonia Energy Association* has calculated the energy requirement for ammonia cracking to be between 0.28 and 0.3 kWh/kg_{NH_3}, in addition to the "loss of hydrogen" in cracking of 1.13 kWh/kg_{NH_3}, which culminates in an efficiency of approximately 76 %, excluding *combined heat and power* (**CHP**) [116]. Approximately 100 ppm of uncracked ammonia is present in the hydrogen stream without purifiers [91], [115].

2.4 Liquid Organic Hydrogen Carriers

The concept of liquid organic hydrogen carriers (LOHC) can be defined, in its broadest sense, as the synthesis or enrichment of carbon-based compounds using hydrogen gas, with the purpose of hydrogen transportation under ambient conditions. This may also be referred to as *organic chemical hydrides* (**OCH**) [2]. The carrier molecules are either destroyed in the process and/or reused, depending on their chemical compositions. Reusability is in this case key to a zero-emissions supply chain, which is why *most* of the literature refers to molecules that are not destroyed when describing the LOHC concept. However, *some* studies may also refer to certain other molecules as LOHCs despite not technically fitting the usual definition [117]. These specific cases are further elaborated in chapters **2.4.1** and **2.4.3**. The first of these is a brief introduction to synthetic fuels, which is somewhat related to LOHCs. **Figure 11** illustrates the different supply chains.

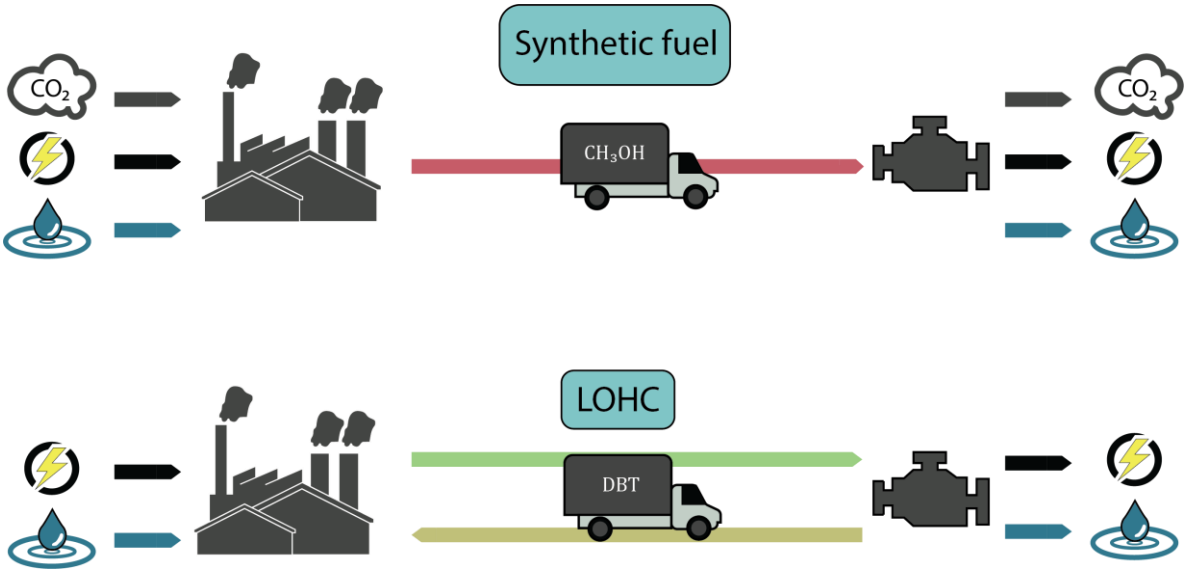

Figure 11: Synthetic fuel and LOHC supply chains.

2.4.1 Synthetic fuels

Fuels can be synthesised using hydrogen gas as a primary component, and subsequently decomposed into water, etc., after use. One example is *methanol* (**CH_3OH**) which is already produced worldwide from organic matter, natural gas, or coal. However, it can also be created by combining H_2 with CO_2 (captured from industrial processes or the atmosphere). The latter is determined by **reaction equation** (**xv**) to (**xvii**) [118], [119] ...

$$CO_2\ (g) + 3H_2(g) \rightarrow CH_3OH\ (l) + H_2O\ (l) \qquad \Delta h = -131.5\frac{kJ}{mol} \qquad \textbf{(xv)}$$

$$CO_2\ (g) + H_2\ (g) \rightarrow CO\ (g) + H_2O\ (l) \qquad \Delta h = -41.2\frac{kJ}{mol} \qquad \textbf{(xvi)}$$

$$CO\ (g) + 2H_2\ (g) \rightarrow CH_3OH\ (l) \qquad \Delta h = -128.7\frac{kJ}{mol} \qquad \textbf{(xvii)}$$

…where the water-producing side reaction (**xvi**) can be discouraged with high pressure (optimal process around 760 °C and 100 bar) [120]. Methanol can be used as a *hydrogen* carrier for regular fuel cell systems or as an *energy* carrier for both direct methanol fuel cells and internal combustion engines [121], [122]. When burned under stoichiometric conditions CO_2 is produced in amounts equal to what was harvested from the atmosphere when creating the methanol, making it a carbon neutral fuel in this case (provided the H_2 is generated from electrolysis with renewable electricity) [120]. The chemical structure of methanol is visualised in **Figure 12**.

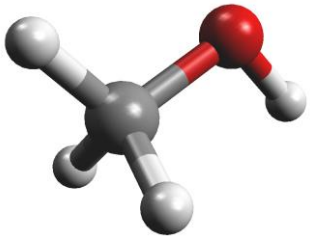

Figure 12: Molecular model (ball and stick) of methanol.

2.4.2 Reusable hydrocarbons

The LOHC concept is defined by the principle that unsaturated hydrocarbons (with double and/or triple covalent bonds) have available electron pairs that can be rearranged into new single bonds, incorporating additional atoms into the molecule. Crucially, this process can also be reversed, extracting the added elements, and reverting the molecule to its original form. The two subprocesses are referred to as hydrogenation and dehydrogenation, i.e., storing and releasing additional hydrogen atoms into and out from a carrier molecule. The strength of the bonds makes LOHC a virtually lossless storage method. However, this also means that *releasing the hydrogen requires energy*. Conversely, *storing the hydrogen releases energy* in the process [2]. Typically, only 1 % of the hydrogen's energy content is required for hydrogenation, whereas 20 % is required for dehydrogenation [11]. However, this will vary depending on the carrier molecule, chosen catalysts and process integration.

In theory any unsaturated hydrocarbon can be used, but in practice there are several factors to consider: The ideal hydrogen carrier is liquid at operating temperatures, safe and easy to transport, and has a sufficient hydrogen capacity to achieve meaningful energy efficiencies. This capacity can be defined as the number of available bonds per carrier atom, or as wt.% H_2.

Figure 13 shows the hydrogenation/dehydrogenation cycle of the cycloalkene toluene. The three double bonds (per seven carbon atoms) are all rearranged to support a total of six additional hydrogen atoms. This gives the molecule a maximum hydrogen capacity of 6.2 wt.%, which, considering a practical dehydrogenation limit of 95 %, translates to 1500 kWh/m^3 [123]. Upon use, the excess hydrogen is released, and the base molecule is ready for another cycle.

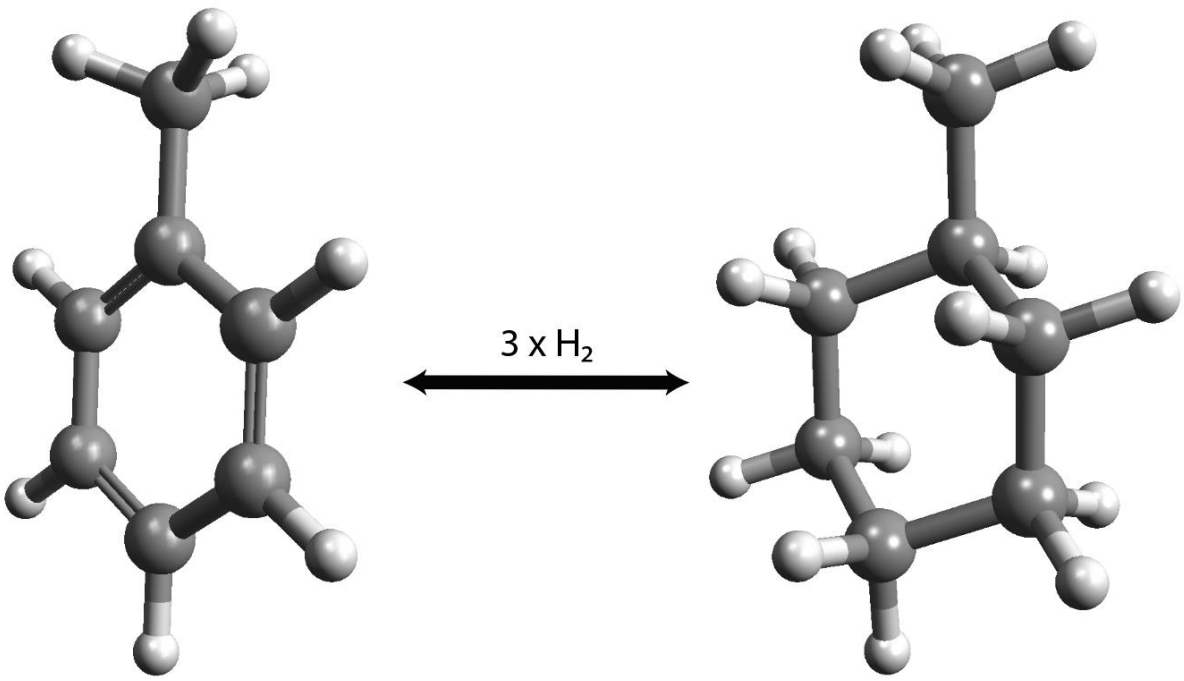

Figure 13: Hydrogenation/dehydrogenation cycle of toluene.

2.4.3 Carriers, challenges, and combinations

There exists a handful of studies that provide comprehensive overviews of potential candidates for LOHC systems, most notably Markiewicz, et al. (2015) and Niermann, et al. (2019) [123], [124]. However, some examples are presented in **Table 5** to provide adequate context. The most relevant factors for energy calculations are given, but safety factors must also be considered when selecting a carrier. Toxicity is compared using the TPI scale (Toxic Potential Indicator), which is a combination of several German health and environmental classifications, denoted as units of TPI/mg. This scale ranges from 0 (entirely harmless) to 100 (extremely harmful). Note that only the initial chemical composition of a substance is considered, and not by-products from exposure, combustion, etc. [125]. The toxicities of the saturated and unsaturated molecules are often similar, or one of the two is unknown. Where they vary significantly, the most severe indicator is presented.

Table 5: A comparison of reusable LOHC molecules [123], [126]–[128]

LOHC (unsaturated / saturated)	Hydrogen capacity [c] [wt. %]	Liquid temp. range [°C]	Ignition temp. [°C]	Density at 20 °C [d] [kg/L]	Viscosity (dynamic) at 20 °C [d] [mPa · s]	Toxicity [TPI/mg]
N-ethylcarbazole (NEC) / perhydro-N-ethylcarbazole	5.8	68 -> 270 / <20 -> 208	186 / 146	1.10 / 0.94	121 / 5.9	5.1
Diphenylmethane (DPM) / dicyclohexylmethane (DCM)	6.7	25 -> 265 / -19 -> 250	130 / N/A	1.00 / 0.87	2.43 / 4.15	N/A
Toluene / methylcyclo-hexane (MCH)	6.2	-95 -> 111 / -127 -> 101	535 / 260	0.88 / 0.77	0.6 / 0.7	19.3
Dibenzyltoluene (DBT) / perhydro-dibenzyltoluene	6.2	-39 -> 390 / -45 -> 354	450 / N/A	1.04 / 0.91	49 / 425	13.8

The clearest distinction between the molecules is seen in the liquid temperature ranges. NEC is a solid below 68 °C, but this can be mitigated with limited dehydrogenation (90 %), allowing a liquid phase down to 20 °C [123]. Alternatively, solvents can be added, but this could potentially pollute catalysts, etc. DPM has a significantly higher hydrogen capacity, but also has the same solidity issue at lower temperatures. Han, et.al (2019) propose to solve this by creating a eutectic mixture with another LOHC, namely biphenyl. Both molecules hydrogenate fully and efficiently on the same catalyst, and this kind of solution could be possible for other LOHC systems as well [127]. For example, DBT has a very wide liquid temperature range, but Müller, et.al. (2015) show that the dynamic viscosity of the hydrogenated DBT increases significantly at lower temperatures, from 425 cP @ 20 °C to 1520 cP @ 10 °C [128]. To counter this, Jorschick et.al. (2020) propose a mixture of 20 wt.% *benzyltoluene* in dibenzyltoluene, decreasing the viscosity by 80 % (@ 10 °C), while also increasing the hydrogen release rate by up to 16 % [129]. Further details in **chapter 2.4.4**.

A related, and equally crucial metric for LOHC systems is the dehydrogenation temperature. It is not listed in **Table 5** due to the variance in possible catalysts, but temperatures close to the boiling point, from 100 °C up to 450 °C, are required to extract most of the excess hydrogen [123]. This is considered the main drawback of most LOHC technologies, as the high energy demand makes dehydrogenation difficult to integrate.

Additionally, it is always possible that the individual molecules decompose or bond with others during the hydrogen cycle, and the probability increases with temperature. This in

[c] Theoretical maximum values.

[d] + 5 to 10 °C depending on the source data. Table values are adequate for rough estimates.

turn decreases the lifetime of the LOHC with respect to a certain tolerable concentration of by-products. The limit may vary because cracking the molecules does not necessarily decrease the hydrogen capacity of the mixture. On the other hand, it is possible that these new molecules are more difficult to hydrogenate or dehydrogenate on certain catalysts. Furthermore, by-products can have significant effects on other properties like viscosity, melting point, boiling point, toxicity, etc. [130].

Finally, it is noted that substances like methanol, acetone, etc., in addition to their potential as synthetic fuels, can also be used inside a power system for *transfer hydrogenation.* This is -simply put- adding and subtracting hydrogen in a chemical reaction without creating H_2 in the process. The mechanism theoretically enables combined LOHC solutions where the hydrogen is transferred from the main carrier to the end point (for example a fuel cell) via a second carrier, meaning no gaseous hydrogen is present in the system. In addition to this obvious safety benefit, higher energy efficiencies may be achieved as the transfer reactions can occur at significantly lower temperatures than typical catalytic LOHC dehydrogenation [117], [131].

2.4.4 DBT production

Dibenzyltoluene is regarded by many as the most suitable LOHC so far, and it is the main focus of the EU hydrogen infrastructure project HySTOC [132]. DBT's relatively high hydrogen capacity, high thermal stability, and low flammability are some of the reasons cited for its adoption [133]. Another major "selling point" is its availability due to existing use as an industrial heat transfer oil. In this context DBT is perhaps better known by brand names like Marlotherm SH, or Jarytherm DBT [134]. **Figure 14** shows the chemical structure of some dibenzyltoluene isomers.

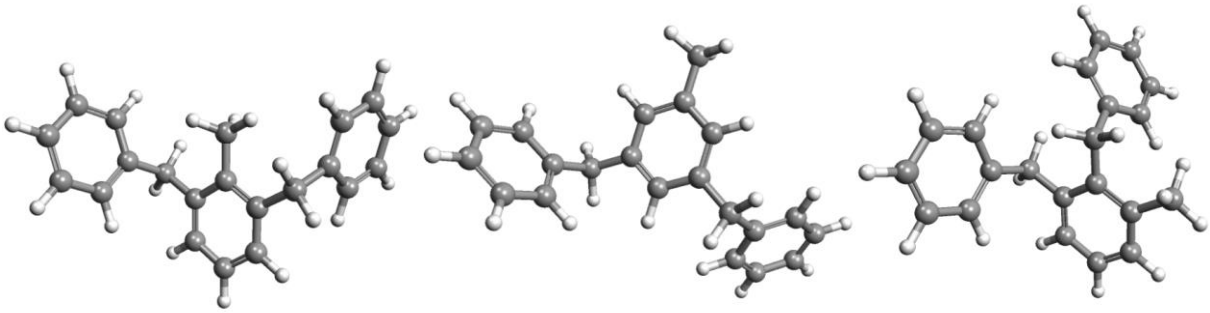

Figure 14: Chemical structure of three different DBT isomers.

To create this molecule, only two main components are needed: Toluene and chlorine. The first is a petroleum product which is primarily distilled from two different process streams: Most common is catalytic reforming, a process designed to produce high-octane aromatic compounds. Alternatively, cracking heavy hydrocarbons in an inert atmosphere produces pyrolysis gasoline, which is a mixture of toluene and various other aromatic compounds, paraffines, etc. Finally, toluene is also created directly as a by-product of styrene production [135], [136].

Some of the toluene is reacted with chlorine gas, for example under UV light, to create benzyl chloride. Although other compounds are also made, the desired reaction is favoured by carefully managing the process conditions (below 1:1 molar ratio of chlorine and toluene, atmospheric pressure, and temperatures between 65 °C and 100 °C) [134].

To form the final dibenzyltoluene product, benzyl chloride and the remaining toluene is reacted by Friedel-Crafts alkylation using a Lewis acid. There are multiple reactions that happen in series, and several possible reaction sets, but they are all typically carried out around 100 °C and atmospheric pressure, except dechlorination which may require temperatures of up to 390 °C. Further details and explanations of the chemical process are found in the HySTOC (D8.4) DBT production cost estimation study from 2019 [134].

The conclusion, with regard to energy use, is that a plant producing 3500 tons per year of DBT requires an estimated 2435 kW + 1990 kW for low and medium pressure steam, respectively + 420 kW of electricity [134]. Assuming constant operation this equates to 42.4 GWh annually, which of course is unrealistic, but no approximate uptime is given for this production level. It is also estimated that a total of 9000 tons of DBT is currently produced worldwide annually [134].

2.4.5 Hydrogen cycle and longevity

Storing hydrogen in dibenzyltoluene requires a metal catalyst (typically Platinum or Ruthenium based), with a temperature of at least 150 °C in the reaction chamber and a hydrogen pressure of up to 50 bar. These conditions and a 0.25 mol% Ru/Al_2O_3 catalyst fully hydrogenates a batch of DBT in 240 minutes [12]. Commercial systems use up to 250 °C with pressures between 25 – 50 bar [10]. Detailed knowledge of these systems, for example the chosen catalyst material and structure, is currently unavailable, but **Table 6** summarises the key properties of the LOHC system currently offered by the German company Hydrogenious.

Table 6: Hydrogenious StorageBOX and ReleaseBOX base module properties [133]

	Hydrogenation	**Dehydrogenation**
Hydrogen inlet/outlet	0.9 kg/h	0.9 kg/h
LOHC production/demand	20 l/h	20 l/h
Heat supply/demand	8 kW	11 kW
Load range	50 – 100 %	
LOHC stream	P ≥ 0.1 barg, T ≥ 15 °C	

This clearly illustrates the difference between loading and unloading an equal amount of hydrogen: Hydrogenation *releases* 8 kW, whereas dehydrogenation *requires* 11 kW of thermal power. Supplying this heat is a key challenge of implementing LOHC systems. Efficiencies are not specified, and they cannot easily be calculated without further information. However, the hydrogen must be pressurised before the LOHC is hydrogenated, as illustrated in **Figure 15**. Hurskainen, et.al. (2020) suggest using a

compressor with 75% isentropic efficiency [137]. The total electrical efficiency for DBT hydrogenation is therefore set to 74% in this thesis, not including waste heat utilisation.

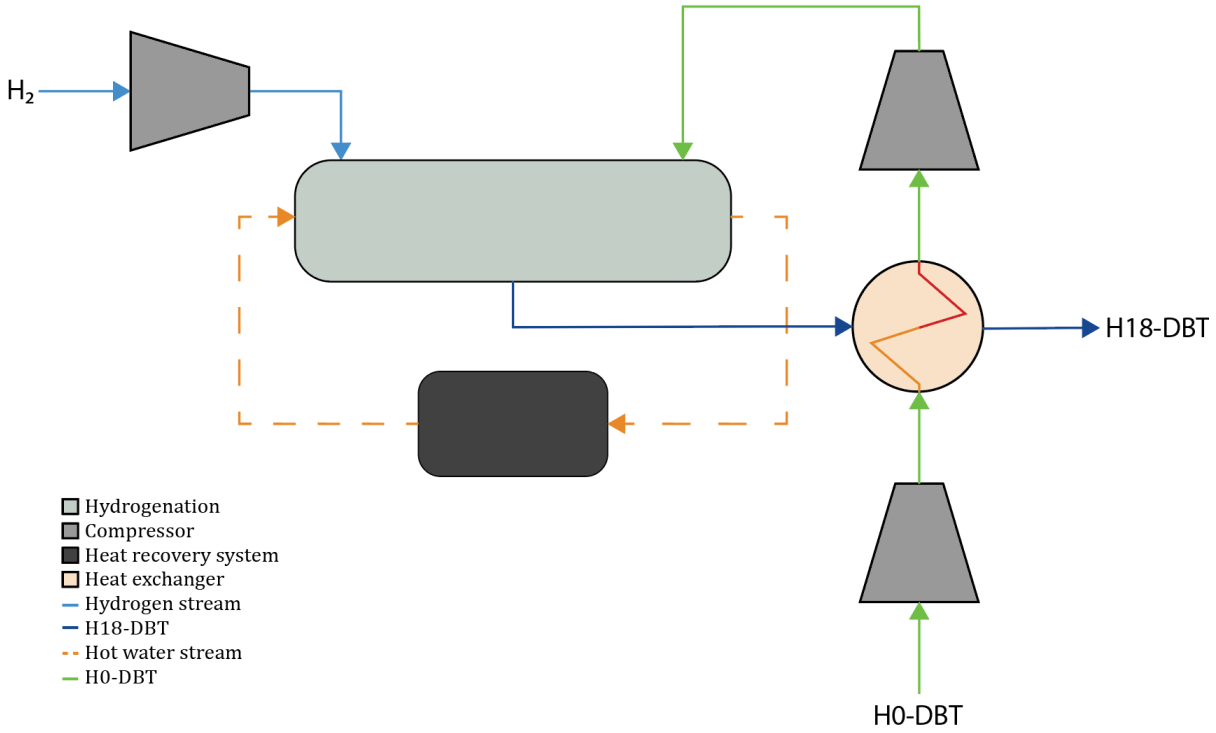

Figure 15: Hydrogenation process, inspired by Eypasch et al. [138]

Releasing hydrogen from dibenzyltoluene also requires a metal catalyst (typically Palladium or Ruthenium based), with temperatures of 310 °C or more at atmospheric pressures. Using a Ru/C (carbon supported) catalyst at these conditions dehydrogenates DBT to 97% in 120 minutes [12]. Commercial systems use around 300 °C with 1-3 bar pressure [12], [133]. Lower temperatures significantly reduces reaction rates [12]. The dehydrogenation limit results in a *practical* hydrogen capacity of 6.0 wt% for DBT, with a corresponding volumetric energy density of 1800 kWh/m³ [123]. **Table 6** shows that the dehydrogenation process requires 12 kWh / kg_{H_2} of heat.

Note that both the storage and release systems require the DBT to have a temperature of at least 15 °C at the inlet, despite the substance being liquid down to -39 °C. This is likely to counter the rapid viscosity increase that occurs when going below 20 °C, as mentioned in **chapter 2.4.3**, which is partially due to the large number of isomers that DBT may contain [123]. To illustrate this, **Table 7** compares the viscosity of DBT with some common fluids.

Table 7: Viscosities of common fluids and DBT [128], [139], [140]

Temperature [°C] (± 1 degree)	H0-DBT [cP]	H18-DBT [cP]	Acacia Honey [cP]	Olive oil [cP]
0	340	-	9360	-
10	-	1520	-	-
15	-	790	-	-
20	49	425	1370	75
30	-	155	270	52
40	17	72.1	-	38
60	8.2	22.4	-	20

It becomes clear that the aforementioned 80 % reduction in viscosity that is achieved with a 20/80 wt% BT/DBT mixture can be vital for application in colder climates, as the handling becomes easier and energy requirements for pumping and/or heating are reduced. Furthermore, a 12 to 16 % increase of dehydrogenation rates can be achieved, compared to pure DBT on the same porous Pt catalyst (silica- or alumina supported). This may be due to the BT molecule's smaller size matching better with the catalyst pores. It is also noted that transfer hydrogenation between the different compounds can occur under these kinds of conditions, meaning the BT or DBT species hydrogenate each other instead of releasing H_2 gas. This would reduce the process efficiency [129].

Handling, storage, and transport

Dibenzyltoluene is a fairly large molecule with properties very similar to regular diesel fuel [133]. Neither diesel nor DBT is «one thing», per se, but rather a range of similar substances and/or isomers [128], [141]. The similarities include low flammability, storage in regular plastic or steel tanks at ambient conditions, and low or nonexistent risk of explosions during storage and transport. The main toxicity hazard to humans is in both cases related to ingestion of the substance, although prolonged skin contact should also be avoided [141], [142]. It is therefore considered a viable option to adapt the existing mineral oil infrastructure to supply dibenzyltoluene instead [10].

Storage conditions for DBT are defined as 20 °C and 1 atm (see **chapter 2.1.3** for further explanation). The temperature is chosen to compensate for increased viscosity at lower temperatures, assuming pure DBT is used.

It is also necessary to return the dehydrogenated DBT using the existing infrastructure. H0-DBT (dehydrogenated) has similar properties to H18-DBT (hydrogenated) but is more viscous and therefore more easily pumped. Heavy transport both ways leads to increased CO_2 emissions (if the supply trucks run on fossil fuels), but the project described by the HySTOC deliverable 8.2 shows that the energy demand for dehydrogenation is the primary source of emissions if the electricity is supplied from non-renewable sources [143].

Longevity and by-products

Another source of GHG emissions could be the dehydrogenation process itself. Modisha & Bessarabov (2020) showed how DBT can degrade under catalytic hydrogenation, as well as under the high temperatures that occur when dehydrogenating, by simulating a large number of cycles with accelerated stress tests (**AST**). A multitude of by-products can be created by cracking the DBT molecule, including methane which has a global warming potential of 28-36 CO_2 equivalents (over 100 years) [130], [144]. The AST indicates that 89 hours of dehydrogenation at 300 °C creates 7.4 mol% of by-products, and **Table 8** is a summary of the hydrogenation tests. Note that only one of the seven identified by-product reaction pathways produce methane [130].

Table 8: By-products created from hydrogenation on Ni-based catalyst [130]

By-product limit [mol%]	0.5	5	15	25	35
Number of cycles [e]	7	130	404	678	951

As mentioned in **chapter 2.4.3**, the various by-products can have vastly different effects on the mixture properties. Cracking DBT into smaller molecules *generally* yields lower viscosity, which might be beneficial, but also higher vapour pressure resulting in a greater potential for carbon contamination of the hydrogen stream. Wunsch, et.al. (2018, 2020) propose to counter this with either multi-stage dehydrogenation and intermediate hydrogen purification, or by using *palladium-silver* (**PdAg**) membranes in the reactor [145], [146]. The presence of certain by-products also impacts safety. For example, DBT can crack into BT and benzene, both of which are significantly more toxic than the base molecule [12]. The relative hydrogen capacity, however, would not be impacted in this case (only single bonds are broken), assuming that the catalyst and process conditions result in effective hydrogenation and dehydrogenation of the by-products as well.

Hydrogenious have stated that their LOHC systems already provide 300 cycles of use before the DBT must be rejuvenated by distillation, and they have a goal of reaching 1000 cycles [147]. It is unknown how they intend to achieve this and what the corresponding by-product limit may be. Furthermore, their latest presentations indicate a switch to BT, which may be related to longevity issues but is clearly also motivated by higher efficiencies; BT can be dehydrogenated at only 200 °C using a reactive distillation column [148].

[e] 0.33 hours reaction time

2.5 Applications

2.5.1 A summary of fuels and hydrogen carriers

Hydrogen can be used in either fuel cells or heat engines for energy production.

L-H_2 is directly applicable in both cases, whereas ammonia is usually cracked (and DBT dehydrogenated) before the hydrogen gas can be utilised. Ammonia may be used directly in fuel cells and combustion engines as well, as elaborated in **chapter 2.5.4**. The combustion of synthetic fuels is always an option, but the associated release of CO_2 makes carbon neutrality more difficult to achieve. Note the fact that LOHCs are not "used up" like the other fuels, which means that an LOHC power system will contain a nearly constant mass throughout the cycle. **Table 9** compares the most relevant properties of liquid hydrogen, ammonia, methanol and dibenzyltoluene. ISO 8217 *marine gasoil* (**MGO**) [149] is also included because this is *probably* the fuel currently used by MV Rubin[f].

Table 9: Thermophysical properties of select fuels and hydrogen carriers.

Fuel [data sources]	**ISO 8217 RMK-700** [150]	**L-H_2** [27], [63], [151]	**Ammonia** [91], [92], [152]	**Methanol** [117], [122], [153]	**DBT (H0/H18)** [123], [128]
LHV [MJ/kg]	40.077 [g]	120	18.6	20.26	-
Laminar flame velocity [m/s]	N/A	2.91	0.07	0.523	-
Ignition temperature [°C] [h]	60 (Δ)	560 (∇)	630 (∇)	465 (∇)	450 / N/A
Hydrogen capacity [wt%]	-	100	17.8	12.5	6.2
Fuel density [kg/m³] [i]	1010.0	70.8	680	795	1044 / 913.4
Hydrogen density [kg/m³]	-	70.8	121	99.4	56.6
Dynamic viscosity [cP] [i]	707 [j]	0.013	0.25542	0.544	49 / 425 [k]

[f] ISO 8217 RMK-700 is the recommended fuel for the main engine on *MV Rubin*, 9L20, see **chapter 2.6.1**.

[g] Calculated using empirical formula from ISO 8217 (2017) appendix H.

[h] Δ is flash point, ∇ is autoignition temperature. Missing marker means unspecified in source.

[i] At storage conditions, see **chapter 2.1.3**.

[j] Calculated by multiplying kinematic viscosity at 50 °C with the density at 15 °C, assuming the latter is approximately the same at 50 °C.

[k] At 20 °C, increases *significantly* at lower temperatures, see **chapter 2.4.4 - Table 7**

2.5.2 Fuel cells

A fuel cell is used to convert chemical energy into electrical energy. The theoretical process of a fuel cell is the reverse process of the electrolysis prosses described in **chapter 2.1** [27], [154]. A fuel cell is comprised of electrodes separated by an electrolyte, and is categorised as a redox cell [27]. Many different types of electrolyte may be used, though the four most notable technologies (*for hydrogen*) are *alkaline fuel cells* (**AFC**), *polymer electrolyte membrane fuel cells* (**PEMFC**), *high temperature PEMFC* (**HTPEMFC**), and *solid oxide fuel cells* (**SOFC**), all of which are named after its electrolyte and/or operation conditions [27].

Fuel cells are generally divided into two categories: Low- and high temperature fuel cells, operating at below and above 200 °C, respectively (Léon, chapter 5.6) [27]. The theoretical efficiency of a fuel cell is defined by the cell potential (voltage) and the current density (ampere per areal) [154], with the maximum possible efficiency defined as the change in Gibbs free energy divided by the change in enthalpy [2]. In this thesis however, the simpler thermodynamic definition is used, as presented in **equation (3)** …

$$\eta = \frac{E_{out}}{E_{in}} = 1 - \frac{E_{loss}}{E_{in}} \tag{3}$$

…where η is efficiency, E_{out} is the energy delivered by the system, E_{in} is energy added to the system, and E_{loss} is the amount of energy lost due to heat, friction, etc. [155]. Note that energy units may be substituted by power or specific energy. This definition simplifies the preliminary system-wide efficiency calculations [155]. Efficiencies presented in this chapter are all system-wide efficiencies, and not stack efficiencies [2].

Alkaline fuel cells

Alkaline fuel cells are the earliest type of fuel cells, best known for their application in NASAs space shuttles [156]. They usually contain nickel anodes and silver (**Ag**) cathodes (Léon, page 173) [27]. The electrolyte in an AFC is typically an alkaline potassium hydroxide (**KOH**) solution. The chemical cell reaction is presented in **reaction equation** (**xviii**) to (**xx**)…

$$Anode: 2H_2(g) + 4OH^-(aq) \rightarrow 4H_2O(l) + 4e^- \tag{xviii}$$

$$Cathode: O_2(g) + 4e^- + 2H_2O(l) \rightarrow 4OH^-(aq) \tag{xix}$$

$$Overall: O_2(g) + 2H_2(g) \rightarrow 2H_2O(l) \tag{xx}$$

…with a typical electrical efficiency for AFC, $\eta_{AFC,el}$, of about 62-63 %, according to *Institute for Energy Technology* and *Miranda.* An AFC has an operating temperatures around 60-100 °C at ambient pressure [2], [154], [157]. Multiple cells may be stacked using graphite-based bipolar plates (Léon page 175)[27]. A basic illustration of an AFC is presented in **Figure 16**.

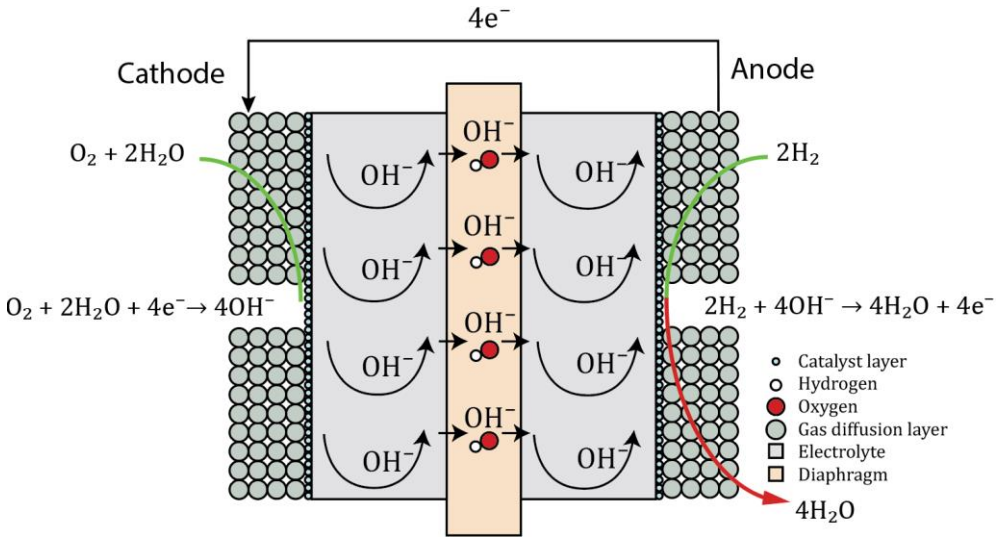

Figure 16: Basic principle of an alkaline fuel cell, inspired by Keçebaş [47]

In order to keep the alkaline fuel cell performing reliably over a long period, it is essential that the oxygen supply is extremely pure, because of the risk of reaction between CO_2 and the electrolyte which will consume the electrolyte [11], [154] as shown in **reaction equation** (**xxi**) and (**xxii**) (Lèon, page 174) [27]**.**

$$CO_2(g) + 2OH^- (aq) \rightarrow CO_3^{2-} (aq) + H_2O (l) \quad \textbf{(xxi)}$$

$$CO_3{}^{2-} (aq) + 2K^- (aq) \rightarrow K_2CO_3 (s) \quad \textbf{(xxii)}$$

In order to keep the alkaline fuel cell performing reliably over a long period, it is essential that the oxygen supply is extremely pure, because of the risk of reaction between CO_2 and the electrolyte which will consume the electrolyte [11], [154]. This could possibly be remedied by combining liquid hydrogen storage with AFC's. By supplying a heat exchanger with extremely cold hydrogen vapour from the liquid hydrogen storage, ambient air can be significantly chilled. Since CO_2 freezes at a much higher temperature than oxygen [69], the CO_2 is easily separated from the air. The cold air is also used to cool the fuel cell, and could effectively reduce the boil-off loss during operation to 0 %, as suggested by *Ahuja* [154], [158]. **Figure 17** is a simplified process diagram of the solution.

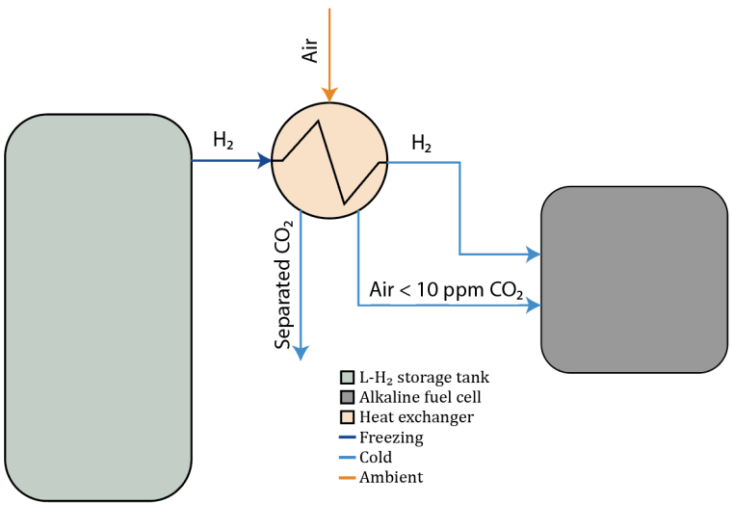

Figure 17: Simplified diagram of an AFC fuelled by liquid hydrogen [131]

Alkaline fuel cells supplied with pure hydrogen are expected to have a operational lifetime of 75 000 hours [157]. However, combined heat and power (CHP) is difficult because of the low operating temperature [159].

Polymer electrolyte membrane fuel cells

PEMFCs are the most common fuel cells today, being applicable in a variety of different operations. They are comprised of platinum-based electrodes and the electrolyte is made of an acidic polymer, typically Nafion [154]. The hydrogen molecules are oxidized at the anode and single hydrogen ions (protons) are transported through water pockets in the polymer membrane, while the electrons are transported through an outer circuit. The oxygen molecules are reduced to oxygen ions at the cathode, and then react with pairs of hydrogen ions, forming water, as presented in **reaction equation** (**xxiii**) through (**xxv**).

$$Anode: 2H_2(g) \rightarrow 4H^+(aq) + 4e^- \quad \textbf{(xxiii)}$$

$$Cathode: O_2(g) + 4e^- + 4H^+(aq) \rightarrow 2H_2O(l) \quad \textbf{(xxiv)}$$

$$Overall: 2H_2(g) + O_2\,(g) \rightarrow 2H_2O(l) \quad \textbf{(xxv)}$$

The membrane electrode assemblies follow the same basic principles as those of PEMEC, described in **chapter 2.1.2**. To remain operable, the electrolyte needs to be hydrated, which in turn limits the operational temperature of PEMFC to about 50 - 80 °C. The typical electrical efficiency, $\eta_{PEMFC,el}$, is about 50-60 %, though some claim it to be as low as 30-55 %, and CHP is difficult because of the low operating temperature [2], [157], [159]. PEMFC can only tolerate hydrogen with less than 20 ppm of CO [27]. PEMFCs are illustrated in **Figure 18**. Specialised kinds of PEMFCs may also operate on methanol. This is known as a direct methanol fuel cell (**DMFC**). They operate at 20 – 90 °C and are considered viable for portable, low power applications [27], [154].

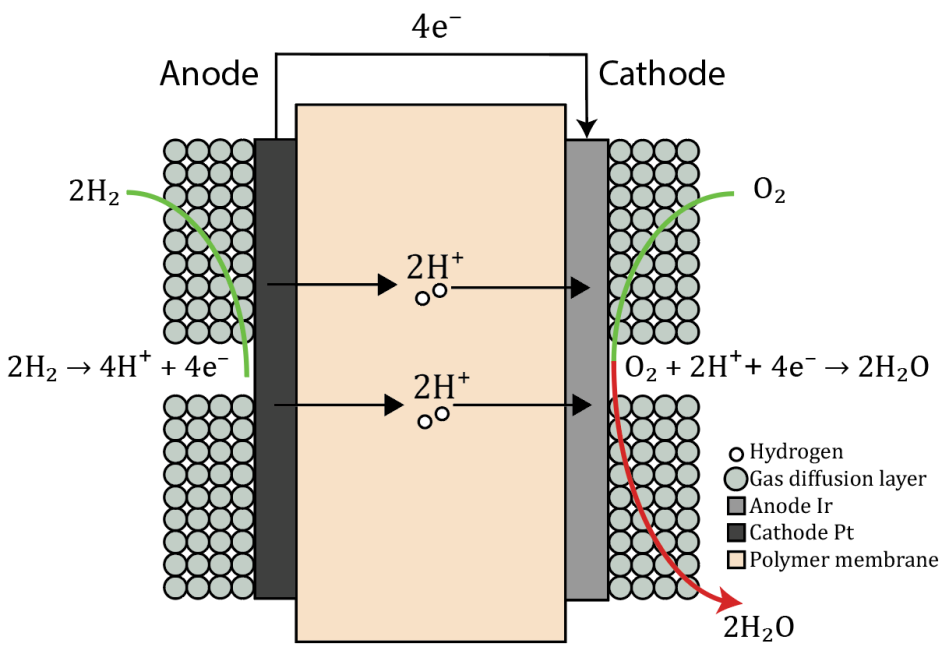

Figure 18: Basic principle of a PEM fuel cell.

Utilising a different polymer-electrolyte, polybenzimidazole (**PBI**) doped with phosphoric acid, increases the temperature tolerance of the electrolyte up to 200 °C. A high temperature polymer electrolyte membrane fuel cell (HTPEMFC) has a lot of the same qualities as a regular PEMFC, but this modification makes it a lot more tolerable to impurities in the fuel; It may even tolerate several percent of CO [27]. The typical electrical efficiency, $\eta_{el,HTPEMFC}$, is 50-60 %, though the higher operating temperature means CHP is possible and the potential degree of utilisation may be higher [159]. Note that the water becomes highly corrosive when mixed phosphoric acid, which is an important factor to consider when designing systems based on HTPEMFC [160]. According to DNV GL, a stationary PEMFC and HTPEMFC has an estimated service lifetime of 60 000 hours, while mobile fuel cells only have 5 000 hours [11]. Note that this is primarily because of membrane wetting caused by operating in short bursts at a time, which is mainly the case for automobiles [161].

Solid oxide fuel cells

SOFC is the second most common fuel cell today and has an even higher operational temperature than HTPEMFC, with the most common forms operating at 600 – 1000 °C [154]. This would be perfectly suited in combination with ammonia cracking and LOHC dehydrogenation, as these processes also require high temperature heat input in order to operate (see **chapters 2.3.3** and **2.4.5**). The high temperature leads to low reaction times, which alleviates the need for costly platinum catalysts. SOFC is also flexible regarding fuels, as the high temperature may reform for example LNG directly in the fuel cell [154], though the main focus in this thesis is the application of hydrogen is SOFC, presented in **reaction equation** (**xxvi**) to (**xxviii**):

$$Anode: 2H_2(g) + 2O^{2-}(aq) \rightarrow 2H_2O(l) + 4e^- \quad \textbf{(xxvi)}$$

$$Cathode: O_2(g) + 4e^- \rightarrow 2O^{2-}(aq) \quad \textbf{(xxvii)}$$

$$Overall: 2H_2(g) + O_2\,(g) \rightarrow 2H_2O(l) \quad \textbf{(xxviii)}$$

In contrast to PEMFC, SOFC transports *oxygen ions* through the ceramic electrolyte, as shown in Figure 19. The electrolyte is made from thin and porous ceramic materials, which increases the difficulty of handling, and in turn the cost of manufacturing. It also complicates the start-up and shutdown procedures [154]. The typical electrical efficiency, $\eta_{SOFC,el}$, is approximately 50-60 % [2], [116], though the potential degree of utilisation, $\eta_{SOFC,ut}$, may be as high as 85 % if used in CHP-designs, because of the high operating temperature [154], [159]. The thermal efficiency, $\eta_{SOFC,th}$, is approximately 30-40 % [116], and lifetime of operation is estimated to be upwards of 90 000 hours [11]. The thermal efficiency, and therefore the heat generated in a SOFC makes it possible to crack the ammonia directly in the cell [162].

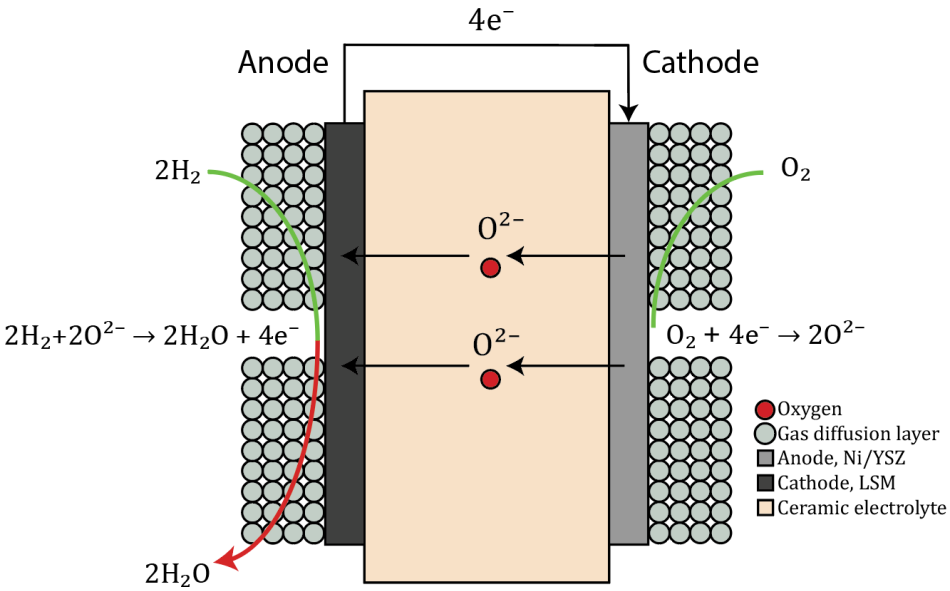

Figure 19: Basic principle of a solid oxide fuel cell.

It should be noted that ammonia fuelled SOFC is associated with some NO_X emission [163], and that air exposed to temperatures above 1200 °C *may* lead to formation of NO_X, known as thermal NO_X [164]–[166].

Summary of fuel cell technologies

Data presented in this chapter is organized and presented in **Table 10** as a comparison of the different fuel cell technologies, with colour coded cells.

Table 10: Comparison of different fuel cell technologies.

Fuel cell type	AFC	PEMFC	HTPEMFC	SOFC
Fuel flexibility	low	low	moderate	high
Sensitivity of impurity	high	high	medium	low
Pure electrical efficiency	high	moderate	moderate	moderate
Degree of utilisation	low	low	moderate	high
Responsiveness	high	high	moderate	low
Electrode cost	low	high	moderate	moderate
Life expectancy	moderate/high	moderate/high	moderate/high	high
Handling and complications	low	low	high	medium

= bad = good = moderate/medium

When considering which technology to choose, the hydrogen carrier determines what properties one should favour. When considering ammonia or LOHC, heat is needed for the cracking/dehydrogenation process, which means that SOFC or HTPEMFC must be considered, as they have a high temperature of operation. One should also consider if the waste heat is usable in other processes. Liquid hydrogen may be converted directly in the fuel cells presented in **Table 10** which means that secondary processes determine whether the waste heat is usable or even necessary to consider.

2.5.3 Electric motors and batteries

When applying fuel cell technology in a vessel, an electromechanical motor is also needed to convert the electrical energy into mechanical energy. This has been done from the time of *Jacobi*'s small boat experiments in the 1830s until today, with the electricity for propulsion being supplied from a generator (typically powered by a diesel engine). The electric motor is coupled to the propeller shaft, either directly or through a single reduction gear if another prime mover (a gas turbine, for example) is involved [167]. Mechanical transmissions (i.e., several interchangeable gears) are usually not required due to the electric motor's instantaneous torque and wide range of possible operating speeds. Efficiencies typically range from 70 to 96 % depending on motor type, duty, etc., with *ABB*'s synchronous *alternating current* (**AC**) motor holding the world record at 99.05 % measured in testing [168], [169]. **Figure 20** shows a family of ABB motors. Speed controllers for both AC and DC motors are also typically over 90% efficient [170], [171].

Figure 20: A variety of motor sizes from ABB [172]. © ABB.

Some of the electrical energy needs to be stored long term in batteries to supply peak loads that the fuel cell is unsuited for (*peak shaving*), thereby contributing to both stable power delivery and increased fuel cell longevity [173]. The *Panasonic "2170"* Lithium-ion cells used in current generation *Tesla* electric vehicles have an energy density of 260 Wh/kg, which is reduced to roughly 150 Wh/kg when packing them into battery modules, but the company aims to reach 400 Wh/kg (per cell) by 2025 [174]. Development trends so far indicate that the volumetric energy density increases more than the gravimetric energy density, but there are also a great number of other factors to consider when selecting and dimensioning batteries, as elaborated in a recent study by DNV-GL [173].

The low energy densities of current batteries are inadequate for powering larger ships, but the Norwegian company *EVOY* is developing electrical systems for smaller boats, both outboard and inboard, including a battery pack of up to 378 kWh and an electric inboard motor with 300 kW continuous and 600 kW peak power, weighing 2725 kg in total [175]. 600 kW is roughly equivalent to 800 horsepower, for those more familiar with piston power metrics.

2.5.4 Heat engines

Heat engines are used to convert chemical energy directly into mechanical energy. Both hydrogen and ammonia can be utilised in heat engines, either separately or in a mixture [176]. Ammonia is not widely used as a combustion fuel today, mainly because of its high auto ignition temperature and relatively low burning velocity [92], [177]. These properties (shown in **Table 9**, **chapter 2.5.1**) lead to difficulties getting ammonia to maintain a proper combustion.

Despite this, a steam engine locomotive running off a simple ammonia burner was constructed in England as early as 1822 [178]. A century later, in 1933, Norsk Hydro rebuilt an *internal combustion engine* (**ICE**) vehicle to run on hydrogen (stored as ammonia, cracked before use), and this very car is shown in **Figure 21** [179]. Hydrogen and ammonia combustion has been slowly but continuously researched over the following decades, generally in response to various fuel crises, with a "renaissance" from the turn of the millennia until today [93].

Figure 21: Early hydrogen-car, with permission from Norsk Industriarbeidermuseum [179].

Piston engines

A piston ICE works by igniting a mixture of air and fuel in a closed cylindrical chamber, where one of the chamber walls is the top of a movable piston. The piston decreases the pressure at first, by increasing the volume of the cylinder, and air is pulled in. When the piston returns the cylinder volume is reduced, the air is compressed, and fuel is injected (the exact timing depends on the engine). The mixture is then ignited, leading to an explosive expansion of the gases, and the piston – which is eccentrically connected to an axle – is pushed back down and rotates said axle. The mixture may be ignited in two different ways (or in combination); Either with a spark plug, or by piston compression to the point where the mixture self-ignites. A crucial parameter is therefore the *compression ratio,* which is the relationship between the maximum and minimum cylinder volume (due to the piston's motion). The entire process can be completed in two or four *strokes* [26], [155], [180]. **Figure 22** illustrates a four-stroke Diesel cycle.

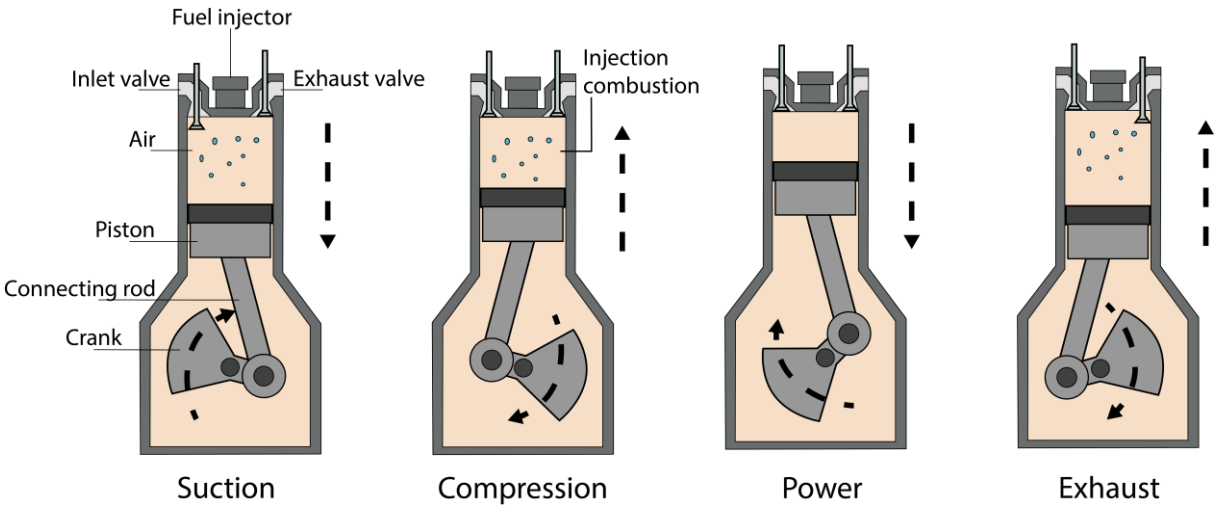

Figure 22: Four stroke Diesel cycle, inspired by Motordynasty.com [181].

In ICEs with compression ignition (ex. Diesel cycle), the combustion properties of ammonia are less of a concern, as the pressure and temperature from the compression is typically sufficient to ignite the fuel. Note that the engine is also preheated using glow plugs. Ammonia fuelled engines have been tested at operational compression ratios from 100:1 down to 35:1. Further reduction may be achieved by co-burning the ammonia with diesel, which results in working compression ratios as low as 15.2:1. This makes it possible to increase power density, but will also increase emissions. Spark ignited engines (ex. Otto cycle) *may* run on ammonia by having a sufficiently powerful spark or multiple spark plugs, but these engines are generally less efficient than compression ignited engines and are therefore not considered further [26], [177], [180]. Note that this need not be an either-or-scenario; For example, *Mazda* has in recent years developed a *spark controlled compression ignition engine* (**SPCCI**) for passenger cars called *Skyactiv-X*, which they claim offers «*[…] the best of both diesel and gasoline engines with none of the disadvantages*» [182]. This includes increased power and torque as well as greater fuel efficiency and lower emissions.

Designing or rebuilding ICEs to run exclusively on ammonia is, however, technically viable regardless of ignition method. Some other important considerations are material choices (for cylinder jackets, gaskets, etc.), and co-ignition or flushing with less corrosive fuels,

both of which contribute significantly to the life expectancy of the engine [177]. Ammonia fuelled ICEs are within range for practical applications, given that the fuel is available. Both MAN and Wärtsilä are developing ammonia engines for maritime use [183]. The MAN model is intended for larger ships, based on a well-tested multifuel- / methanol engine, which is already designed to handle a very corrosive and toxic fuel with low laminar burning velocity [184]. In its original configuration the engine can output between 5350 kW and 82440 kW continuous power. **Figure 23** is an illustration of said engine [185].

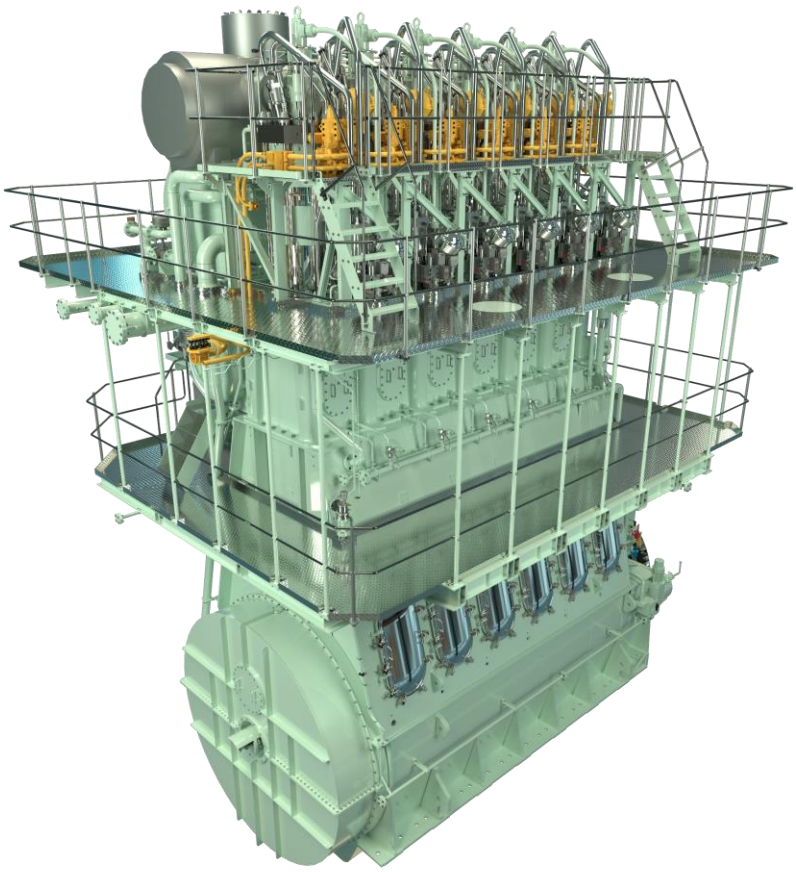

Figure 23: MAN ME-LGIP, the base for the ammonia engine [185]. Yes, those are stairways. © MAN ES

Ammonia combustion ideally follows reaction equation (**xxix**) [92].

$$4NH_3\ (g) + 3O_2\ (g)\ \rightarrow 2N_2\ (g) + 6H_2O\ (l) \qquad \Delta h = -383\ \frac{kJ}{mol} \qquad \textbf{(xxix)}$$

Nitrogen oxides (**NOx**) may also be produced by ammonia combustion, through multiple reaction pathways. However, a remedy may be designed into the cycle, as the fuel itself can also be used to *clean* NOx from exhaust gases, as shown in **reaction equation** (**xxx**) and (**xxxi**) [93]…

$$4NO\ (g) + 4NH_3\ (g) + O_2\ (g) \rightarrow 4N_2\ (g) + 6H_2O\ (l) \qquad \Delta h = -1632.4\ \frac{kJ}{mol} \qquad \textbf{(xxx)}$$

$$6NO_2\ (g) + 8NH_3\ (g) \rightarrow 7N_2\ (g) + 12H_2O\ (l) \qquad \Delta h = -2733.6\ \frac{\mathrm{kJ}}{\mathrm{mol}} \qquad \textbf{(xxxi)}$$

…which describe NO_X reaction by selective catalysis using ammonia as the reducing agent [93]. It should be noted that this can be done both for piston engines and turbines, but it becomes a balancing act, especially in flow machines, because the release of pure ammonia is also undesired [176], [177]. Note that this kind of solution could alleviate some of the complexities of the engine support systems, compared to the same exhaust treatment applied to diesel engines [93].

While ammonia combustion is difficult to sustain because of the low flame speed, etc., *hydrogen* combustion is challenging for precisely the *opposite* reasons: It ignites readily and burns rapidly (see **chapters 2.5.1** and **3.2.5**), creating low flame stability and high NO_X emissions despite being a non-nitrogenous fuel [186]. Pure hydrogen ICEs are being developed by companies like *MAN*, *Wärtsila*, *Mitsubishi* and *Scania* (the latter in cooperation with *Westport Fuel Systems*) [187]–[190]. *BeHydro* launched their multifuel diesel-hydrogen engine in late 2020 and aim to have a monofuel hydrogen engine ready by the second quarter of 2021 [191]. Fewer technical details are available for these engines than for ammonia engines because they are at an earlier stage in development. Previous attempts at H_2 ICEs have burned *premixed* air and fuel, resulting in limited power, intake flashbacks, engine knocking, pre-ignition, etc., which translates to poor efficiency and usability. Co-burning with diesel solves most of these issues but re-introduces carbon emissions. Babayev, et.al. (2021) simulated and tested *non-premixed* direct injection of hydrogen in a compression ignition engine and found that optimisation of this solution requires the opposite strategy to what has been employed in commercial diesel engines since the 70s, i.e., using less injection pressure not more [192]. The hydrogen combustion reaction is the same as for fuel cells, see for example **reaction equation** (**xx**).

Alternatively, co-burning hydrogen and ammonia could also be feasible, as investigated by Wang, et.al. (2021). A 30/70% hydrogen/ammonia mixture will likely improve performance in a marine diesel engine (compared to pure NH_3 combustion) but also increase NO_X emissions which must be dealt with using *exhaust gas recirculation* (**EGR**) and/or catalytic treatment as previously mentioned [193].

Material choices are also vital in the case of burning pure H_2, not because of corrosivity but rather to avoid *hydrogen embrittlement* a.k.a. *hydrogen induced stress cracking* (**HISC**) in the main construction, and also to prevent gas leakages from gaskets [2], [194].

There are multiple ways to calculate the efficiency of an internal combustion engine depending on use case and available data. Most ICE manufacturers include the *specific fuel-oil consumption* (**SFOC**), a.k.a. the *brake specific fuel consumption* (**BSFC**), as well as information about the fuel used to calculate this value. This is necessary because the SFOC/BSFC value changes with fuel composition [195]. The efficiency of the engine is calculated as presented in **(4)**…

$$\eta_{ICE} = \frac{3600}{BSFC \cdot h_n} \quad \textbf{(4)}$$

... where η_{ICE} is the ICE efficiency, *BSFC* is the specific fuel consumption, and h_n is the (specific) LHV, usually denoted in units of kg/kWh and kJ/kg, respectively. With these units the 3600 kJ/kWh conversion factor must also be part of the equation.

Diesel engines are typically categorised as low-, medium- and high-speed engines. Engine speed, BSFC, and efficiencies are presented in **Table 11**.

Table 11: Engine speeds and efficiencies for large maritime ICEs [196]

	Engine speed [rpm]	BSFC [g/kWh]	η_{ICE} [%, h_n=42.7 MJ/kg]
Low speed engines	50 - 300	155 – 175	54.4 – 48.2
Medium speed engines	300 – 1000	175 – 200	48.2 – 42.2
High speed engines	1000 – 3000	195 – 225	43.2 – 37.5

To reduce energy losses in an ICE, the exhaust heat and pressure is commonly utilised in a *turbocharger*, shown in **Figure 24**, which expands the exhaust gases in a radial turbine and creates rotation that is in turn used to drive a radial compressor, increasing intake air pressure. Exhaust (orange) is being pushed out and expanded; Air (blue) is being sucked in and compressed. Benefits include increased performance and reduced emissions [195].

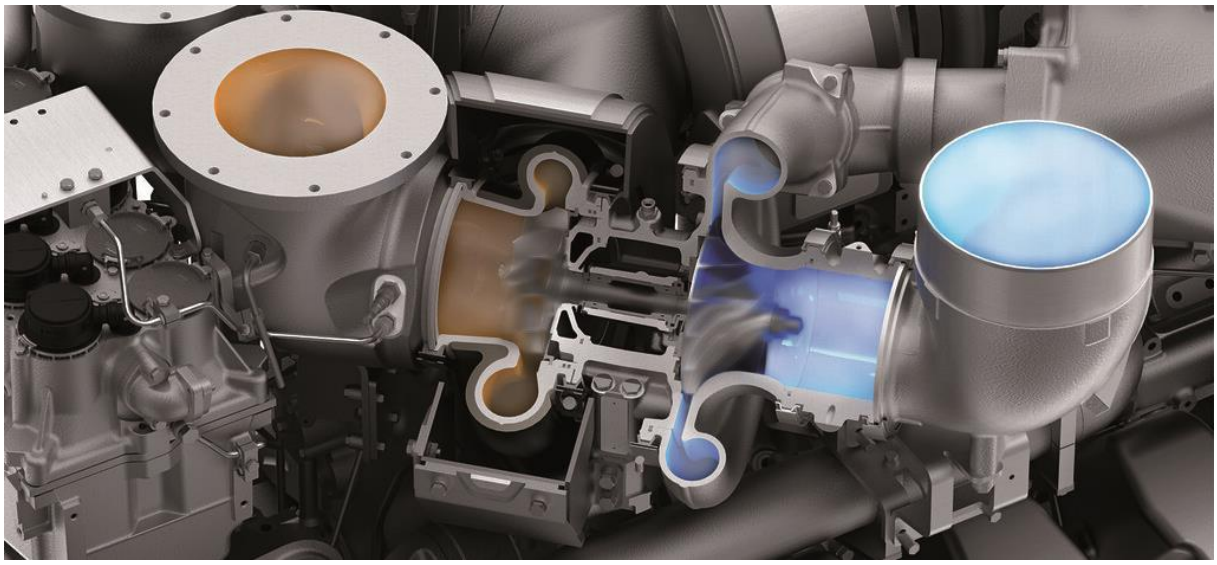

Figure 24: Cutaway illustration of a turbocharger [197]. CC license, © Rolls Royce Power Systems AG.

Gas turbines

Gas turbines are also used as part of maritime propulsion systems, with *Rolls Royce* being one of the major producers supplying for example navy ships the world over [198]. These machines have four main components illustrated in **Figure 25**.

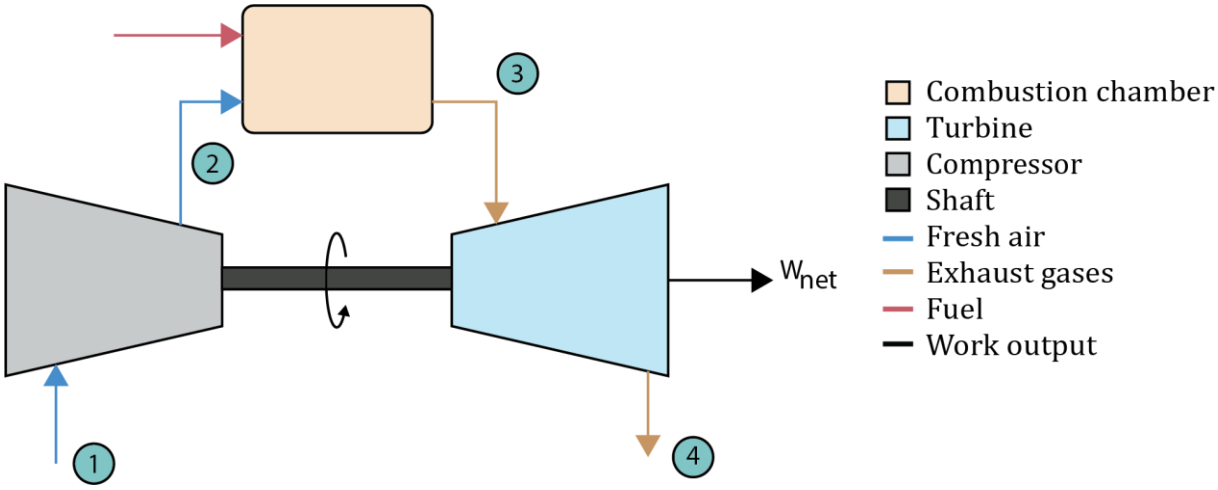

Figure 25: Working principle of a gas turbine [26].

A rotating compressor and a turbine are both connected to the same axle, with a combustion chamber in between. Intake air is compressed by a set of rotating blades which push the air through another set of stationary blades. This usually occurs in multiple stages, which allows the air to cool before being further compressed, reducing the required compression work and increasing efficiency. High-pressure air is then lead into the combustion chamber where fuel is injected, mixed, and ignited. The resulting gas expansion is forced through another set of rotating blades, this time oriented in the opposite direction, extracting mechanical energy from the pressure differential. The blades themselves have profiles similar to aeroplane wings but are in this case applied to generate rotation instead of lift. Part of the harvested energy is used to rotate the intake compressor, either directly through the common axle or indirectly (by electricity) through a generator and a motor in a dual-axle setup [195]. The remaining energy is used for propulsion or electricity generation, depending on the application.

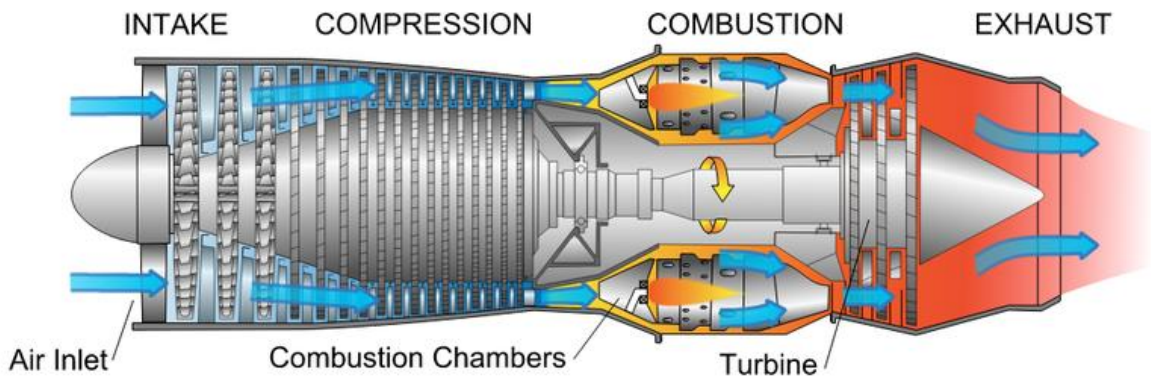

Figure 26: A jet engine, i.e., a gas turbine optimised for exhaust gas pressure [199]. CC license.

When burning ammonia in gas turbines, Kobayashi, et.al (2019) used a special burner, creating spiralling flames that compensate for the slow flame speed. The quicker the flame spirals, the greater the resulting temperature because more of the ammonia is burned before leaving the combustion chamber [92]. Using different gas mixtures yields various results: Ayaz, et.al. (2018) determined that a 20/60 % ammonia/methane blend in a micro gas turbine results in a more environmentally benign process (based on several different sustainability factors) [200]. Valera-Medina et.al. (2019) showed that a 70/30 % ammonia/hydrogen blend creates a stable burn while simultaneously providing enough unburnt ammonia in the exhaust for non-catalytic reduction of NO_X emissions. On the other hand, the efficiency of the turbine in question was significantly reduced compared to its regular methane burning performance [176].

As with piston engines, ammonia and hydrogen burning pose very different problems in gas turbines. Development of pure hydrogen turbines has proven more difficult due to the high flame speed increasing risk of flashback, autoignition and NO_X emissions just like in piston engines [201]. Nevertheless, *Siemens Gas and Power* already have *wet low emissions* (**WLE**) gas turbines that can run on 100 % H_2, and they aim to develop *dry low emissions* (**DLE**) units by 2023 because the water used for WLE steam needs to be pure (to avoid excess wear and tear in the turbine), and clean water is a very precious resource in many parts of the world [202]. Ditaranto, et.al. (2019) also determined that DLE is preferrable when burning high concentrations of hydrogen, despite WLE being more efficient [203].

The efficiency of gas turbines can also be defined in a multitude of ways depending on the chosen cycle, etc. Alternatively, **equation (4)** using the brake specific fuel consumption (*BSFC*) and lower heating value h_n can also be applied to turbines, with typical shaft-efficiencies of 30-40 % and CHP-efficiencies over 60 % [196], [204], [205].

Methanol combustion is also the subject of recent research. It is most suitable for compression ignition engines because of its high auto-ignition temperature. Methanol also produces a lot less soot than traditional fuels because of its relatively low carbon content [206]. However, this technology is not considered further in this thesis.

NO_X and N_2O emissions from combustion

Both nitrogen oxides (NO and NO_2) as well as nitrous oxide (N_2O) negatively affect the ozone layer. The former also contributes to smog and acid rain, while the latter is -in its base form- a potent GHG with a GWP of 265-298 CO_2 equivalents (over 100 years). Combustion can produce these molecules whether the fuel itself contains nitrogen or not. NO_X is generally a product of high temperature combustion, and one strategy to prevent this by-product is to burn lean, premixed air and fuel which results in lower temperatures. However, this may increase N_2O emissions [207], [208]. An alternative strategy is to use EGR, which may be frowned upon due to carbon being deposited in the EGR valve in gasoline / diesel ICEs, but this is assumed to be irrelevant when using ammonia or pure hydrogen as fuel.

Further details about emissions can be found in other parts of the thesis. There is a small note about possible methane emissions from LOHC dehydrogenation towards the end of chapter **2.4.5**, while chapter **3.2.4** describes emissions related to the transport and use of the various hydrogen carriers, and the following chapter (**2.6**) provides more insight into an existing powertrain based on combustion engines.

2.6 Large carrier MV Rubin

By comparing the three hydrogen carriers and their technologies in a case study, a more realistic comparison is hopefully achieved. As mentioned in **chapter 1.3**, Ocean Hyway Cluster wishes the case to cover a medium size vessel, and *MV Rubin* of *Frøy-gruppen* [209], depicted in **Figure 27**, is chosen.

Figure 27: MV Rubin unloading fish food at a fish farm [210].

Constructed by *Crist S.A.* in 2014 [211], MV Rubin is a fish feed carrier and *DNV GL-class* vessel, with a module-based cargo loading system, which makes it possible to transport raw materials during the off-season. Select specifications are presented in **Table 12**:

Table 12: MV Rubin, Technical information [211], [212].

Built	2014
Length overall (LOA)	69,9 m
Beam width	15 m
Draft	6,5 m
Dead weight	3200 t
Class	DNV GL
Bulk capacity	2000 t
Ballast water	1334 m^3
Travers SWL	10 t | crane 2 t
Ballast and cooling system	Closed
Fuel tank	250 m^3

The cargo-modules are loaded using a crane traverse with a safe working load (**SWL**) capacity of 10 tons, whereas the crane alone has a SWL capacity of 2 tons. Featuring

dynamic positioning (**DP**), MS Rubin is capable of remaining stationary when unloading unto fish farms, even "midt-fjords"[1]. The ballast water capacity is 1334 m^3 and the system is closed, to keep contaminated ballast water from being released into the fjords [211]**.** The boat is 70 meters long, has a 15 m beam width, and 6.5 m draft depth. It has a *dead weight tonnage* (**DWT**) of 3200 tons and bulk capacity of 2000 tons [210]**,** as presented in **Table 12.** DWT a measurement of the ships total carrying capacity, including fuel, crew, ballast water etc., excluding the ships own weight [214].

2.6.1 Engines and machinery of *MV Rubin*

As with most bulk carriers of this size, MV Rubin has both a main engine and auxiliary engines. Supplied from Wärtsilä, the main engine is an internal combustion engine that has a maximum power output rated at 1800 kW at 1000 revolutions per minute (**rpm**), combined with a *Stamford* 300 kVA electric shaft generator. The auxiliary power is delivered by two *Baudouin* engines (ICE) at 700 kW with *Leroy Somer* electric generators at 875 kVA each. There are two electric tunnel thrusters, *Brunvoll (FU-63-LTC-1750)* at 500 kW each [211]. The main engine is rated to run on ISO 8217 RMK700 fuel oil [215]. The machinery is presented in **Table 13:**

Table 13: Power output and specific fuel consumption – machinery MV Rubin .

	Power output	**Specific fuel oil consumption or efficiency**
Wärtsila 9L20	1800 kW	190 g/kWh
Leroy Somer LSA 49.1	875 kVA	95,4 %
Baudouin 12M26.2	700 kW	197 g/kWh
Stamford HCM434F	300 kVA	94,1 %

2.6.2 Operating profile and shipping route of *MV Rubin*

With a home port in Tromsø, MV Rubin usually loads fish food at *EWOS*'s factory at Bergneset near Tromsø, with a corresponding shipping route in Nordland, Troms, and Finnmark [212]. However, automatic identification system-data (**AIS**) from *marinetraffic.com* [220] for February 2021, suggests that MV Rubin supplies fish farms along almost the entire western coastline of *Norway*. From Midthordaland in Vestland all the way to Troms and Finnmark as presented in **Figure 28** [221]. During the southern part of the route, MV Rubin docks in Florø.

[1] As Petter Solberg would say it [213].

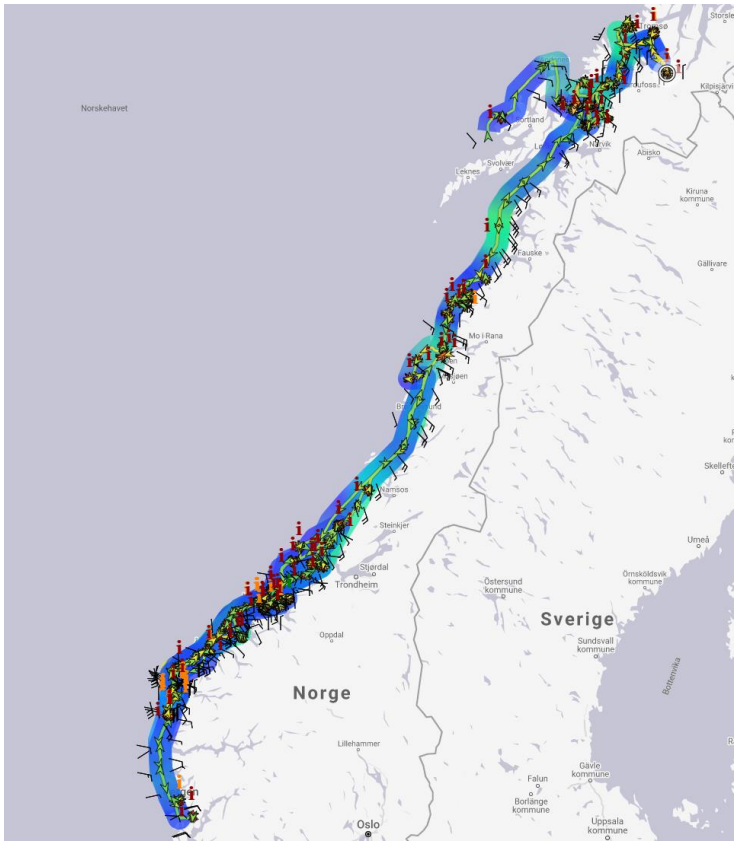

Figure 28: MV Rubin shipping route for February 2021 [221]

The AIS-data is exported to a *comma separated value* (**CSV**)-file, and further analysed in **chapter 3.3.1**. The bride bridge crew of MV Rubin states that the average fuel consumption varies between regular sailing and during loading. The DP-system requires 400 kW on standby in order to remain stationary. During full operation of thrusters and machinery, the power load is 1400 kW, not including the main engine's 1750 kW, presented in **Table 14**, as well as in **Attachment 1**.

Table 14: Operating profile of MV Rubin

	Daily sailing	**(un)loading**
Auxiliary power consumption [kW]	100	400
Utilities daily fuel consumption [m³]	5	7

Further analysis of operation as well as alternative fuel solutions are presented in **chapter 3.3.**

3. Analysis

3.1 Methods

The literature review methodology described in **chapter 2** is continued in this chapter, but with a greater focus on industry experience rather than theoretical background. Furthermore, a case study is conducted, using both first-hand information from the crew aboard MV Rubin and AIS tracking data courtesy of web sites like *myshiptracking.com* and *marinetraffic.com*. The data is analysed both manually and using Python programming.

This thesis is largely based on approximations and assumptions regarding subjects that are still being researched. Incorrect results may be a consequence, but the methodology as described in the following chapters can be re-applied with corrections. The main bulk of the analysis is divided in two: This first part is a general comparison of the selected hydrogen carriers. The second part is a threefold system design for MV Rubin, illustrating technical readiness and more a realistic energy comparison.

3.2 Comparison of hydrogen carriers and their supply chains

3.2.1 Energy densities including storage tanks

Although this thesis compares liquid hydrogen, ammonia, and dibenzyltoluene, it is beneficial to put said comparison into perspective by including other fuels. MGO (ISO 8217) is chosen because it is likely the fuel used in MV Rubin, and LNG is chosen because many consider it an adequate compromise between traditional fossil fuels and renewable fuels, in regards to emissions [222]. Although LNG produced from fossil sources is a fossil fuel - by definition. All of these are presented in **Figure 29**.

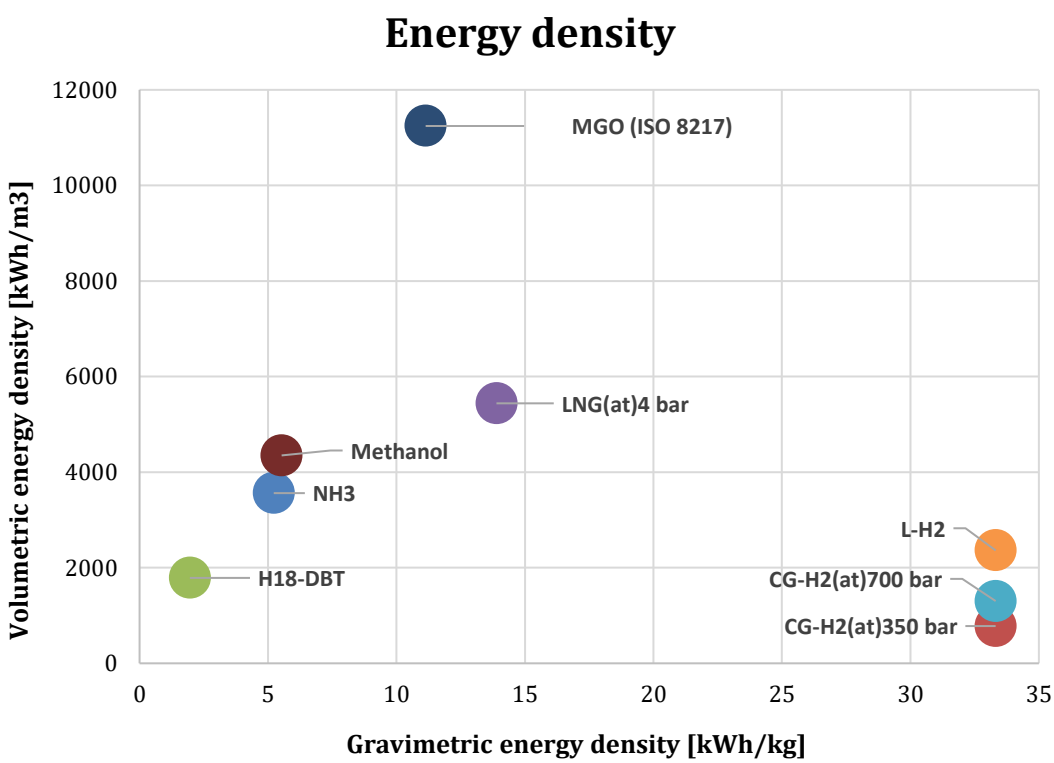

Figure 29: Comparison of energy densities of different fuels.

The energy densities for L-H_2, NH_3, and DBT are all presented in prior **chapters 2.2**, **2.3**, **2.4**, and **2.5.1**. LNG and CG-H_2 (at 350 and 700 bar) are sourced from Léon, table 6.1 [27], and the energy content of this specific MGO is calculated in **chapter 3.3.2**. All calculations are presented in **Attachment 1** as well. Battery technology is not considered, as gravimetric energy densities in the sub-kWh/kg range are unsuited for medium-to-long distance voyages, as mentioned in **chapter 2.5.3**.

One of the biggest challenges when transitioning to renewable fuels is the energy density. MGO has 3, 5, and 6 times the *volumetric* energy density than that of NH_3, L-H_2, and DBT, respectively. Similarly, the *gravimetric* energy density of MGO is *twice* that of NH3 and 6 times that of DBT. This is not necessarily a problem, as the weight of the fuel is only a small part of a what a ship can carry. This is particularly true for large seagoing vessels where the fuel only takes up 1-2 % of the ships loading capacity [22]. The volume requirement is more difficult to overcome, however, and may potentially lead to more frequent bunkering and shorter voyages. It is important to keep in mind that the efficiency of fuel cells generally is 20 to 25 percent point higher than that of ICE, as presented in **chapter 2.5.2** and **2.5.4**.

The storage systems for the three fuels considered in this thesis are all defined by storage conditions in chapters **2.2.3**, **2.3.2**, and **2.4.5**, and it is therefore possible to define a simple, generalised storage solution for all three hydrogen carrier solutions, where the added mass and volume is calculated into the energy densities.

According to *SUSI Partners*, as well as *CNHi Industrial*, the volumetric energy density of liquid hydrogen is approximately 1200 kWh/m^3 including the added volume of a tank, *SUSI* also reports that the added mass of the tank corresponds to a gravimetric energy density L-H_2 of about 2 kWh/kg [78]. Furthermore, they estimate that the specific gravimetric and volumetric energy densities of ammonia including storage tanks are 3.4 kWh/kg and 2300 kWh/m^3, respectively [78].

DBT, on the other hand, does not require specially constructed, heavy tanks, as it is non-toxic, non-explosive, and is stored at ambient conditions. One can argue that the added mass (and volume) for DBT storage is negligible, as the existing fuel tanks on any given MGO or MDO powered ship may be repurposed into H18-DBT-tanks, which significantly lowers the cost of installation as well. Determining the actual decreased volumetric- and gravimetric energy density is not possible as, at the time of writing this thesis, there are no details available of DBT systems in use. However, the added mass and volume may simply be estimated by using the governing standard for double jacketed fuel oil storage tanks, EN-12285, as presented on engineeringtoolbox.com [223]. Using the largest of the tanks, the volumetric energy density for H18-DBT including storage is calculated using the following **equation (5)** …

$$u_{H18-DBT+tank} = \frac{\left(\rho_{H18-DBT} * V_{tank,inner} * h_{H18-DBT}\right)}{V_{tank,outer}} \quad \textbf{(5)}$$

…where $u_{\mathrm{H18-DBT}+tank}$ is the total volumetric energy density, including the tank, $\rho_{\mathrm{H18-DBT}}$ is the density of H18-DBT, $V_{tank,inner}$ is inner volume of the tank, $V_{tank,outer}$ is the outer volume of the tank, and $h_{\mathrm{H18-DBT}}$ is the gravimetric energy density of H18-DBT. This yields a total volumetric energy density of 1714 kWh/m^3.

The gravimetric energy density including storage is calculated by the following **equation (6)** ...

$$h_{H18-DBT+tank} = \frac{\left(u_{H18-DBT+tank} * V_{tank,outer}\right)}{\rho_{H18-DBT} * V_{tank,inner} + m_{tank}} \quad \textbf{(6)}$$

...where $h_{\mathrm{H18-DBT}+tank}$ is the total gravimetric energy density, including the tank, m_{tank} is the mass of the tank. This yields a total gravimetric energy density of 1.71 kWh/kg.

The full calculations are available in **Attachment 1**, and the results are presented in **Figure 30**.

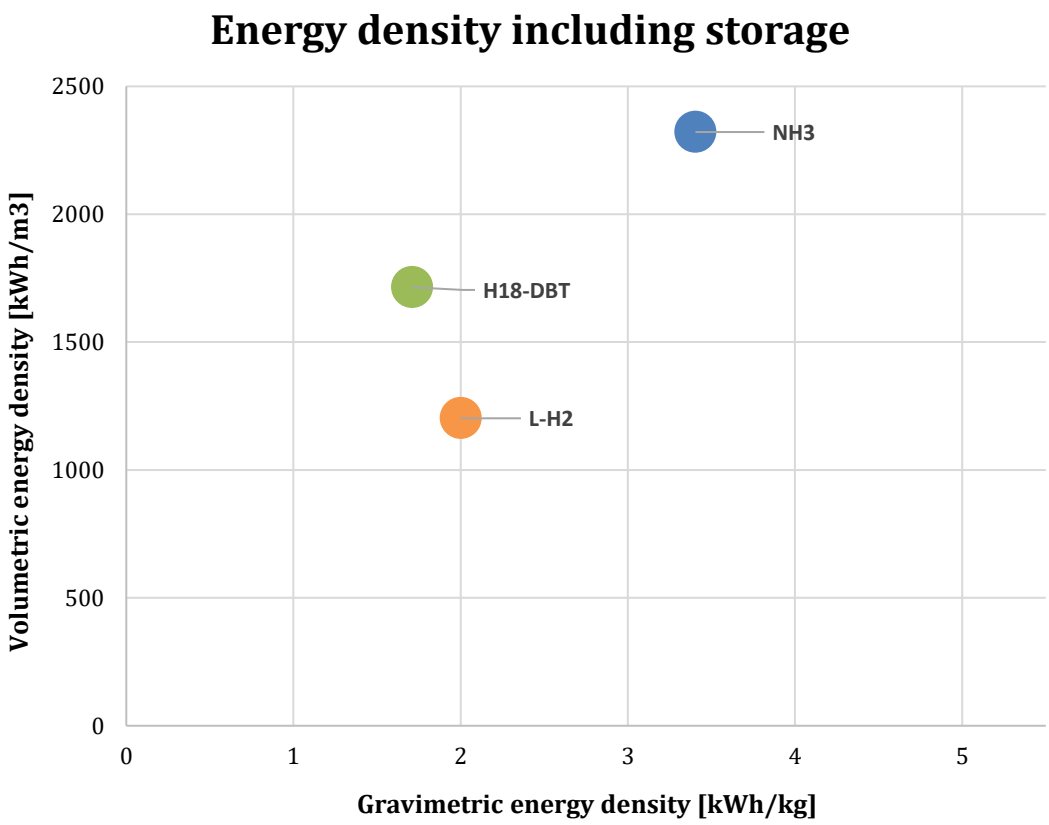

Figure 30: Comparison of energy densities of different fuels, including storage.

While the gravimetric energy density of liquid hydrogen has decreased with a factor of 16, ammonia and dibenzyltoluene have barely decreased by a factor of 1.6 and 1.2, respectively. The volumetric energy densities of L-H_2 and NH_3 are almost halved, while DBT remains *almost* unchanged. This is, as stated earlier, a product of the fact that L-H_2 and NH_3 both have complex, heavy storage solutions, because of the challenges associated with handling fluids at such low temperatures and also because of the L-H_2's explosivity and NH_3's toxicity.

A summary of the densities and storage conditions is presented in **Table 15**:

Table 15: Comparison of hydrogen storage solutions [27], [34].

Fuel	L-H2	Ammonia	DBT
Storage temperature [°C][m]	-253	-33.4	> 15
Storage pressure [bar][m]	1 – 10	1 - 10	Ambient
Volumetric energy density [kWh/m3]	2360	3540	1800
Volumetric energy density – including storage system [kWh/m3]	1200	2320	1710
Gravimetric energy density [kWh/kg]	33.3	5.2	2
Gravimetric energy density – including storage system [kWh/kg]	2	3.4	1.7

3.2.2 Supply chain efficiencies

The efficiencies of green hydrogen production methods are presented in chapter **2.1.2**, and the average efficiency of 60% is used as a baseline. The processing efficiency of each hydrogen technology is presented in their respective chapters (**2.2**, **2.3**, **2.4**). To complete the picture and present supply chain efficiencies, a set of assumptions need to be made:

First, a reference amount of hydrogen must be determined. The technical challenges associated with L-H_2 transport, as well as the limited number of available options, makes this carrier the limiting factor. The Linde HYLICS liquid hydrogen container can hold 3 tons of hydrogen [81]. This container can be hauled by a medium size truck using approximately 5 litres of diesel per 10 kilometres, roughly equivalent to 5 kWh/km in fuel consumption [224], [225]. Data from **Table 15**, along with hydrogen densities from **Table 9** (**chapter 2.5.1**), is used to calculate volumes and weights of each carrier for the 3 ton hydrogen scenario. This is summarised in **Table 16**.

Table 16: Truck requirements for transporting 3 tons of hydrogen.

Truck requirements	L-H_2	NH_3	DBT
Storage volume [m^3]	42.4	24.8	53
Storage weight [tons]	50	29.4	58.8

The heaviest load is *not* within the EU limit for net weight of a truck and trailer combo which is 60 tons *including* the truck [226]. (As of January 2020, these combinations are also allowed in Norway [227]). For simplicity's sake, it is assumed that overload

[m] Storage conditions defined in **Chapter 2**.

dispensation is given for the DBT scenario, and that the same tractor unit is used in each case, weighing approximately 12 tons (estimated by checking several models on finn.no).

Second, a distinction between the different cargo weights needs to be made. The estimate given in *Klimakur 2030* (appendix 3, page 631) regarding energy requirements for trucking provides the same average fuel consumption for medium and long distance transport [224]. Therefore, the L-H_2 scenario is chosen as reference and the *somewhat unrealistic* assumption is made that transport energy requirements scale linearly with mass, all other things being equal. Including the tractor unit weight this results in a relative transport energy factor of 0.67 for ammonia and 1.14 for DBT. The return trip is also included for every carrier, with corresponding transport energy factors adjusted to the lower mass.

Third, a reference distance must be determined. Although the road travelled from Mongstad (where an upcoming liquefaction plant will be located) to Florø's Fjord Base is less than 200 km, it is assumed that distribution with *at least* five times this range is desired. This is certainly no problem for diesel trucks, with high energy density fuel and an abundance of filling stations. However, if a zero-emissions supply chain is desired, then a hydrogen electric truck would be required. Nikola Motor estimates that their model Two truck running on compressed hydrogen will have a range of more than 1200 km [228], which is sufficient if fuel is available along the maximum 1000 km route. Alternatively, the truck could theoretically be refuelled from its own cargo. Using a hydrogen truck, and supplying the hydrogen production with renewable energy, would result in a completely emissions free supply chain. However, for this comparison, transport by diesel truck is chosen.

Fourth, a range of efficiencies are usually available for different systems. The lower values, or reasonable averages, are consistently used in order to prevent unrealistic results. Energy demand for cracking of NH_3 and dehydrogenation of DBT assumes that no waste heat from the fuel cell is utilised, which means that all the required thermal energy is supplied directly from the hydrogen by burning it. The waste heat from hydrogenation of DBT also remains unused. In both cases the actual efficiency depends on system integration, which is detailed in chapters **3.3.3**, **3.3.4**, and **3.3.5**.

It is also assumed that the hydrogen is delivered to the end user at an average speed of 70 km/h, resulting in 14.3 hours of driving time. The rules for truck driver resting times in Norway are somewhat complicated, but a 45 minute break is added for every 4.5 hours of driving time [229]. This will affect the total boil-off. A 0.5 vol% loss per day is expected for L-H_2 tanks of these dimensions [230].

Finally, 5 % of the energy content is lost when unloading the liquid hydrogen, unless systems are in place to recompress the resulting hydrogen gas [230]. Only one unloading is required in this scenario. Furthermore, it is assumed that the DBT is kept at a temperature above 15 °C to avoid excess pumping energy requirements. Transfer losses for DBT are therefore considered negligible, and the same goes for NH_3 [107].

In general, the efficiencies are used to calculate energy requirements by either **equation (7)** or **(8)** (both based on **equation (3)**), where the former is applied with pure electrical efficiencies (like in the case of electrolysis or liquefaction) and the latter is applied with combined efficiencies. This is because the Haber-Bosch process and the LOHC

hydrogenation process both utilise some of the chemical energy of the hydrogen in addition to the required electricity. The equations are defined as…

$$E_{in,1} = \frac{E_{H_2}}{\eta_1} \tag{7}$$

$$E_{in,2} = \frac{E_{H_2}}{\eta_2} - E_{H_2} \tag{8}$$

…where E_{in} is the electrical energy demand, E_{H_2} is the hydrogen's energy content, and η is the process efficiency. Finally, an average fuel cell efficiency of 50 % is used, see **chapter 2.5.2**. **Figure 31**, **Figure 32**, and **Figure 33** are the resulting Sankey diagrams of the L-H_2, NH_3 and DBT supply chains, respectively.

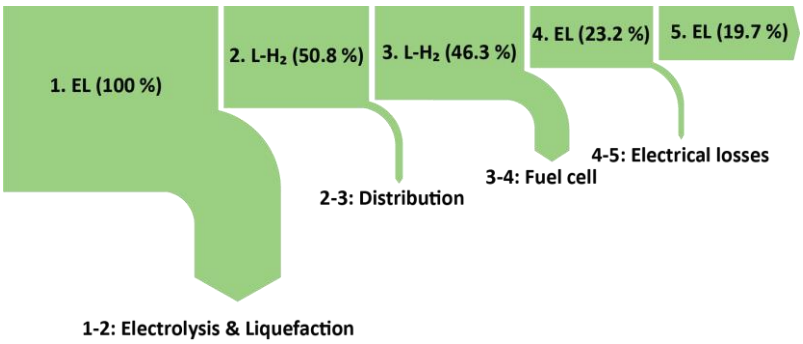

Figure 31: Sankey diagram of liquid hydrogen supply chain.

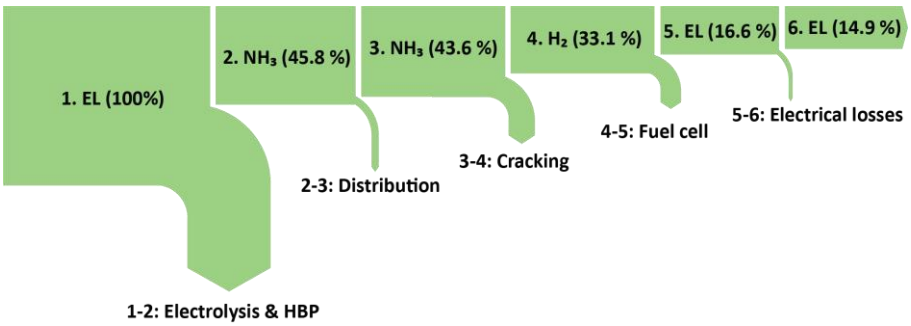

Figure 32: Sankey diagram of ammonia supply chain.

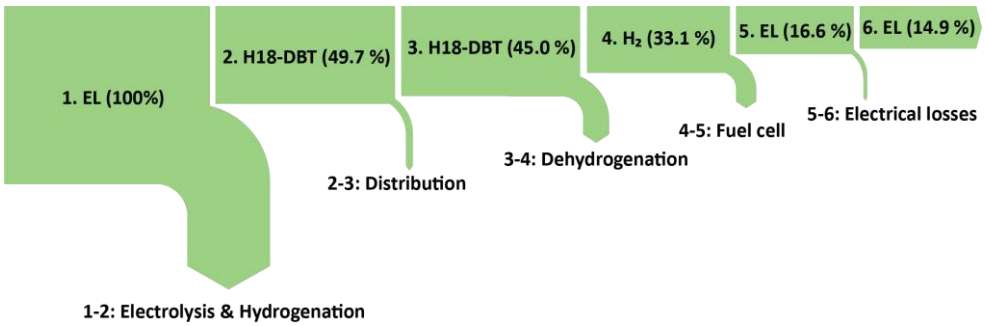

Figure 33: Sankey diagram of dibenzyltoluene supply chain.

The foundation of these energy flow diagrams is found in **Attachment 1**. An estimated water to water efficiency, η_{WtW}, of 20 % is achieved for liquid hydrogen, and 15 % for ammonia and dibenzyltoluene.

3 tons of H_2 is transported 1000 km by diesel truck, a journey taking almost 17 hours (including mandatory driver breaks) at an average speed of 70 km/h. The liquid hydrogen supply yields the most available energy after power conversion, followed by ammonia and then dibenzyltoluene. However, the NH_3 supply *requires* the most energy, followed by DBT and finally L-H_2.

Although liquefaction is a highly energy intensive process, the L-H_2 supply gains efficiency by not requiring energy for a second reforming stage, unlike the other two carriers which have to be cracked or dehydrogenated. Efficiency can be regained by cracking NH_3 inside the fuel cell (see chapter **3.3.4**), and by using waste heat for the dehydrogenation of DBT (see chapter **3.3.5**).

Transport losses are greatest for L-H_2 (including the 5% transfer loss), but the total boil-off at this distance becomes a negligible 0.35 %. The return trip is also included, which impacts L-H_2 and DBT more than NH_3, but all three technologies still have a distribution efficiency of more than 90% at this range. A summary of all the supply chains, with corresponding values, is found in **Figure 34**:

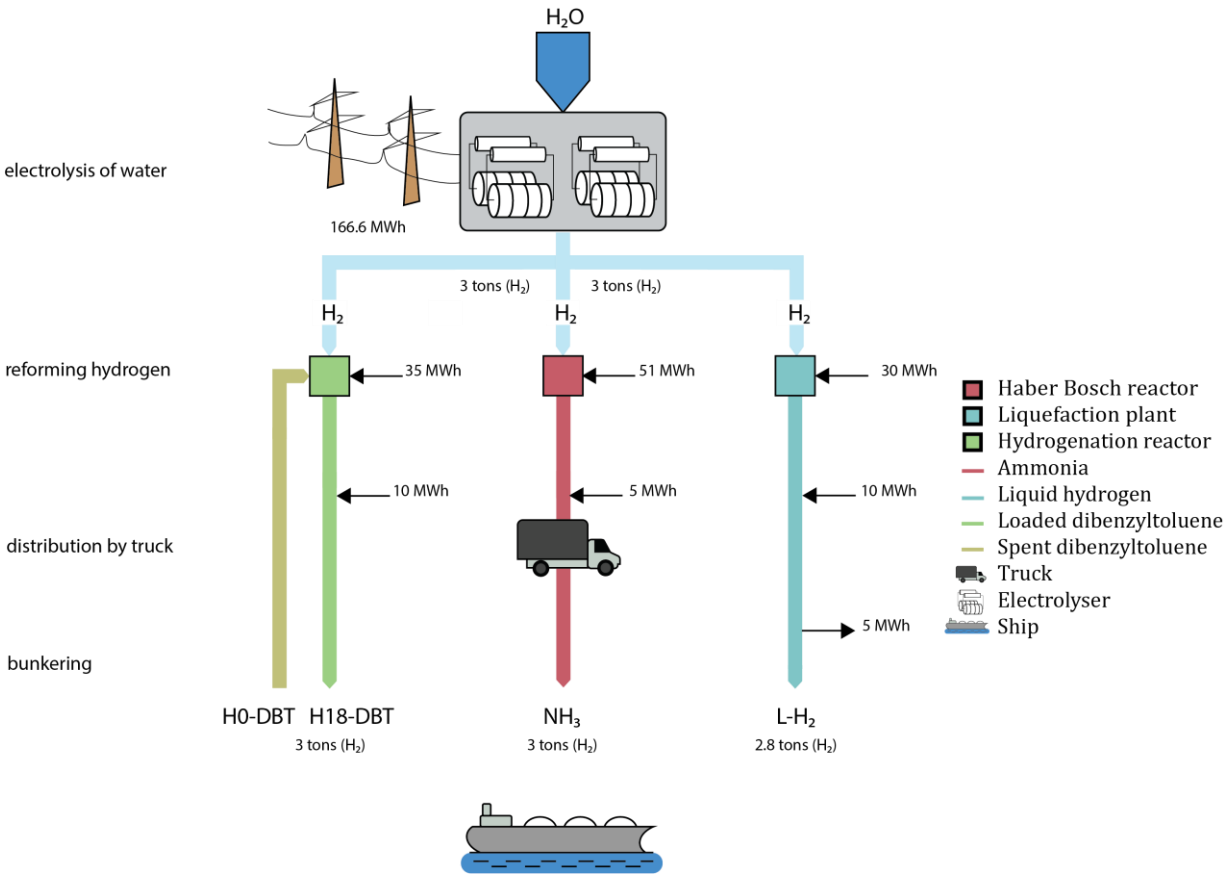

Figure 34: Generalised supply chains of liquid hydrogen, ammonia and dibenzyltoluene.

Note that the boil-off of L-H_2 leads to less hydrogen delivered. Furthermore, H0-DBT and H18-DBT is unloaded and loaded dibenzyltoluene, respectively.

3.2.3 Cost of fuels

Even though a *life cycle analysis* (**LCA**) is not conducted in this thesis, a rough cost analysis is included in order to put the comparison into perspective.

The synthesis report conducted by DNV GL [11] is the baseline, as it analyses multiple studies and reports. Additionally, *The Blue Move* (2017)[31] and the confidential *HyInfra B.0* (2020) report from Ocean Hyway Clusters' members area [34], are utilised for comparison of the capital expenditure (**CAPEX**) estimates of electrolysers. The cost of pure hydrogen is first calculated, and each hydrogen carrier is presented subsequently.

Alkaline electrolysers have a CAPEX of 740 – 1300 €/kW according to *IEA* [231], while *E4Tech* estimates that it will reduce from 2014's 1000 – 1200 €/kW to 370 – 800 €/kW by 2030 [232]. The Blue Move estimates a 1000 – 1200 €/kW CAPEX in 2017, and that it will likely reach 600 €/kW in the following 5-10 year [31]. HyInfra, on the other hand, has received multiple estimates from manufacturers and calculated an average based on the source information, which is currently 750 €/kW and 390 €/kW by 2030 [34]. Summarised in **Table 17.**

Table 17: CAPEX for AEC from multiple analysis

Report	Blue	HyInfra	Shell	IEA	E4Tech	Average
€/kW	1000 – 1200	750	1000 – 1200	740 – 1300	1000 – 1200	900 – 1100
€/kW (2030)	600	390	–	–	370 – 800	680 – 930

E4Tech estimates that the CAPEX of PEM to reach 250 – 1270 €/kW by 2030, compared to the 1900-2300 €/kW of 2014 [232]. *IEA's* estimates 740 – 1300 €/kW [231]. Furthermore, Shell reports that the Norwegian manufacturer NEL claimed, in 2017, to be able to deliver PEM electrolysers at a price of 850 €/kW, and that the price likely should reach 600 €/kW in 2020 and 350 €/kW by 2030 [7]. Blue Move estimates a CAPEX of 1900 – 2100 €/kW, and 760 €/kW by 2030 [31], while HyInfra estimates 1020 €/kW and 758 €/kW by 2030, for comparison [34]. This is all summarised in **Table 18**.

Table 18: CAPEX for PEMEC from multiple analysis

Report	Blue	HyInfra	Shell	IEA	E4Tech	NEL	Average
€/kW	1900 – 2100	1020	3000 - 4000	740 – 1300	1900 – 2300	850	1570 – 2310
€/kW (2030)	760	758	–	–	250 – 1270	350	530 – 780

No estimates are available for current prices of SOECs, which is unsurprising as they are not yet commercialised. Blue Move estimates the CAPEX to be 1500 €/kW [31], while estimates from HyInfra is 760 €/kW [34], both by 2030. This is summarised in **Table 19**.

Table 19: CAPEX for SOEC from multiple analysis

Report	Blue	HyInfra	Average
€/kW	-	-	-
€/kW (2030)	1500	760	1130

Shell estimates that alkaline electrolysers have a lifetime of 60 – 90 thousand hours, and that PEM electrolysers have a lifetime of 20 – 60 thousand hours [7]. Estimates from *Fraunhofer-Institut* estimates 65 – 100 thousand and 30 – 85 thousand hours for AEC and PEMEC, respectively [233]. Fraunhofer-Institut also estimates that the operational expenditure (**OPEX**) for AEC is 13 – 32 €/kW and PEMEC is 6 – 10 €/kW.

Following the example presented by DNV GL [11], it is assumed that the cost of electricity in Norway remains unchanged for corporate customers, and also that electrolysis remains exempt of the electricity fee [11]. NVE estimates that the cost of electricity is 0.32 NOK/kWh (0.032 €/kWh [234]), though may increase to 0.34 NOK/kWh (0.034 €/kWh [234]) by 2030 [235]. According to the example from DNV GL [11], a large production scale translates to a lower hydrogen price, especially if the plant can qualify for the "disconnectable tariff" [236] for corporate customers with installations in the several MW-range, as this will lead to a electricity-network-fee estimated to be as low as 0.02 NOK/kWh (0.002 €/kWh [234]) and a 20 % estimated increase by 2030.

The production scale is based on the annual energy need of a set number of *MV Rubin*-equivalents, assuming that the operating time for the machinery is 8000 hours, and that the efficiency of a hypothetical fuel cell is 50 %, as was done in **chapter 3.2.2**. The voyage described in **Chapter 3.3** is set as the basis for the calculations, presented in **equation (9)** ...

$$m_{H_2,annual} = \frac{\frac{E_{Florø-Tromsø}}{t_{Florø-Tromsø}} * t_{operatingtime}}{h_{n,H_2} * \eta_{fuelcell,general}} * n \qquad \textbf{(9)}$$

... where $m_{H_2,annual}$ is the annual hydrogen production, $E_{Florø-Tromsø}$ is the work done on the voyage, $t_{Florø-Tromsø}$ is the total time spent on the voyage, $t_{operatingtime}$ is the operating time of the machinery, h_{n,H_2} is the gravimetric energy density of hydrogen, $\eta_{fuelcell,general}$ is the efficiency of a hypothetical fuel cell, and n is the number of *MV Rubin*-equivalents, for reference set to 5. This equates to an annual hydrogen production of almost 2800 tons hydrogen.

Utilising the efficiencies presented in **chapter 2.1.2**, assuming the operating time of the plant is 8000 hours equates to a 11.5 MW installation, assuming a discount rate at 4 % and a down payment of 10 years, the annual expenditure is calculated using **equation (10)**...

$$Cost_{annual} = D_v + I_0 * \left(\frac{f * (1+f)^n}{(1+f)^n - 1}\right) \quad \textbf{(10)}$$

... where $Cost_{annual}$ is the annual expenditure, D_v is the total annual OPEX, I_0 is the capital investment, f is the discount rate/100, and n is the total amount of years. The specific cost of hydrogen is calculated by dividing the annual expenditure by the amount of hydrogen produced. Calculations are performed in **Attachment 1**, and the results are presented in **Figure 35**.

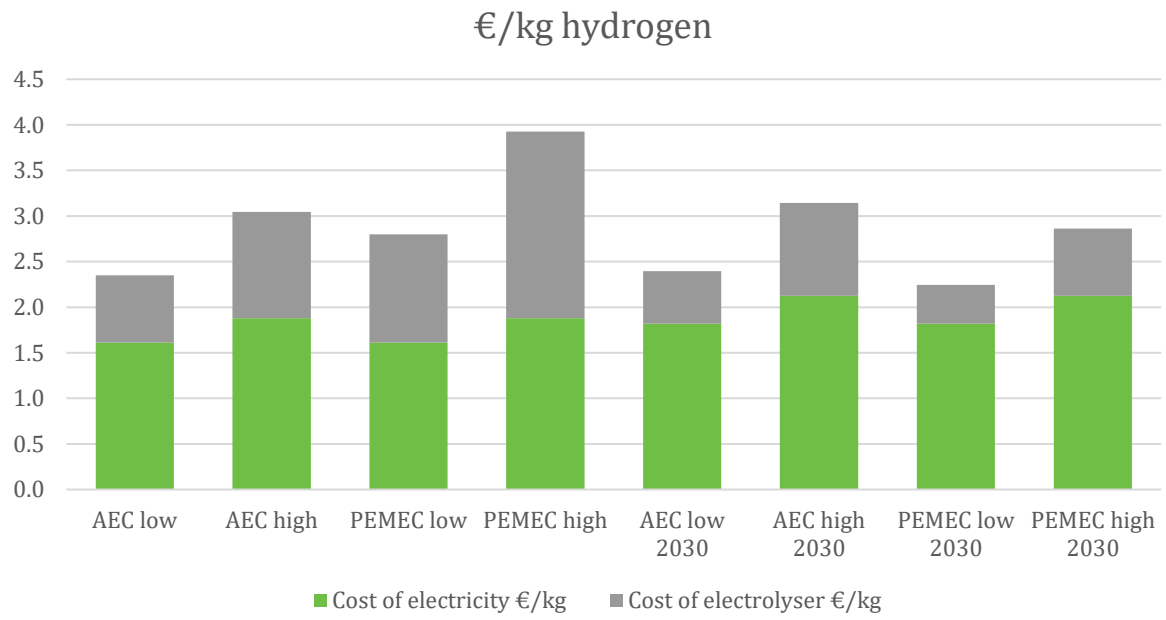

Figure 35: Estimated cost of green hydrogen produced in Norway.

The "low" estimates represent the lowest investment cost and highest efficiencies, and "high" estimates represent the highest investment cost and lowest efficiencies, which corresponds with estimates from *DNV GL* (2019) [11].

Alkaline electrolysers are currently more cost efficient, although this is likely to change within the next 10 years. SOEC is not included on account of no *reliable* OPEX data available. It is important to note that these estimates are based on average values from multiple sources, some of which may even be guesswork.

Based on these estimates, AEC-produced hydrogen will likely increase in specific price, as the estimated price-increase for electricity is greater than the estimated efficiency increase and CAPEX decrease by 2030, while PEMEC CAPEX decreases to such a degree it likely will become more affordable than AEC.

The cost of green, renewable hydrogen is in other words between 2.4 to 4 €/kg and will likely reach 2.3 to 3.2 €/kg by 2030. *IEA* states that hydrogen from natural gas costs 0.7 to 1.6 €/kg without CCS and 1.2 to 2.1 with CCS, and estimates indicate the cost by 2060 to be 2.2 to 2.5 €/kg, and 1.2 to 2.1 €/kg with and without CCS, respectively [237], though these estimates do not include carbon taxing.

Liquid hydrogen

The extreme variance in both CAPEX and OPEX makes it impossible to calculate a general cost for liquefaction plants, as stated by *Maritime Cleantech* [65]. By utilising the forecasted price of *Hyon* which is planned to produce hydrogen in the same scale as this example, a rough estimation can be done in order to calculate the added cost of liquefaction [65]. The Hyon project is forecasted to have an initial investment cost of approximately 90 million $ and a production scale of 15 tons per day, which corresponds to a CAPEX of 16.4 $/kg or 13.6 €/kg [65]. While the OPEX for service and maintenance has proven difficult to acquire, the OPEX for electricity is added, assuming a Claude cycle, as described in **chapter 2.2.1**, which corresponds to an electricity consumption of approximately 30 % of the energy stored in hydrogen, equating to a thermodynamic efficiency of 77 %. Utilising **equation (10)**, the added cost of liquefaction is estimated to be approximately 2 €/kg hydrogen produced, which is somewhat higher than estimates conducted by *the Commonwealth Scientific and Industrial Research Organisation* (**CSIRO**) at 1.54 €/kg [238].

Ammonia

According to *Rivarolo et al.* (2019) the cost of ammonia plants is 2875 €/kW for low capacity (less than 200 ton/day) production [239]. OPEX associated with service and maintenance has proven difficult for HBP as well and is therefore neglected. The power installed is calculated through **equation (11)**…

$$P_{installed,HPB} = \frac{m_{H_2,annual} * h_{n,H_2}}{t_{operatingtime}} * (1 - \eta_{HBP}) \quad \textbf{(11)}$$

… where $P_{installed,HPB}$ is the installed power rating, and η_{HBP} is the typical efficiency for a Haber-Bosch-plant, presented in **chapter 2.3.1**, which equates to approximately 3900 kW. Utilising **equation (10)**, the added cost of ammonia synthesises is estimated to be approximately 139 €/ton_{NH_3} which equates to 0.89 €/kg_{H_2} of hydrogen. Compared to *IOPs* claims that Haber-Bosch plants produces ammonia at 160 $/ ton_{NH_3}, or 132 €/ ton_{NH_3}, even though the market price is approximately 600 $/$ton_{NH_3}$ [240], [241].

DBT

Prices for hydrogenation are scarce and what little is available is difficult to verify. The techno-economic analysis by Eypasch et. al. (2017) [138] includes a polynomial for calculating the installation cost of a hydrogenation plant as presented in the following **equation (12)**…

$$Cost_{hyd,total} = 2840.81 * P_{hyd,max}^{-0.434} \quad \textbf{(12)}$$

…where $Cost_{hyd,total}$ is the CAPEX of reactor and supporting system and $P_{hyd,max}$ is the maximum power rating of the unit. The power rating is calculated utilising **equation (13)** …

$$P_{hyd,max,} = \frac{m_{H_2,annual} * h_{n,H_2}}{t_{operatingtime}} * (1 - \eta_{hyd}) \quad \textbf{(13)}$$

...where η_{hyd} is the efficiency of hydrogenation described in **chapter 2.4.5**. This equates to a specific installation cost of 154 €/kW and a power rating of 3.1 MW. Additionally, *Eypasch et. al.* estimates the unit price of DBT to be 4 €/kg and assumes that each batch can stay in rotation for 300 cycles, as described in **chapter 2.4.5**. Utilising **equation (10)**, the added cost for DBT is approximately 2.33 €/kg_{H_2}.

Toluene and summary

One alternative to DBT is the similar LOHC toluene, currently employed in a supply chain between Brunei and Japan [242]. By applying the same method as with DBT, but with the unit cost of 0.3 €/kg, the added cost of toluene is approximately 1.1 €/kg_{H_2} [137].

Figure 36 represents a comparison of the added cost for all the aforementioned hydrogen carriers.

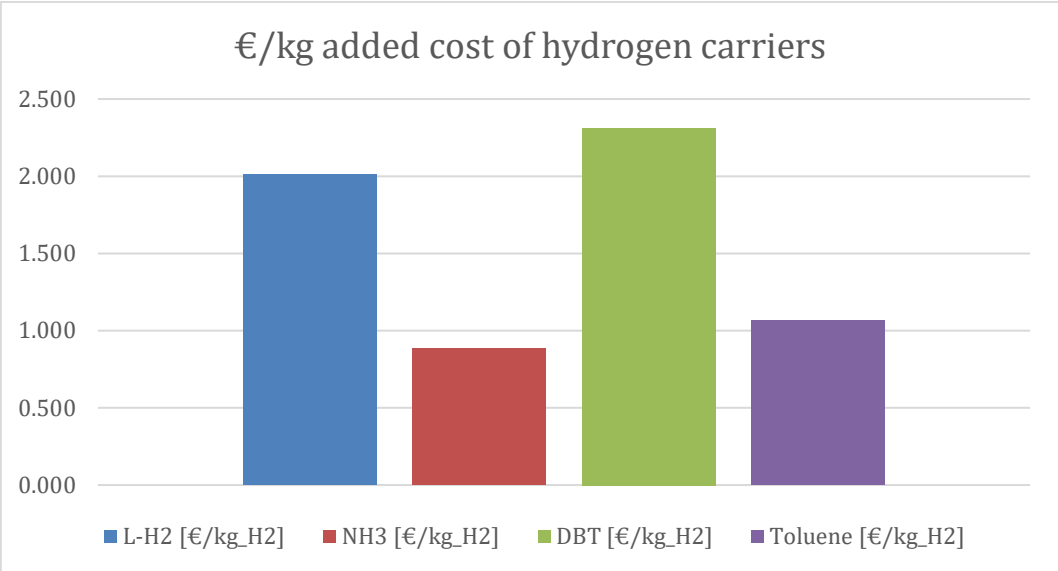

Figure 36: Added cost of hydrogen carriers.

With ammonia being the cheapest hydrogen carrier, the relative cost of hydrogen bound in DBT is more than twice that of NH_3, while L-H_2 *nearly* twice that of NH_3. The cost of toluene is 20% greater than ammonia.

3.2.4 Transportation and emissions

Utilising the example from **chapter 3.2.2**, all the trucks have a storage capacity corresponding to 3 tons of hydrogen, and the hypothetical route is 1000 km. The annual hydrogen production is 2760 tons, or 7.6 tons/day. The number of deliveries per day is calculated in **equation (14)** ...

$$n_{deliveries,daily} = \frac{m_{H_2,daily}}{m_{H_2,trailer}} \quad \textbf{(14)}$$

... where $n_{deliveries,daily}$ is the number of deliveries per day, $m_{H_2,daily}$ is the daily hydrogen demand, and $m_{H_2,trailer}$ is the hydrogen capacity of each trailer.

The time spent on the road was calculated in **chapter 3.2.2** and the maximum number per day is calculated in **equation (15)** …

$$n_{truck,trips,daily} = \frac{24}{t_{total,trip,time} + t_{loading}} \quad \textbf{(15)}$$

… where $n_{truck,trips,daily}$ is the number of trips per day per truck, $t_{total,trip,time}$ is the total trip time, and $t_{loading}$ is time spent unloading (and loading for LOHCs). And lastly, the number of trucks necessary is calculated utilising **equation (16)** …

$$n_{trucks} = \frac{n_{deliveries,daily}}{n_{truck,trips,daily} * availability} \quad \textbf{(16)}$$

… where n_{trucks} is the number of required trucks and $availability$ is the percentage of the time the trucks are available (with regard to service and maintenance). 6 trucks are needed if an annual hydrogen production/delivery is 2760 ton. **Table 20** presents capital cost and OPEX values for a truck and L-H_2, NH_3, and LOHC trailers.

Table 20: CAPEX and OPEX for transportation of hydrogen carriers

	Truck [234], [243], [244]	**L-H_2** [245]	**NH_3** [246]	**LOHC** [247]
Investment cost [€]	180000[n]	725 000	112 000	95 000
Lifetime	8[n]	15[o]	15[o]	15[n]
Fixed O&M [%]		0.4[o]	0.4[o]	0.4[n]
Variable O&M [€/km]	0.1[n]			
Loading time [h]		1+1[o]	1+1[o]	1+1[n]
Fuel consumption [l/km]	0.5[p]			
Fuel price [€/l]	1.21			
Labour cost [€/h]	27.16			
Truck availability [%]	80[n]			

= not applicable

[n] Estimates from *Hurskainen et al. (2020)* [137]

[o] Estimate same value as LOHC

[p] Presented in **chapter 3.2.2**

Assuming a discount interest of 4 % in this example as well, the annuity cost is calculated for each hydrogen carrier by utilising **equation (10)**.

The estimated fuel consumption in **chapter 3.2.2** is based on the specific loading capacity of liquid hydrogen, which, if applied to ammonia or dibenzyltoluene, must be multiplied with the ratio in regard to liquid hydrogen, as shown in **equation (17)** …

$$\text{Ϙ} = \frac{m_{specific,storage}}{m_{specific,storage_{L-H_2}}} \tag{17}$$

…where Ϙ is the specific weight ratio, $m_{specific,storage}$ is the specific weight including storage, and $m_{specific,L-H_2}$ is the specific weight including storage for L-H_2. Assuming a linear relation between the mass transported and the fuel consumption. This ratio accounts for the lower load on the return trip, as presented in **Attachment 1**.

By adding the results to the lowest and highest scenarios from hydrogen production, the total cost of each hydrogen carrier is presented in **Figure 37.**

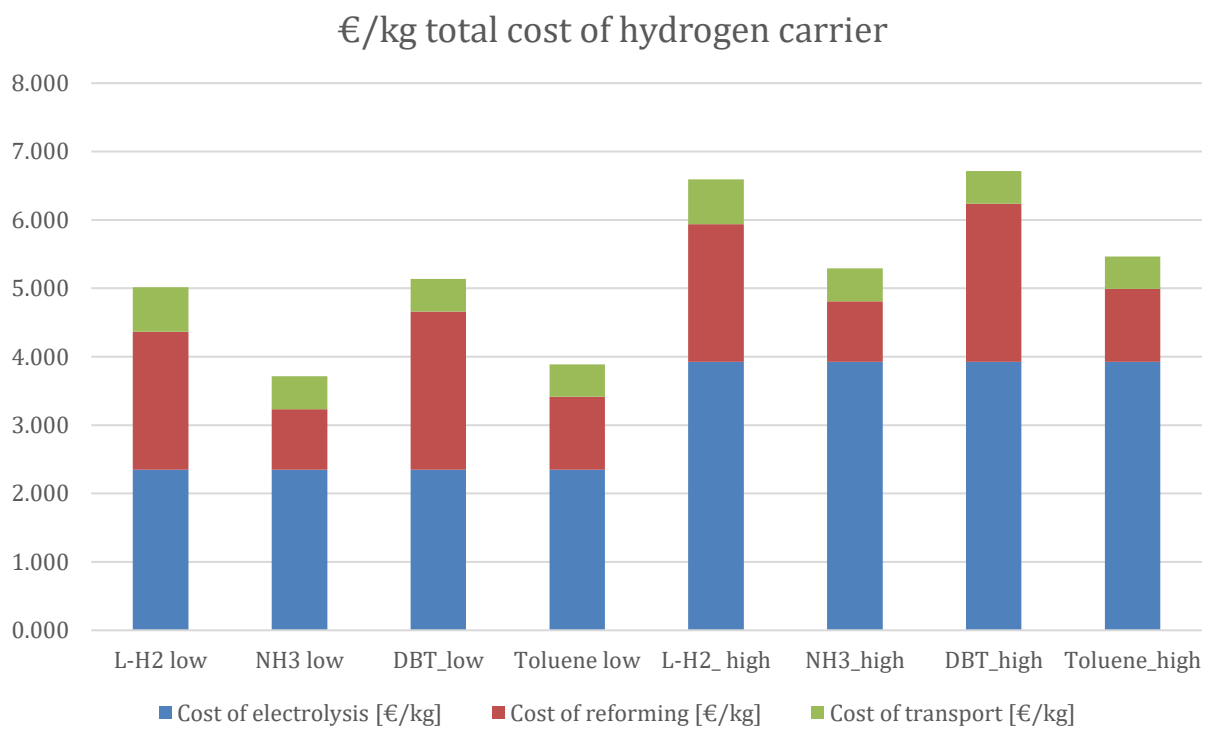

Figure 37: Total cost of hydrogen carrier, lowest and highest scenario

The specific cost of ammonia and toluene is approximately 1.3 – 1.5 €/kg_{H_2} cheaper than that of liquid hydrogen and dibenzyltoluene. The cost of transportation makes up only about 12% of the specific cost of the hydrogen carriers, presented in **Table 21.** All figures are excluding taxes.

Table 21: Total cost of hydrogen carrier, low and high scenario

	L-H2 low	**L-H2 high**	**NH3 low**	**NH3 high**	**DBT low**	**DBT high**	**Toluene low**	**Toluene high**
Cost of electricity [€/kg$_{H_2}$]	1.6	1.8	1.6	1.8	1.6	1.8	1.6	1.8
Cost of electrolysis [€/kg$_{H_2}$]	0.7	2	0.7	2	0.7	2	0.7	2
Cost of production [€/kg$_{H_2}$]	2		0.9		2.3		1.1	
Cost of transportation [€/kg$_{H_2}$]	0.7		0.5		0.5		0.5	
Total cost [€/kg$_{H_2}$]	**5**	**6.6**	**3.7**	**5.3**	**5.1**	**6.7**	**3.9**	**5.5**

Note that the cost of production includes the purchase of the molecule as well as the cost of electricity during loading of hydrogen for the two LOHCs, as stated earlier in this chapter.

Emissions

The *International Maritime Organisation* (IMO) has, as mentioned in **chapter 1.1**, agreed to reduce the GHG-emissions from shipping by 70 % by 2050, relative to 2008, which is the prime reason for hydrogen (and its carriers) as a ship fuel are the fact that the energy conversion onboard has no emissions other than water. There are emissions during production and transportation of fuel, however, varying depending on the source of electricity.

Continuing the scenario from **chapter 3.2.2** and **3.2.3**, the electrolysis plant is located in Norway, which has an associated CO_2 emission from the Norwegian electricity mix of 17 g_{CO_2}/kWh [248]. The figure for fuel consumption in chapter **3.2.2** is the same, which means that it has a fuel consumption of 0.5 l_{diesel}/km and has, according to B.1.1, a CO2 emission of 1.575 kg_{CO_2}/km [225]. The specific fuel consumption of the truck will vary depending on load, and as ammonia has a total specific weight almost half that of L-H2 and LOHC, will have a significantly lower load on the truck, and is estimated by **equation (18)**...

$$m_{CO_2} = e_{consumption} * Dist_{12} * (Ϙ_{loaded} + Ϙ_{unloaded}) \quad \textbf{(18)}$$

... where m_{CO_2} is amount of CO_2, $Ϙ_{loaded}$ is the ratio between the mass of hydrogen with storage system and the mass of the fuel and storing system being shipped, $Ϙ_{unloaded}$ is the ratio between the mass of hydrogen with storage system and the mass of the storage system transported back to the production plant, $e_{consumption}$ is the specific energy

consumption with regard to distance, and $Dist_{12}$ is the distance between the production plant and the bunkering plant. The emissions for production of the dibenzyltoluene (or benzyltoluene for that sake) is not accounted for. The CO_2 emissions associated with transport of hydrogen for 1000 km, including the trip back, is presented in **Table 22**.

Table 22: CO_2 emission of the different hydrogen carriers

	L-H_2	**NH_3**	**LOHC**
Electrolysis [kg_{CO_2}/kg_{H_2}]	0.81	0.81	0.81
Synthesis [kg_{CO_2}/kg_{H_2}]	0.17	0.19	0.15
Transportation [kg_{CO_2}/kg_{H_2}]	1.02	0.53	1.95
Total [kg_{CO_2}/kg_{H_2}]	2.00	1.54	2.05

The total CO_2 emission for L-H_2 and DBT is about 2 kg_{CO_2} / kg_{H_2} or 60 g_{CO_2} / kWh, while NH_3 is only 1.5 kg_{CO_2} / kg_{H_2}on account of its higher gravimetric energy density with regard to the storage system. The trailer is empty when returning to the plant, while DBT and L-H_2 trucks both carry about the same mass (minus the 3 tons of hydrogen) on their return trip. Compared to the well-to-wake emissions of MGO and LNG at 315 and 288 g_{CO_2} / kWh, respectively, which equates to an 81 % reduction of CO_2 for L-H_2 and DBT, and 86 % for NH_3 [249], and an even greater reduction if the transportation of hydrogen is substituted with a zero-emission solution.

The CO_2 emission associated with the production through electrolysis is estimated to be approximately 0.81 kg_{CO_2} / kg_{H_2}, compared to the median emission of hydrogen produced from steam reformed methane (SMR) at 9 kg_{CO_2}/kg_{H_2}, equates to a 91% reduction of CO_2 emission from the production [250], [251].

3.2.5 Safety and handling

Regulations

IMO has strict regulations and clearly defined limitations of properties for marine fuels, most of which is meant for traditional fossil fuels, such as LNG [252]. When hydrogen and its carriers are considered, there are especially a few extra considerations one must take. Green Shipping Programme **(GSP)** points out three regulatory frameworks that needs to be considered:

Safety of Life at Sea (**SOLAS**) is an international convention made by IMO for regulating maritime fuels. It was first formed as a response to the Titanic disaster in 1914 [253]. It is widely regarded as the most important international treaty regarding safety of merchant ships, based on decades of experience. SOLAS focuses on conventional maritime fuels, and does not include safety regulations regarding hydrogen, in any form. It is therefore multiple frameworks being established based on the SOLAS convention taking into account as many hydrogen fuels as possible, with some already published [253], [254].

In 2015 an amendment was made to the SOLAS convention allowing the use of low flashpoint fuels on ships complying with the International Code of Safety for Ships Using Gases or Other Low Flashpoint Fuels (**IGF**). The IGF Code states that some parameters such as safety, reliability and dependability on ships utilising low flashpoint fuels must be equivalent to that of modern conventional oil-fueled machinery, both main- and auxiliary, regardless of whether the machinery is used for propulsion or not. The code only states requirements for LNG as of yet, with other low flashpoint fuels such as ammonia being allowed but requiring separate approvals on a case-to-case basis. This is called *alternative design* by the code, and can be very time-consuming and economically taxing, leading to a higher risk for shipping companies looking to build ships containing energy systems with non-conventional fuels. When it comes to uses besides as fuels, transport in bulk becomes lucrative, as the infrastructure and knowledge already is in place, as is the case with ammonia. The International Code for the Construction and Equipment of Ships Carrying Liquefied Gases in Bulk (**IGC**) provides the standard for carrying liquefied gases in bulk, with a separate chapter on using cargo as fuel. The code will however have to be reviewed in order to allow the use of ammonia or other toxic fuels in the ship carrying the cargo [9], [13], [22].

IMO being the leading authority on maritime safety suffers from the same symptoms as most large bureaucracies, the main one for hydrogen fuels being that rework of the regulatory frameworks is slow. Therefore, Classification Societies such as **DNV** and **Lloyd's Register** often develop sections of the conventions to ease the process of rework, with a Flag Administration accepting the application to ease the *alternative design* approach [9], [13], [22], [255]. There are a multitude of standards to consider regarding the infrastructure necessary for hydrogen fueled maritime transport, with many standards not specifically made for hydrogen at all. One example of this is ISO 20519, which regulates bunkering of LNG. This standard is being used as per 2021 for hydrogen bunkering, while in the next revision in 2022, hydrogen may finally have its own paragraphs, or even its own ISO [256]. The *Ammonia as a Marine Fuel Safety Handbook* by GSP also suggests how to advance the regulatory framework, where a lot of the considerations applies to hydrogen as well [9].

While IMO constructs regulations for safety of maritime fuels in general, not just on ships, there will be different Classification Societies that will have their say in matters related to the necessary infrastructure on land and for bunkering. In Norway, The Norwegian Directorate for Civil Protection (**DSB**) will be the leading authority of these factors, with assistance from other governmental departments such as local fire departments and city planning commissions [257], as presented in **Figure 38**.

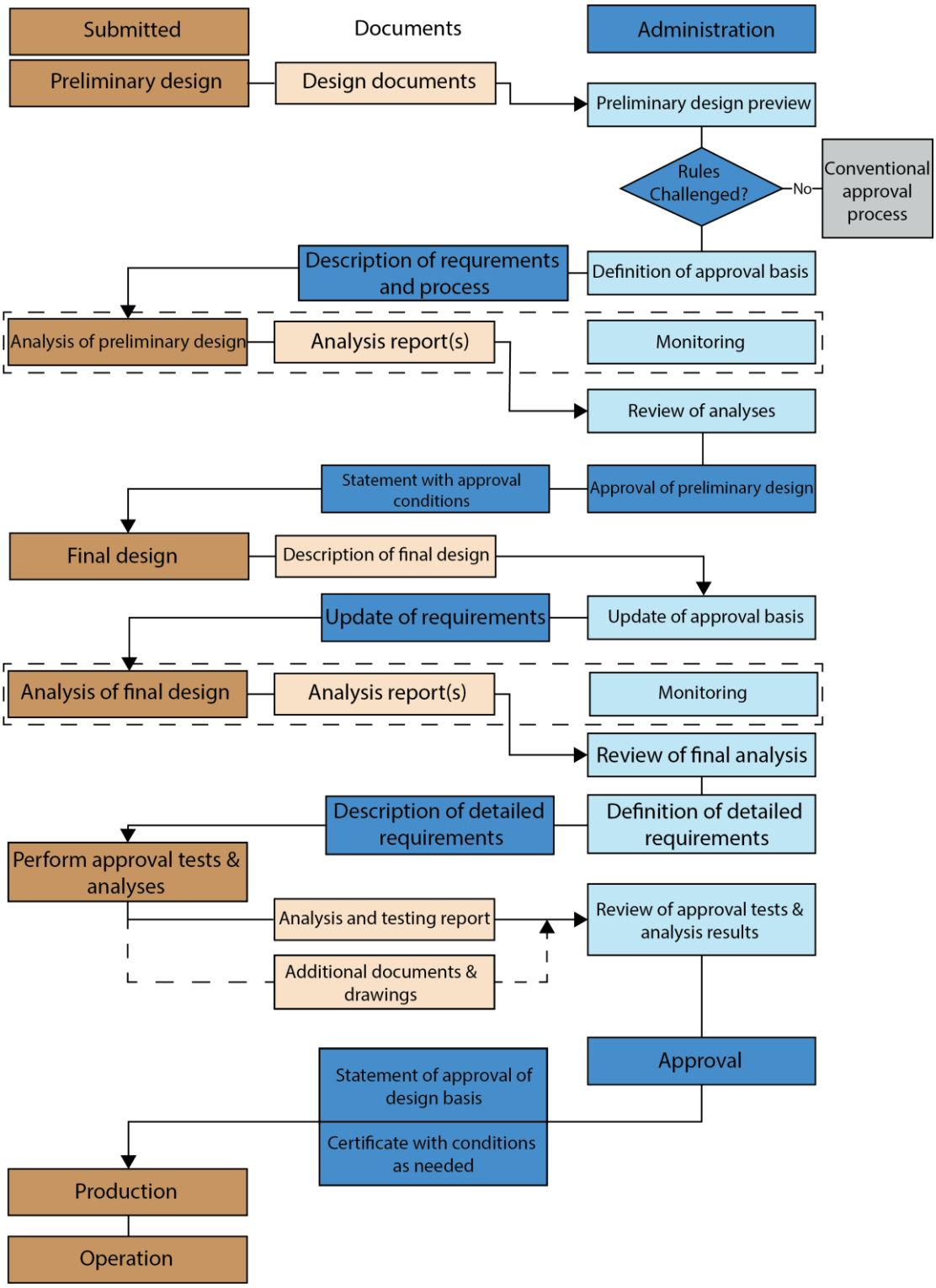

Figure 38: Process of regulatory framework, diagram is inspired by Lloyd's [257].

Safety characteristics of hydrogen fuels

Low flashpoint fuels, such as ethanol, ethane and methanol are attractive as maritime fuels, as they are clean-burning and do not contain any sulphur [258]. Flashpoint must not be confused with auto-ignition temperature, as the latter is the threshold where the fuel self-ignites, while flashpoint is the lowest temperature the fuel vapour will continue burning after the ignition source is removed. Flashpoint can be used to distinguish flammable and combustible fuels, because a fuel with a flashpoint lower than 37.8 °C is flammable, and fuels above is called combustible [259], [260]. IMO categorises low flashpoint fuels as those below 37.8 °C [9], [13], [254].

There are already some systems developed to minimize damage in case of gas leakage in maritime applications, some of which applies to liquid hydrogen and ammonia. There are positives and negatives with most of these systems, as there are several different potential dangers with both fuels. As stated earlier, liquid hydrogen has an outflow velocity of about 50 m/s at 1 bar storage pressure, which can if systems are built around it be beneficial in the way of getting the fuel away from infrastructure and personnel faster. This can be a *double-edged sword* as the ignition temperature of hydrogen in a sufficient mix with air is low (4 to 75 %), and a high velocity exposes the hydrogen to a larger amount of friction as well as the potential for high amounts of hydrogen, depending on the size of fracture on the storage tank [13], [22], [261], [262].

When released into the atmosphere, ammonia and liquid hydrogen behave in seemingly similar ways. While liquid hydrogen evaporates in ambient temperatures, freezing surrounding air forming a cloud while the hydrogen rapidly rises further into the atmosphere, ammonia will form a cloud of toxic vapour that stays near the ground. As described in **2.3**, ammonia is hygroscopic which means that the moisture in the surrounding air will be absorbed, creating a vapour cloud denser than air [9], [261]. Both substances leave behind an area of danger to human life and/or surrounding infrastructure, albeit different dangers. As stated by Olav Roald Hansen [261], liquid hydrogen has a potential of releasing out of a storage container with an outflow velocity reaching 50 m/s at just 1 bar pressure, and more than 100 m/s at 4 bar pressure. The liquid hydrogen will immediately boil when coming into contact with surrounding materials or gasses, such as air, expanding about 120 % per degree K – meaning a temperature difference of 270 K (liquid hydrogen storage temperature of 20K and ambient temperature around the storage tank) will lead to a volumetric increase of 32 400 % in a very short amount of time [261]. This hydrogen gas can, given a sufficient air mixture, ignite and potentially cause an explosion [13], [257], [261].

Until the regulations placed by IMO encompasses hydrogen specifically, other standards and frameworks can be utilised. For now, ISO 20519 has been used, which originally only regulates LNG as a maritime fuel. This standard, among other factors, regulates safety zones, operational procedures, crew training and qualifications, and control of ignition sources [13], [256], [257]. Furthermore, as stated earlier, ships that use a low flashpoint fuels must comply with the IGF code. As the global experience with hydrogen, as well as ammonia, used as a maritime fuel is low, prescriptive rules do not apply, and ships run on hydrogen will have to follow the *alternative design*, as explained earlier [9], [13], [257].

Complications regarding hydrogen in a maritime setting is explained in detail by several parties, including *Olav Roald Hansen*, *GSP* and *DNV-GL*. To mention some of the more

prominent factors when compared to LNG: High chance of leak from fuel tank, valves and other system components, high reactivity with air at high hydrogen concentrations, freezing of surrounding air in the event of a larger release, high risk of *burning fuel* transitioning to *exploding fuel* (DDT, deflagration to detonation transition), as well as a higher laminar burning velocity (≈3 m/s) at high concentrations (≈>12 %) [9], [13], [257], [261]. As with most fuel related accidents, a cascade effect can occur, especially when said fuel is highly exotherm. Heat can warp metal and spread fires aboard ships, causing other systems to fail, escalating the severity of the incident [257].

Since ammonia is a toxic substance, as mentioned in **2.3**, strict regulations are needed if it is to be handled in a safe way, as safety of ammonia transportation is classified as extremely critical [93]. A lot of the groundwork of regulations regarding the handling of ammonia are well established, as the industry has more than 100 years of experience in the handling of ammonia [263]. The use of ammonia as a fuel has a lot of extra requirements, however: Ammonia is gaseous at STP, as mentioned in **2.3**, which means it either needs to be pressurized or cooled for liquification to increase the density for transport. Because of this, a leakage will potentially lead to exposure of both liquid *and* gaseous ammonia as well as risk of frostbite since this process is followed by cooling [264]. The ammonia-to-air weight ratio is 0,6 – ammonia is in other words more buoyant than air. Boiling liquid ammonia (**L-NH_3**) on the other hand, is heavier than air, not unlike liquid hydrogen (**2.2**), which potentially complicates the handling, and needs to be taken into account when working with ammonia [264].

Generally, the use and handling of ammonia include a lot of the same risks as other fuels. It is not flammable, though it will ignite at higher temperatures if a sufficient solution (16-25 %) comes in contact with air [264]. Anhydrous ammonia on the other hand, is not flammable [93], but is drawn to moisture so it will bind itself to eyes, mucous membranes, and other moist parts of the body, because of its hygroscopic nature [264]. Exposure will lead to caustic burns. This is why the American Conference of Governmental Industrial Hygienists (**ACGIH**) has established a limit in regards to the amount of ammonia gas human beings can be exposed to; a maximum of 25 ppm for 8-hour workdays in a 40 hour work week [264], [265]. The Environmental Protection Agency (**EPA**) US, has developed the Acute Exposure Guideline Levels (**AEGL**) for airborne chemicals where *almost* the same conclusion is formed:

Table 23: EPA Acute Exposure Guideline Levels [265], [266]

	10 min	**30 min**	**60 min**	**4 h**	**8 h**
AEGL 1 (ppm)	30	30	30	30	30
AEGL 2 (ppm)	220	220	160	110	110
AEGL 3 (ppm)	2700	1600	1100	550	390

AEGL 1*: Notable discomfort, irritation, or certain asymptomatic non-sensory effects. However, the effects are not disabling and are transient and reversible upon cessation of exposure.*

AEGL 2: *Irreversible or other serious, long-lasting adverse health effect or an impaired ability to escape.*

AEGL 3: *Life-threatening health effects or death.*

As seen by *Hydrogenious'* presentation [267], DBT in particular is not flammable to any great extent, while ongoing studies are examining its toxic properties regarding marine organisms, as well as its effect on internal and external exposure on human wellbeing. Safety issues regarding DBT cannot be measured by the same standards that L-H_2 or ammonia can, as potential dangers surrounding DBT on a human's well-being presumably only applies when ingested, or during other long-term exposures, as described in **2.4.5**.

TPI (Toxic Potential Indicator) is used to indicate some of many toxicity dangers of substances, and is calculated based on differing parameters based on the country/region doing the calculations [268], [269]. While the TPI is high for DBT relative to some other known LOHCs, as shown in **Table 5**, it is still quite low in comparison to some LOHC's, and is being studied further at time of writing regarding toxicity and danger to marine life [270], [271]. When it comes to fuel tank spill, specifically into open water such as the ocean, it is assumed the same regulations regarding safety will apply to DBT, as does for conventional maritime oil-based fuels. In contrast to liquid hydrogen and ammonia, DBT does not evaporate when subjected to ambient conditions, as described in **2.4.3**, meaning a fuel tank spill is predictable in its outcome**.** This may not be the case for simpler toluene derivatives, due to higher vapour pressures. Depending on the state (loaded/unloaded) of the DBT, it has a higher buoyancy than water, meaning the same methods for retrieval and clean-up can be applied in the case of a fuel tank spill as for conventional maritime oil-based fuels. This does not take into account whether a fuel tank spill occurs at a location where the temperature of the ocean is below 10 °C or not, as further studies on DBT are needed to say anything about its buoyancy and viscosity at this temperature.

Below is a table listing some of the most important safety related data regarding liquid hydrogen, ammonia, dibenzyltoluene and liquid natural gas. For ammonia toxicity see **Table 23** and the surrounding text.

Table 24: Safety related properties, bullet points [13]

	L-H_2	**Ammonia**	**DBT**	**LNG**
Main hazard	Explosive, flammable, cryogenic	Toxic, flammable	Ingestion, prolonged skin contact	Explosive, flammable, cryogenic
Material strain	H_2-embrittlement, cryogenic	Corrosive in water solutions	None	Cryogenic
Smell threshold	Odourless	5-50ppm	Irrelevant	Odourless
Flame colour	Invisible	Yellow-green	Orange	Blue to orange

Table 25: Safety related data on liquid hydrogen, ammonia, dibenzyltoluene and liquid natural gas

	L-H_2	**Ammonia**	**DBT**	**LNG**
Maximum flame velocity [m/s] [13]	3	0.07	-	0.4-0.45
Ignition temperature [°C] (Table 9)	560	630	450	465
Auto-ignition temperature [°C] [22]	571	651	-	540
Ignition energy [mJ] [13], [272]	0.017	680	-	0.29
Combustion energy (HHV) [MJ/kg] [13]	142	19	-	56
Flammability in air (vol%) [22]	4-75	15-28	-	5-15
Detonatable concentration with air [%] [13]	15-60	-	-	5-15
Storage pressure [bar] (Table 15)	1-10	1-10	Ambient	1-10
Combustion pressure, closed space [bar] [13]	7.1	5.4	-	7.9
Boiling point [°C] [13]	-253	-33.2	-	-162
Adiabatic flame temperature [°C] [13]	2254	1800	-	1963
Speed of sound @ STP [m/s] [13]	1290	440	-	450
Toxicity (relative, 0 - 4) [93]	0	3	1	1
Flammability (relative, 0 - 4) [93]	4	1	1	3

Note that DBT's smell threshold is irrelevant, as in this safety context the smell of spilled DBT should warn no danger, other than potentially slippery surfaces. This may be subject to change, when further DBT-studies becomes available.

Incidents and accidents

Documentation regarding hydrogen related incidents vary widely, based on the governing company or nation, understanding and matureness of technology, as well as the time of the incident. As seen in the report for incidents on the mainland of the United States of America [273], documenting 67 incidents from 1969 to 2020, the cause of the incident ranges from human error to a variety of system part failures. Most of these incidents had no severe consequences, with some leading to a fire developing or explosion, and a few leading to fatalities and loss of human life [273].

Probably the most famous accident involving hydrogen is the *Hindenburg Disaster* in 1937. While this accident often comes up in the media as an example of how dangerous hydrogen can be, it only paints a small part of the greater picture that is hydrogen safety. Other famous accidents involve the space industry, with rockets filled with liquid hydrogen and liquid oxygen in enormous fuel tanks with a rocket engine at the bottom,

exploding either on the launch pad or high up in the air, as in a spectacular pyrotechnic show on steroids. Other more recent events are the meltdown of the *Fukushima* nuclear reactor, where exploding hydrogen was part of the accident, or the many smaller accidents involving trucks carrying hydrogen bursting into flames [13]. The most recent accident happening in Norway is the 2019 explosion of a hydrogen refuelling station at *Kjørbo*, leading to a shutdown of all hydrogen fuel station in the country as well as a set-back politically for the hydrogen industry [13], [274], [275]. Ammonia, as a hydrogen carrier, has seen its fair share of accidents as well, both in industrial settings as well as near communities. Such as the 1985 *Herøya* incident, where an ammonia plant exploded, damaging surrounding infrastructure in a 400 m radius, as well as the death of two plant employees [13], or the three fatalities at the Canadian indoor hockey arena in *Port Alberni* following an ammonia gas leak where the exposure to gaseous ammonia was the cause of death, not an explosion or fire [276]. There are several times more ammonia leak incidents than explosions or fires, but ammonia leakage can be just as fatal, as half an hour exposure to 2-3 000 ppm ammonia in breathable air may be fatal, and 5-10 000 ppm is rapidly fatal [9]. As an example, a direct blast to the face is the main cause of death regarding anhydrous ammonia, and when large amounts are inhaled, the throat swells shut, and suffocation occurs [9].

Despite the many accidents and incidents, there is no reason to believe there will be more hydrogen fuel related accidents than there are fossil fuel related accidents as per today, especially in the maritime sector, as hydrogen fuel will have to comply with stricter regulations than MGO, MDO or LNG, as described earlier. If the necessary precautions are made, and appropriate maintenance is done, neither leaks nor fires/explosions should happen in any greater degree than existing fuel solutions.

Almost 200 million tons of ammonia are produced and used in various ways annually on world basis, with few accidents relative to other highly toxic and/or explosive/flammable substances [13]. It is estimated that the fatality rate related to the use and production of ammonia is 2 per billion, which is extensively lower than for fuels such as ordinary car fuel grade diesel or gasoline [13], [277]. While fatalities are low, accidents and injuries are still relatively common, with almost one thousand ammonia related accidents in a 15-year period in the US, with on average 1,6 injuries per accident [13]. The low fatality rate can somewhat be explained by the fact that ammonia releases a strong smell that becomes unbearable to be near, causing both humans and animals to evacuate quickly, as long as the concentration is low enough to not endanger life immediately [13]. A very recent (April 2021) accident involving ammonia is the ammonia leak on the tanker anchored in *Port Klang* in Malaysia, causing one fatality and three injured [278], [279].

Accidents related to the use of LOHC as a fuel is undocumented, as LOHC is a relatively new technology. DBT shares many properties with mineral oil, and fuel tank spills of DBT *can* have the same consequences as the many oil spills throughout history.

3.3 Case: MV Rubin

As mentioned in **chapter 2.6**, the fish feed carrier MV Rubin was selected by Ocean Hyway Cluster as the subject of a case study. The following chapters outline strategies for determining the energy requirements of this ship based on both AIS data and the average fuel consumption of the existing system. Analysis of the shipping route also helps to determine the minimum required range of the ship in the current use case.

The study culminates in a threefold proposal for retrofit systems using L-H_2, NH_3 and DBT as fuel instead of MGO. Considerations regarding available space are not taken, and the ship is assumed to have an approximately constant mass during every voyage because of ballasting requirements. The goal of this analysis is to determine energy efficiencies while also considering practical limitations like cold-starting, waste heat management, etc.

3.3.1 Analysing the shipping route

In order to analyse the shipping route from the CSV-file mentioned in **chapter 2.6.2**, the distance between coordinates needs to be calculated. Since coordinates are defined by the locations on a sphere, the distance may be calculated using the *Spherical Law of Cosine* [280],

$$cos(c) = cos(a)\,cos(b) + sin(a)\,sin(b)\,cos\,(C) \qquad \textbf{(19)}$$

...where C is the angle of "the spherical triangle" (positioned on the North Pole in this case), while a, b, and c are the arcs between said points.

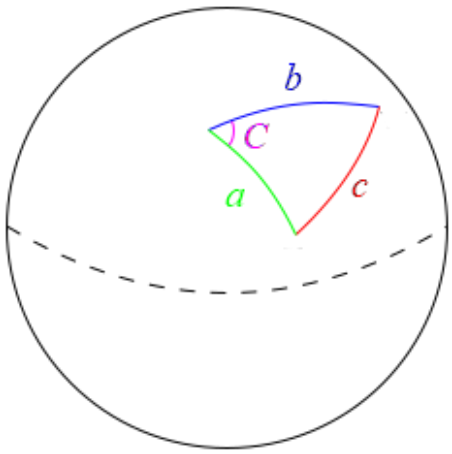

Figure 39: An illustration of the arc lengths [281] (modified from Public Domain figure).

When applied to coordinates, the formula is expressed as *Cosine Rule with Latitudes* [280],

$$cos(Dist_{12}) = sin(\lambda_1)\,sin(\lambda_2) + cos(\lambda_1)\,cos(\lambda_2)\,cos(L_1 - L_2) \qquad \textbf{(20)}$$

...where $Dist_{12}$ is the distance between the two points, λ_1 and λ_2 are the latitudes, L_1 and L_2 the longitudes for points 1 and 2, respectively.

<u>Note:</u> The longitudes are subtracted because both points are on the same side of the Greenwich Meridian, as is the case for all the 592 datapoints. If this had not been the case, they would have been added instead [282].

The coordinates in **Attachment 1** are expressed in decimal degrees, which needs to be converted to radians by simply multiplying by $\pi/180$ [283]. The distance needs to be multiplied by the earth's radius, 6378 km [284], in order to get the result in kilometres. It should be noted that this equation assumes the earth is a perfect sphere – *which obviously is not the case* – although the small distance between each coordinate point yields negligible errors using said assumption [285].

Furthermore, the distances must be categorised to calculate and separate each individual voyage, as well as the idle time on each supply point. In order to be able to discern each stop, the coordinates are analysed using google maps [286] and cross-referenced to barenswatch.no, which has a large, comprehensive database containing the fish farms of the Norwegian coastline [66].

Some of the datapoints are missing. These have been substituted using Google Maps. Each point that has been manually adjusted in **Attachment 1**, has an orange cell-colour as to be easy to identify.

By analysing the shipping route presented in **Table 26** and assuming this is a typical operational profile of the vessel, an average voyage requirement may be calculated.

*Table 26: MV Rubin's shipping route for February, see **Attachment 1.***

One roundtrip – Tromsø			**Florø – Tromsø**			**One roundtrip – Florø**		
Distance [km]	**Sailing time [hours]**	**Loading time [hours]**	**Distance [km]**	**Sailing time [hours]**	**Loading time [hours]**	**Distance [km]**	**Sailing time [hours]**	**Loading time [hours]**
532,7	42.3	9.9	1221,4	68,7	8,7	886,5	28,6	8,5
Ålesund – Florø			**Bergen – Ålesund**			**Florø - Bergen**		
Distance [km]	**Sailing time [hours]**	**Loading time [hours]**	**Distance [km]**	**Sailing time [hours]**	**Loading time [hours]**	**Distance [km]**	**Sailing time [hours]**	**Loading time [hours]**
122,2	5,1	-	649,2	55,4	3,5	135,3	7,1	-
One roundtrip - Florø			**Ålesund - Florø**			**Florø - Ålesund**		
Distance [km]	**Sailing time [hours]**	**Loading time [hours]**	**Distance [km]**	**Sailing time [hours]**	**Loading time [hours]**	**Distance [km]**	**Sailing time [hours]**	**Loading time [hours]**
805,3	41,9	6,7	167,4	8,6	-	465,7	26,0	7,4
Måløy - Florø			**Meløy - Måløy**			**Average voyage**		
Distance [km]	**Sailing time [hours]**	**Loading time [hours]**	**Distance [km]**	**Sailing time [hours]**	**Loading time [hours]**	**Distance [km]**	**Sailing time [hours]**	**Loading time [hours]**
40,5	2,5	-	852,1	52,6	11,1	773,3	45,1	7,9

Note that the longest route is almost twice the length of the average route and is therefore the dimensioning factor when the energy requirement is to be calculated, the total time spent sailing is the sum of sailing time and loading time.

Using the cosine rule with latitudes on the corrected dataset, a total travelled distance of 6517 km was calculated for MV Rubin between 26. Jan and 26. Feb 2021.

Automation of this procedure becomes very useful when high resolution AIS data and speed-power-curves are available, presented in **Attachment 4**.

3.3.2 Average energy and power requirements

The layout of the machinery on *MV Rubin* is not readily available. The ship is therefore assumed to have a power schematic as presented in ***Figure 40***, based on typical layouts for non-diesel-electric ships [287]. The main engine is presumably coupled directly to the axle which drives the propeller. The Stamford shaft generator mounted on the axle, is capable of producing approximately 300 kVA, which is distributed at the switch board. Note that shaft generators are typically capable of running in two modes: *Power Take Out* (**PTO**)-mode and *Power Take In* (**PTI**)-mode [288]**.** In PTO-mode the main engine supplies electrical power through the shaft generator, while in PTI-mode the shaft generator supplies additional mechanical power by working as an electrical motor, which increases the power output at the propeller [288]. It is assumed that the system on MV Rubin has this ability.

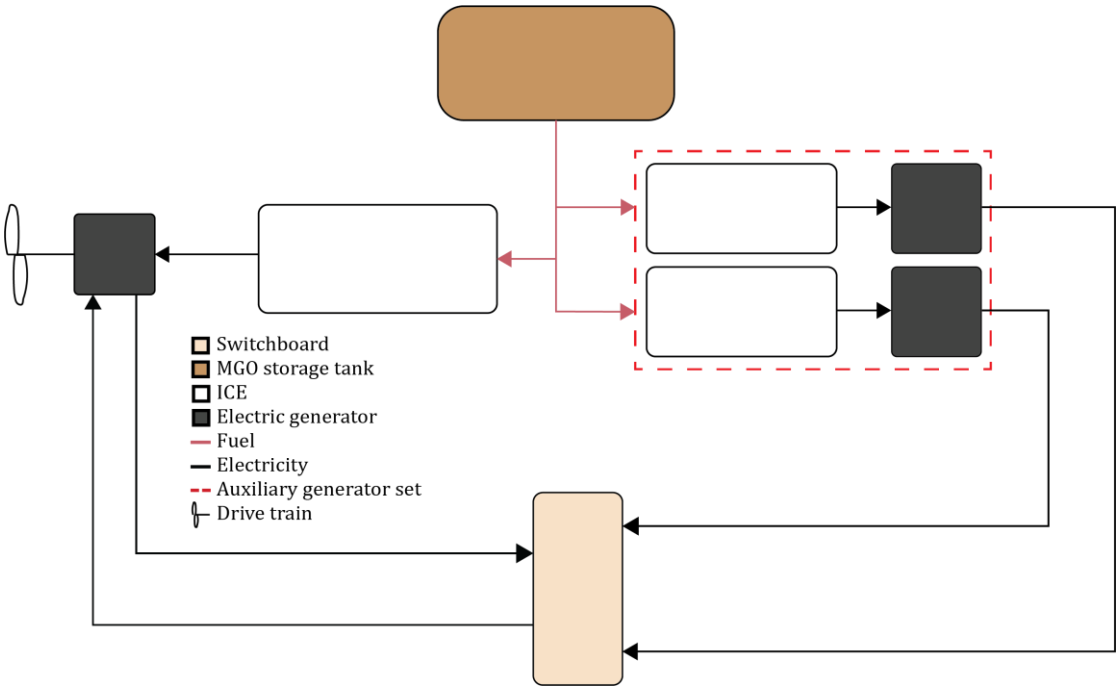

Figure 40: A possible power schematic diagram for MV Rubin [287]

The auxiliary power gensets are the main source of power for the supporting systems on the ship. However, the following calculations assumes that the main engine is the prime mover during regular sailing. During loading, it is assumed that the additional fuel consumption is attributed solely to the auxiliary gensets. This simplification, though imprecise, is a necessary step to take if the energy requirement is to be calculated despite lack of power curves, etc.

In order to propose alternative fuel- and power solutions, the *net energy requirement* must be calculated. This is the total average mechanical (and electrical) work done by *MV Rubin*, calculated by estimating the energy consumption of the internal combustion engines which is then multiplied with their respective efficiencies. The electric generators are all listed with direct efficiencies in their respective manuals, but the combustion engines are not because of variability in fuel energy content (see **chapter 2.5.4**). It is therefore necessary to calculate said efficiencies for the given fuel. Further assumptions (for the sake of simplification) are lossless electrical grid and lossless mechanical transfer, which are easily rectified if data for power curves and system diagrams become available.

Main engine

As stated in **chapter 2.6.1**, the main engine of *MV Rubin* is a *Wärtsilä 9L20*. (Note that the crew of the ship states that it is an 8L20, see ***Attachment 2*****,** although a very thorough maritime article as well as the manufacturer themselves both state that it is in fact a 9L20 [211], [289]). The manual from Wärtsilä states that the SFOC at ISO-conditions is rated at approximately 190 g/kWh. The fuel oil in question is ISO 8217 F-RMK 700 [150], [215]. In order to calculate the efficiency of the engine, the LHV for said fuel must be calculated. ISO 8217, appendix H includes an empiric equation for calculating the lower heating value [150], shown in **(21)**…

$$h_{n,ISO\ 8217} = (46.704 - 8.802\rho_{15}^2 * 10^{-6} + 3.167\rho_{15} * 10^{-3}) * [1 - 0.01(W_w + W_a + W_s)] + 0.094 * 2W_s - 0.024 * 49W_w \quad \textbf{(21)}$$

… where $h_{n,ISO\ 8217}$ is the lower heating value expressed in MJ/kg and ρ_{15} is the density of the fuel at 15 $°C$ and atmospheric pressure. $W_w, W_a, and\ W_s$ is the weight percentage of water, ash, and sulphur, respectively [150]. The sulphur content is locally regulated by countries, which in Norway corresponds to 0.1 % [290].

By using **equation (21)** the lower heating value for ISO 8217 is estimated to be approximately 40.08 MJ/kg, as shown in **Attachment 1**. This is further used in **equation (4)** to calculate the efficiency of the 9L20 engine in this scenario, which is approximately 0.473, as shown in **Attachment 1**.

Auxiliary engines

The auxiliary engines are *Baudouin 12 M26.2* engines, as mentioned in **chapter 2.6.1**. According to articles regarding *MV Rubin*, as well as statements by the bridge crew, the auxiliary engines operate at approximately 700 kW (see **Attachment 2**) [211]. This corresponds to a specific fuel-oil consumption of 197 g/kWh in the manual from *Baudouin*, which also includes the lower heating value used to calculate the fuel consumption, at 42.7 MJ/kg [219].

By utilising **equation (4)** the efficiency of the auxiliary engines is estimated to be 0.428, as presented in **Attachment 1**.

Energy requirements

As stated at the end of **chapter 3.3.1**, the longest of the voyages presented in **Table 26** is the trip between Florø and Tromsø, estimated to be 1221 km long, with 69 hours spent sailing between stops, and 9 hours in total spent loading onto fish farms. By assuming that

bunkering of fuel is possible in both Florø and Tromsø, the following calculations aim to *at least* cover the energy required for this distance. Furthermore, as actual power curves for the ship are unavailable for the authors of this thesis, it is necessary to operate with average values – average fuel consumption and average efficiency of the system which are presented in **Table 13, Table 14**, and the efficiencies estimated in this sub-chapter.

The average fuel consumption was estimated by the bridge crew to be 5 m^3/day during sailing, as presented **Table 14**, while consumption during loading is higher, because of the dynamic positioning system, at about 7 m^3/day as reported in **Attachment 2**. These daily values are multiplied with a conversion factor as well as the amount of time spent preforming the task at hand, as shown in **equation (22)**…

$$W_{task,net} = \dot{V}_{daily} * \frac{1\ day}{24\ h} * t_{task} * \rho_{15} * h_{n,ISO\ 8217} * \Pi(\eta) \qquad \textbf{(22)}$$

… where $W_{task,net}$ is the average work done with regard to the task at hand, $\dot{V}_{daily}$ is the daily fuel consumption (expressed in m^3), t_{task} is time spent performing the task (expressed in hours), ρ_{15} is still the density of ISO 8217 at 15 °C, $h_{n,ISO\ 8217}$ is the lower heating value for *ISO 8217*, and $\Pi(\eta)$ is the product of efficiency for system in question.

Utilising **equation (22)**, the total average work done is calculated and presented in **Table 27**, calculations are presented in **Attachment 1**.

Table 27: Total average work done by MV Rubin on its longest journey between Jan. & Feb. 2020.

	Daily sailing	**Unloading**	
Power source	Main engine	Main engine	Auxiliary engines
Daily fuel consumption [m^3]	5	5	2
Total efficiency $\Pi(\eta)$	0.473	0.473	0.408
Average work done [kWh]	76082	9598	3315
Total average work done [kWh]	**88 996**		

The total work done by *MV Rubin* is, as presented in **Table 27**, approximately 89 000 kWh (or 320 GJ), which is the basis for the system calculations in the following chapters.

Note that the aft and bow thrusters, as well as PTI-mode would decrease the auxiliary efficiency even further. The solution presented in **Chapters 3.3.3**, **3.3.4**, and **3.3.5** are all electrically driven, which means that these efficiencies remain unchanged, and are therefore neglected. All three of the following proposals involve electrical motors with power ratings high enough for MV Rubin, but the analysis ignores this because of the aforementioned lack of power schematics and operational data for the ship. In other words, the *energy demand* is the focus of this analysis. Battery dimensioning for peak shaving, as mentioned in **chapter 2.5.3**, is not considered here. The use of backup generators for cold starting the systems is deemed necessary, but not elaborated further.

The required amount of hydrogen (and storage weight and volume) is determined by doing almost the same calculations as in **chapter 3.2.2**, except in reverse. Most of the assumptions apply in these cases as well.

The goal of a retrofit or redesigned powertrain using hydrogen is emissions reductions. According to SINTEF, the average well-to-wake emission for 4-stroke engines running on MGO is 685 to 734 g_{CO_2} / kWh, which equates to between 129.7 and 139 tons of CO_2 for this voyage [291] (see **Attachment 1** for calculations).

3.3.3 Liquid hydrogen system

The first system proposal involves the use of L-H2 stored in cryogenic tanks. By combining alkaline fuel cells with a heat exchanger for freezing the CO_2 out of the air by utilising the cold, newly evaporated hydrogen, as mentioned in **chapter 2.5.2**, the air may be used directly in the fuel cell, as it is extremely pure with regard to CO_2. This is desired, as the alkaline fuel cells generally have a higher efficiency, as well as not requiring precious metal electrodes. **Figure 41** illustrates a simplified system schematic for the proposed propulsion system.

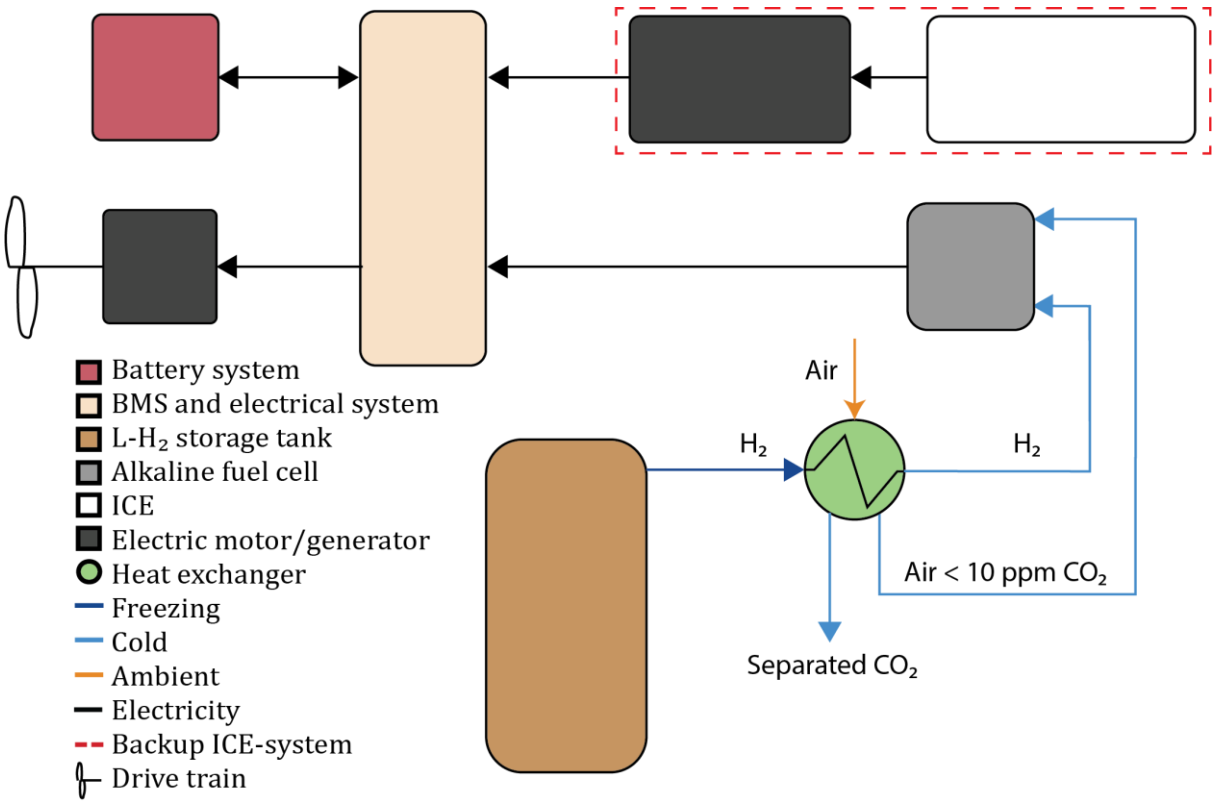

Figure 41: Propulsion system for MV Rubin with liquid hydrogen and alkaline fuel cells.

The efficiencies in **chapter 3.2** was chosen from the lowest estimates in **chapter 2.5.2**, as there were no system optimalisation or recycling of waste heat. In the tree next examples, however, the higher estimates are applied, as waste heat is utilised.

Assuming the same efficiency of the electrical grid, including the electrical motor as in **chapter 3.2**, and 63 % electrical efficiency for the alkaline fuel cell, the ship has a hydrogen demand at bunkering of approximately 4.9 tons. Utilising the specific volumetric and gravimetric energy densities in **Table 15**, the total mass and volume for

the storage system is 82.6 tons and 137.6 m³, respectively, which is well within the loading capacity of *MV Rubin* illustrated in **Table 12**.

Assuming the liquid hydrogen is produced and distributed from the Mongstad-base mentioned in **chapter 2.2.1**, which is approximately 180 km and 3 hours from Florø [292], equates to 8.3 MWh or 250 kg of lost mass, on account of the boil-off (0.5 % per day and 5 vol% during bunkering). The amount of hydrogen liquefied is therefore about 5 tons. Energy requirements for liquefaction is 30 % of the available energy in hydrogen, as stated in **chapter 2.2**, and shown in **equation (23)** …

$$\eta_{liquefaction} = \frac{h_{n,H_2}}{h_{n,H_2} + \left(h_{n,H_2} * 0.3\right)} \quad \textbf{(23)}$$

… where $\eta_{liquefaction}$ is the thermodynamic efficiency of liquefaction, which is 77 %, and $\left(h_{n,H_2} * 0.3\right)$ is the electrical input, as illustrated in **Figure 42.**

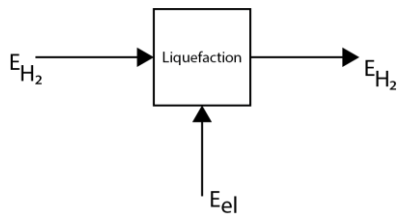

Figure 42: Liquefaction efficiency.

The electrolysis is carried out by a PEM electrolyser, as this is the only technology with a pure enough hydrogen for liquefaction without further purification, as described in **chapter 2.1.2** and **2.2.1.**

The total electrical input for hydrogen production is 290 MWh, which equates to a total *water to water* (**WtW**) efficiencies of about 30.6 % and an associated CO_2-emission of 4.9 $tons_{CO_2}$ for production. The emission from distribution is calculated utilising **equation (18)** and corresponds to 0.5 $tons_{CO_2}$.

The Sankey-diagram in **Figure 43** illustrates the losses through the supply chain.

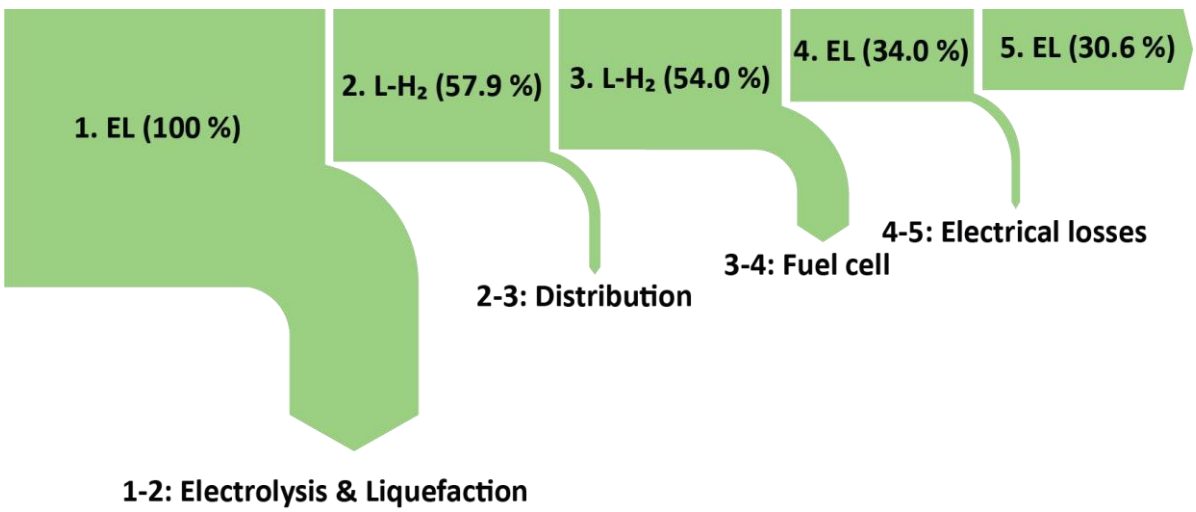

Figure 43: Sankey-diagram illustrating the supply chain of liquid hydrogen for MV Rubin.

3.3.4 Ammonia system

The second system proposal involves the use of NH_3 stored in a cooled or slightly pressurised state (or a combination of the two). Boil-off during distribution is neglected on account of unreliable data. Cracking ammonia directly in a SOFC should yield a substantially higher theoretical efficiency than if an external cracker were to be utilised.

Assuming the energy required for cracking ammonia is 1.34 kWh/ kg_{NH_3} as described in **chapter 2.3.3**, and that the thermal efficiency of a SOFC is 40 %, as presented in **chapter 2.5.2**, **equation (24)** illustrates the available heat energy with regard to the required energy for cracking …

$$q_{SOFC} = h_{n,NH_3} * \eta_{SOFC,th} \quad \textbf{(24)}$$

… where q_{SOFC} is the specific waste heat available, h_{n,NH_3} is the lower heating value for ammonia, and $\eta_{SOFC,th}$ is the thermal efficiency of SOFC. This equates to a specific available waste heat of approximately 1.60 kWh/ kg_{NH_3}, which should be enough, assuming lossless heat transfer and stationary stream. The Norwegian research company *Prototech* aims to be able to deliver direct ammonia SOFC by 2024 for the *Viking Energy* project [293] with efficiencies from 60 to 70 % (see **Attachment 3**). By utilising the higher estimate in **chapter 2.5.2**, an electrical efficiency of 60 % is chosen, which coincides with the lower estimates from Prototech. The system diagram presented in **Figure 44** illustrates the recycling of ammonia with a heat exchanger in order to utilise as much of the high-quality heat as possible.

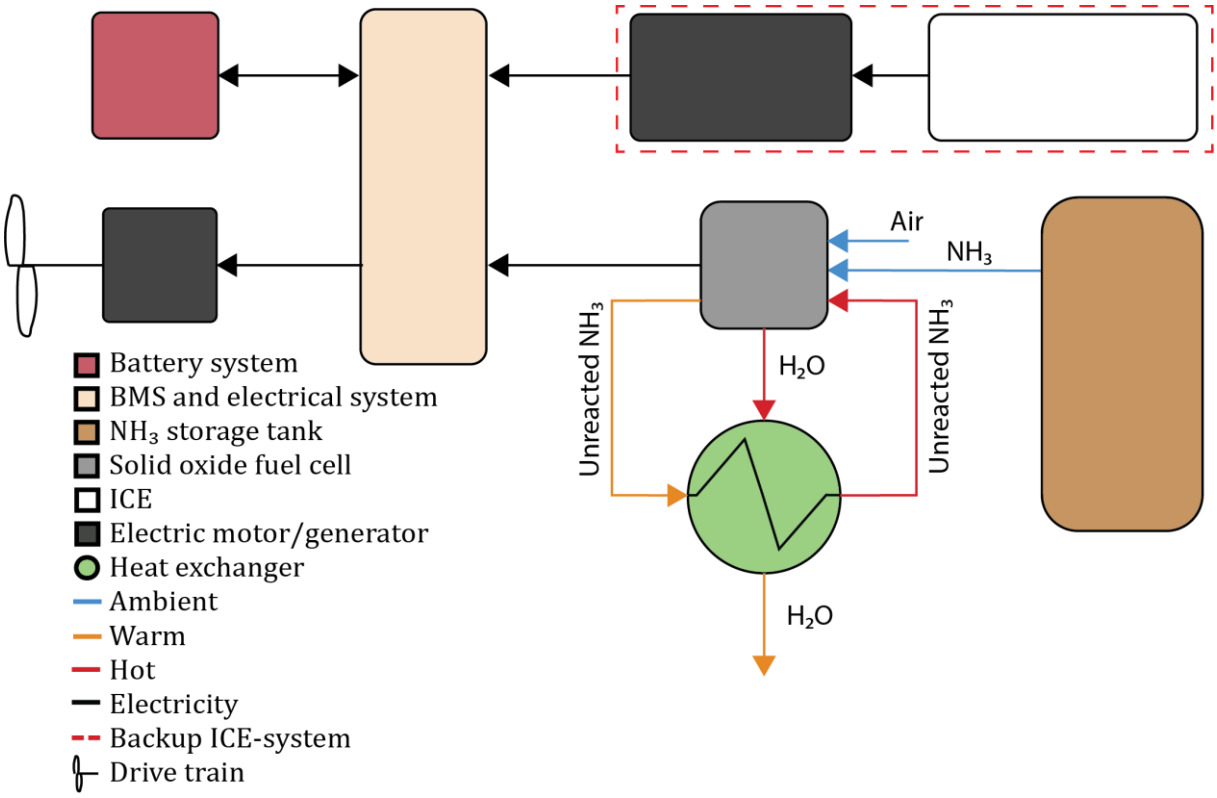

Figure 44: Propulsion system for MV Rubin with ammonia and Solid oxide fuel cells

Assuming the same electrical system efficiency as with the L-H_2 example, the amount of ammonia needed at bunkering equates to about 31.6 tons of ammonia (or 4.9 tons of hydrogen). Utilising the specific volumetric and gravimetric energy densities in **Table 15**, the total mass and volume for the storage system is 48.5 tons and 71.0 m^3, respectively, nearly half that of L-H_2.

Assuming the green ammonia from *Yara*, mentioned in **chapter 2.3.1,** is available on the open market, a distribution route from *Herøya* to *Florø* is approximately 545 km and 8 hours [294].

The energy required for synthesising 31.6 tons of ammonia is calculated utilising **equation (8)** and the 66 % efficiency presented in **chapter 2.3.1**. Producing the hydrogen using *either* PEM or alkaline electrolysers, with an upper efficiency of 70 %, as stated in **chapter 2.1.2**, results in a total electricity consumption for the production of ammonia at 320 MWh, which equates to a total water to water (WtW) -efficiency of approximately 27.0 %.

Future WtW-efficiencies *may* reach as high as 38.3 %, utilising a SOEC and HBP combination, if one is to believe the estimates from *Topsøe*, mentioned in **chapter 2.3.1**. **Figure 45** illustrates the losses through the supply chain.

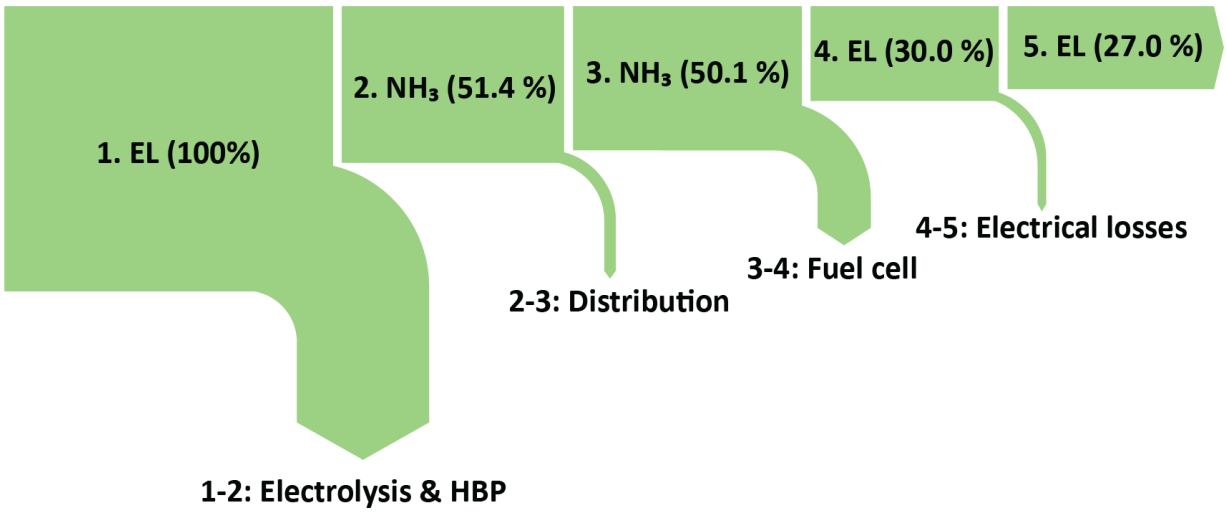

Figure 45: Sankey-diagram illustrating the supply chain of ammonia for MV Rubin.

The CO_2 from the production is approximately 5.5 $tons_{CO_2}$, assuming emission-values with regard to the CO_2 equivalents from the Norwegian mixed-electricity estimates mentioned in **chapter 3.2.4**. Calculating the emissions from the distribution is done by utilising **equaton (18)**, which equates to about 0.9 $tons_{CO_2}$.

3.3.5 LOHC system

The third and final system proposal involves the use of dibenzyltoluene stored in regular fuel tanks. The LOHC is hydrogenated at Fjord Base in accordance with HyFuel's plans [16], and it is assumed that some of the process waste heat is used to keep the viscosity of the H18-DBT reasonably low, which means transport losses are negligible.

Once the on-board system is warmed up (using electrical power from land, or electrical and thermal energy from the diesel backup generator), waste heat from the SOFC is used to maintain the required temperature for the H18-DBT. **Equation (24)** is re-applied, using the LHV of hydrogen instead of ammonia, and a 40% thermal efficiency for the SOFC (see **chapter 2.5.2**), to find the available specific thermal energy of 13 kWh / kg_{H_2}.

According to **Table 6** (**chapter 2.4.5**), the dehydrogenation requires 12 kWh / kg_{H_2}.

Several heat exchangers are needed, and **Figure 46** shows why: In addition to using the waste heat from the SOFC, the heat from the recently dehydrogenated DBT is also recycled. Doing the heat exchange in further stages may also be necessary, as the SOFC waste heat has a temperature of *at least* 600 °C whereas dehydrogenation requires only 300 °C (and temperatures above this significantly decreases the lifetime of DBT). Assuming ideal conditions and heat transfer efficiencies, the LOHC system is self-sustaining after start-up.

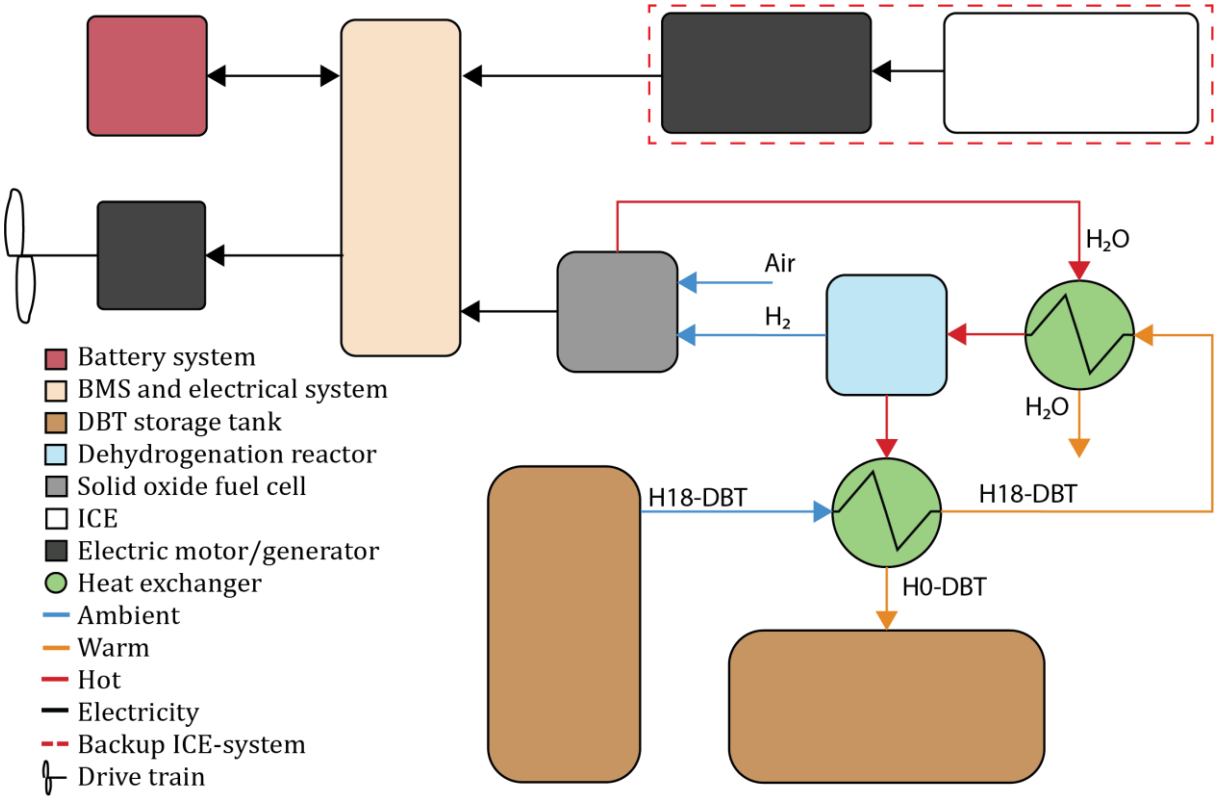

Figure 46: Propulsion system for MV Rubin using DBT and SOFC, created in Illustrator.

Considering the fact that most of the SOFC waste heat is used to further release hydrogen from the carrier, a higher efficiency (or rather, *degree of utilisation*) is achieved. The electrical system losses are the same as for the other two carriers.

Using **equation (8)**, **equation (24)** and **Table 15**, it is estimated that 5.9 tons of hydrogen is required to supply this scenario, which equates to 101 tons of DBT and a total storage weight and volume of 116 tons and 115 m^3, respectively, which is 84 % of the L-H_2 system's volume but 140 % of the mass. Nevertheless, all this DBT, and more, can be stored in the existing fuel tank on MV Rubin, which has a capacity of 250 m^3.

Producing this hydrogen, and bonding it to the carrier molecule, requires 351 MWh of electricity. This results in a 25 % water to water efficiency, as illustrated in **Figure 47**:

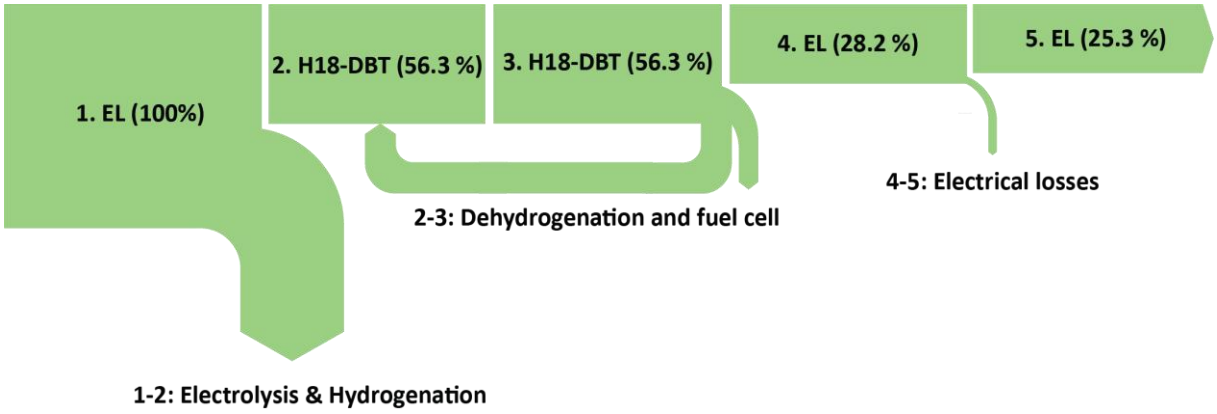

Figure 47: Sankey-diagram illustrating the supply chain of dibenzyltoluene for MV Rubin.

Some of the hydrogenation energy may be regained or utilised for other purposes if enough waste heat is available from the process (after heating up the H-18 DBT to 15-20 °C for pumping).

While the DBT is not transported by diesel truck, the production still uses the same electrical power mix as the other two (see **chapter 3.2.4** or above), resulting in an estimated 6 tons of CO_2 emissions for this case.

4. Discussion

Chapter **2** lays the foundation for evaluating the different hydrogen carriers, while chapter **3** explores the resulting efficiencies, both in a generalised scenario and in a case study. Safety, cost, and emissions are also considered. The following elaboration is intended to provide further insight.

4.1 Renewable hydrogen

While the shipping industry may be successfully decarbonised using either hydrogen carrier technology, care must be taken to not "shift" the emissions elsewhere. The first step is ensuring that the hydrogen is produced in a sufficiently sustainable manner. In this regard any colour of hydrogen will do, except brown and grey, provided the EU CertifHy criteria are also met (as mentioned in **chapter 2.1.1**). As the majority of today's available hydrogen is produced from fossil fuels, *without* carbon capture, ensuring that these emissions are captured and either stored or utilised will be a major priority until renewable hydrogen production has grown in scale. If the demand for hydrogen grows quicker than the available energy from hydropower, solar, wind, etc., then nuclear power *must* be considered as an alternative [295], [296]. Today's nuclear technology is, after all, much safer than it was 35 years ago [297].

The second step is to determine other emissions associated with the production, storage or transportation of hydrogen or the specific carriers. While hydrogen itself has previously been considered entirely harmless in this regard, ongoing research by Cicero suggests that hydrogen gas *may* deplete the ozone layer, as mentioned in **chapter 2.2.3**. If this is the case, transport and storage of pure hydrogen becomes highly undesirable due to the possibility of leaks and boil-off. Ammonia can also boil off, but this is less challenging to handle, and primarily a safety issue (albeit a serious one, see chapter **3.2.5**). Toluene based LOHCs all have the potential to detach the methyl group and form methane as a by-product during hydrogen loading or unloading (elaborated in **chapter 2.4.5**) but these are otherwise very stable molecules.

The third step is evaluating the transport solutions. Trucks running on hydrogen will soon be available, as mentioned in **chapter 3.2.2**, which potentially enables a zero-emissions supply chain within *at least* 5-600 km of the hydrogen production facility, and further if hydrogen is available along the route (or the truck is refuelled from its own cargo). Until then, transport by diesel truck is necessary. According to **chapter 3.2.4** a *total* CO_2 emissions reduction of more than 80 % (compared to MGO and LNG) is achieved for the hydrogen supply chain, regardless of the chosen carrier technology. L-H_2 and DBT transport have similar emissions on account of their similar mass, while ammonia is far more efficient in this regard. Experiments are being done to determine whether some Norwegian roads can allow up to 74-ton truck and trailer combinations, which could further increase the efficiency of the hydrogen transport (and thus reduce emissions), but the results so far indicate excessive wear on the road surface in the spring [298].

A side note regarding transport and supply chain efficiency, is the fact that L-H_2 and DBT solutions carry an almost equal mass *both ways*, creating far higher energy demand for transport than NH_3. This is why methanol, ethanol, or similar synthetic fuels could also be considered as alternatives to achieve carbon *neutrality*. With all the research being done on carbon capture from industry or atmosphere, it would at least make more sense to

utilise the CO_2 rather than pump it into an old oil well and hope it stays there [299]. However, carbon neutral fuels require coordinated efforts between multiple industries.

Finally, **chapter 2.5.4** shows that the combustion of hydrogen or ammonia in ICEs or turbines will likely lead to some emissions as well. Both nitrous oxide and nitrogen oxides have severe environmental effects and must be avoided. The former can be managed by sufficiently high combustion temperatures, but this favours formation of the latter, even in the case of pure hydrogen combustion. However, NO_X exhaust treatment is a well-developed technology. Similarly, although *hydrogen* engine research has only recently gained traction, it builds upon 145 years of experience [300]. It might therefore be conceivable that future ICEs can operate with minimal or zero emissions [301]. Until this is proven, fuel cells are considered the cleaner option, with no potential emissions except thermal NO_X or unreacted hydrogen or ammonia. They are also generally more efficient.

4.2 Sustainable technology

Certain fuel cells, however, do have some *sustainability* issues: Materials and longevity.

Precious metals, primarily platinum, are required for PEM and solid oxide fuel cells and electrolysers (see **chapters 2.1.2** and **2.5.2**). There are great reserves of this metal, but the mining process is associated with significant GHG emissions, energy and water use, and human rights violations [302], [303]. These factors make the use of platinum problematic. As mentioned in **chapter 2.4.5**, platinum is also used for the catalysts in hydrogenation reactors. Both these technologies may require adaptation to other metals before they can be considered sustainable. Similar issues are also reported for the mining of cobalt, a mineral currently used in lithium-ion batteries [304]. Batteries are also necessary in a fuel cell system to provide peak shaving and general load stabilisation (see chapters **2.5.2** and **2.5.3**). This not only benefits the system performance, but also helps to maintain the fuel cell (which deteriorates quicker with greater load variability, especially PEMFC).

One crucial factor that has so far been omitted from this thesis is the *power* requirement. If the power demand varies in a greater range than the chosen fuel cell is suited for, then the battery pack must be dimensioned accordingly. The greater the variability, the larger the battery, and the less weight capacity and volume is available on board for the hydrogen system. In this regard, ICEs are far more flexible (see **chapter 2.5.4**).

When using internal combustion, the fuel purity also becomes far less of an issue. For example, if methane is released from the LOHC during dehydrogenation, then it would simply be burned in the engine and not released to the atmosphere. That being said, it is wise to prevent cracking of the LOHC molecule as much as possible. Although the by-products *can* be filtered out or burned, the utility value of an LOHC is directly related to its longevity. LOHC *blends* may be the key to solve this (see **chapter 2.4.5**).

Either BT or DBT or a mixture can potentially be used interchangeably in an LOHC supply chain, with lower dehydrogenation temperatures and therefore higher efficiencies. Much like various diesel fuels are evaluated for combustion purposes using the *cetane number* (or benzene/gasoline using the *octane number*), it would also be beneficial to have a similar metric for BT/DBT mixtures supplied to different systems and locations depending on local climate and other factors.

A final note regarding sustainability is the potential for synergies with for example the seafood industry. Electrolysis combined with LOHC hydrogenation produces oxygen *and* heat, both of which are useful for onshore fish farms. Additionally, a hydrogen-electric fish feed carrier vessel should make far less noise when unloading food at offshore fish farms, reducing stress on the fish and increasing welfare [305].

4.3 Water to water efficiency

From production to expenditure, the analysis of a generalised case in **chapter 3.2.2** finds that the liquid hydrogen supply chain is 20 % efficient, while the supplies of ammonia and dibenzyltoluene are both 15 % efficient. However, generalisations are generally flawed, and this one is no exception.

The first issue regards liquid hydrogen boil-off, which is considered negligible assuming a conservative 1000 km range and smooth sailing (or, rather, trucking) the entire way. This may not be the case, and longer routes, traffic jams, driver stops, ferry crossings, etc., will result in more time on the road and therefore increased boil-off.

Second, an equal distance travelled is idealised, and transport losses for real cases like MV Rubin must be calculated based on the relative positions of the production and bunkering sites. **Chapters 3.3.3**, **3.3.4**, and **3.3.5** show the impact of this consideration, particularly with DBT production at Fjord Base allowing for complete omission of transport losses.

Third, while liquid hydrogen does not require additional energy supplied before use (except some low-quality ambient heat), ammonia and dibenzyltoluene require hydrogen separation. In the generalised case, the energy required for this process is supplied by burning the hydrogen directly, which negatively impacts the total efficiency. When proposing systems for MV Rubin, this loss was remedied by using the waste heat of a SOFC to crack and dehydrogenate the NH_3 and DBT, respectively. This is not possible with the other fuel cell types, as the operating temperatures are far too low. However, ICEs running on ammonia or hydrogen may be able to supply this thermal energy from the exhaust.

Liquid hydrogen also gains efficiency in the powertrain: The hydrogen is used to cool intake air, thereby cleansing it of CO_2, allowing for the use of an alkaline fuel cell with greater efficiency than a PEMFC or SOFC would have in this scenario.

Considering the above, a ship like MV Rubin has an L-H_2 supply efficiency of 31 %, while the NH_3 supply is 27 % efficient and the DBT supply is 25 % efficient. The liquid hydrogen is produced at Mongstad, the ammonia is produced at Herøya, and the dibenzyltoluene is, as mentioned, produced at Fjord Base, near the bunkering site, in Florø. Optimisation of the hydrogen production is not considered, other than the use of waste heat from the hydrogenation to maintain 15 – 20 °C in the H-18 DBT, to compensate for the increasing viscosity at lower temperatures.

While L-H_2 is the more efficient solution in both cases, ammonia or LOHC systems may have beneficial properties that make them more suitable for maritime applications.

4.4 Determining factors for the maritime use of hydrogen

Directly related to the energy efficiency is cost. A less efficient supply requires more energy for the same amount of useful work, which means the ship operation becomes more expensive. **Chapter 3.2.3** compares estimates of the capital and operational expenses of different electrolysers and includes the price of electricity to find a generalised fuel cost for all three hydrogen carrier technologies. This is carried over into **chapter 3.2.4** where transportation costs (corresponding to the generalised case) are included as well. L-H_2 and DBT are both estimated to cost between 5 and 6.7 €/kg_{H_2}, while NH_3 and the simpler LOHC toluene are roughly 1.5 €/kg_{H_2} *cheaper*.

Equipment costs for powertrain components are not considered in this thesis, as prices are either difficult or downright impossible to acquire. Furthermore, ship specific design considerations will also have a significant impact on the cost of a hydrogen retrofit or a new ship. Similarly, space requirements are not considered either, but this *is* a major disadvantage for liquid hydrogen which has to be stored on deck to minimise the risks and consequences of explosions [13].

The most critical consideration, aside from energy efficiency, is therefore safety. Lower risk of harm to personnel and environment is more ethical, and directly impacts system complexity (i.e., space requirements) and costs. **Chapter 3.2.5** examines the most relevant safety concerns of the three hydrogen carrier technologies.

Liquid hydrogen, turned gaseous before use, is extremely volatile. It ignites easily, burns in a wide range of concentrations in air, and is also explosive (albeit in a slightly narrower range). Furthermore, the gas is colourless and odourless, meaning hydrogen detectors and venting systems are required in every application. An L-H_2 leak will not immediately evaporate but stays on the ground like a dense gas, freezing the surroundings. If the liquid hydrogen is ignited in cold, purified air, the resulting explosion becomes even more violent.

Ammonia carries much lower risk of flammability and explosions, but is highly toxic. Although one can very easily smell a leak, this inhalation might well be a sailor's last. Skin exposure is equally undesirable, meaning protective gear must be worn by technicians and engineers. Spills of ammonia are also a danger to sea life.

Dibenzyltoluene is *barely* flammable, non-explosive, behaves like diesel fuel, and is an aromatic compound, which means leaks are easily detectable without technicians being in immediate danger. Prolonged skin exposure may have adverse health effects, and ingestion is very likely fatal, but this is easily avoidable. However, a downside to the use of DBT is the potential for large oil spills due to the sheer volume of fuel required. Benzene based compounds are also carcinogens, which becomes an increasing concern with simpler LOHCs like BT or toluene because of higher vapour pressures and smaller molecules.

While every risk is manageable with appropriate procedures and advances in technology, it is worth invoking what is today known as Murphy's Law, more eloquently elaborated by the British engineer Alfred Holt in 1877 [306]:

"*It is found that anything that can go wrong at sea generally does go wrong sooner or later, so it is not to be wondered that owners prefer the safe to the scientific. It is also found that it is almost as bad to have too many parts as too few; that arrangements which are for exceptional and occasional use are rarely available when wanted, and have the disadvantage of requiring additional care. Their very presence, too, seems in effect to indispose the engineer to attend to essentials. Sufficient stress can hardly be laid on the advantages of simplicity. The human factor cannot be safely neglected in planning machinery. If attention is to be obtained, the engine must be such that the engineer will be disposed to attend to it*."

Although Holt clearly referred to the steam powertrains that drove ships at the time, his comment still holds true today: A simpler and safer system is inherently more reliable and cost effective because humans are the primary cause of incidents and accidents, no matter how many sensors and safety systems are employed.

5. Conclusion

Hydrogen is undoubtedly a viable vector for renewable energy, and its use for ship propulsion has the potential to greatly reduce greenhouse gas emissions. The hydrogen carrier technologies are sustainable if the issues regarding precious metals and longevity (for both fuel cells and LOHCs) are solved.

Although the energy densities of L-H_2, NH_3 and DBT are very dissimilar, the differences are significantly reduced when including storage. This favours DBT, which can be stored in regular fuel tanks.

Liquid hydrogen is the most efficient carrier technology among those considered in this thesis, but the required system complexity and the high risk of fire and explosions are both considered unacceptable trade-offs.

Ammonia, the second most efficient carrier, has different problems but the same conclusion is drawn; Designing systems where people are at risk of exposure to highly toxic substances is a steep price to pay for a few extra percent efficiency and a slightly lower fuel cost.

Dibenzyltoluene as a liquid organic hydrogen carrier, although not completely harmless, is by far the safest alternative, with only a few percent reduction in energy efficiency compared to the other carrier technologies. The added cost of fuel and transport may well be recuperated by the DBT system being simpler and safer. Smaller ships like MV Rubin have more than enough room in the fuel tank for a sufficient amount of DBT, but doing the same on bigger ships might become a challenge.

6. Suggested further work

If liquid organic hydrogen carriers are to be implemented in colder climates, a thorough investigation of viscosities at lower temperatures must be conducted. An interchangeable selection of additives and/or LOHC mixtures could be proposed for varying climates.

Furthermore, powertrains using LOHCs in conjunction with fuel cells or combustion engines (or both) must be designed and tested.

Methane emissions from toluene based LOHCs are hitherto insufficiently scrutinised.

Thermal NOx from SOFCs is also a concern that must be investigated.

Further development of the Python code in **Attachment 4** could be useful for future projects.

7. References

[1] "Techno-economic assessment of zero-carbon fuels," Lloyd's Register, Mar. 2020. Accessed: Feb. 02, 2021. [Online]. Available: https://www.lr.org/en/insights/global-marine-trends-2030/techno-economic-assessment-of-zero-carbon-fuels/

[2] P. E. Miranda, *Science and Engineering of Hydrogen-Based Energy Technologies: Hydrogen Production and Practical Applications in Energy Generation*. Elsevier Science, 2018. [Online]. Available: https://books.google.no/books?id=e5t5DwAAQBAJ

[3] European Commission, "Reducing emissions from the shipping sector," *Climate Action - European Commission*, Nov. 23, 2016. https://ec.europa.eu/clima/policies/transport/shipping_en (accessed Feb. 12, 2021).

[4] IMO, "Reducing greenhouse gas emissions from ships," *International Maritime Organization*. https://www.imo.org/en/MediaCentre/HotTopics/Pages/Reducing-greenhouse-gas-emissions-from-ships.aspx (accessed Feb. 25, 2021).

[5] Norsk klimastiftelse, "Utvikling av brenselcellen som skal brukes i Eidesviks Viking Energy," Jun. 04, 2020. https://www.youtube.com/watch?v=iOXvN3DKHyk&ab_channel=Norskklimastiftelse (accessed Apr. 13, 2021).

[6] "World first for liquid hydrogen transportation.," *Lloyd's Register*. https://www.lr.org/en/insights/articles/world-first-for-liquid-hydrogen-transportation/ (accessed Apr. 12, 2021).

[7] Shell, "Shell hydrogen study," Wuppertal Institut, Hamburg, Germany, 019–0039, 2017. Accessed: Mar. 18, 2021. [Online]. Available: https://www.shell.com/energy-and-innovation/new-energies/hydrogen/_jcr_content/par/keybenefits/link.stream/1496312627865/6a3564d61b9aff43e087972db5212be68d1fb2e8/shell-h2-study-new.pdf

[8] T. Stensvold, "Wärtsilä-motor til Stord for å teste ammoniakk i fullskala," *Tu.no*, Jun. 30, 2020. https://www.tu.no/artikler/wartsila-motor-til-stord-for-a-teste-ammoniakk-i-fullskala/495140 (accessed Apr. 12, 2021).

[9] DNV GL, "Ammonia as a Marine Fuel Safety Handbook," DNV GL, Norway, Safety Handbook, 2021. Accessed: Feb. 15, 2021. [Online]. Available: https://www.dnvgl.com/Publications/ammonia-as-a-marine-fuel-191385

[10] S. Huang, "Hydrogen stored as an oil!," Erlangen, Oct. 2020.

[11] DNV GL, "Produksjon og bruk av hydrogen i Norge," Klima- og miljødepartementet, Norge, 019–0039, Jan. 2019. Accessed: Oct. 03, 2021. [Online]. Available: https://www.regjeringen.no/contentassets/0762c0682ad04e6abd66a9555e7468df/hydrogen-i-norge---synteserapport.pdf

[12] N. Brückner *et al.*, "Evaluation of Industrially Applied Heat-Transfer Fluids as Liquid Organic Hydrogen Carrier Systems," *ChemSusChem*, vol. 7, no. 1, pp. 229–235, Jan. 2014, doi: 10.1002/cssc.201300426.

[13] O. R. Hansen, "Hydrogen and Ammonia Infrastructure - Safety and Risk Information and Guidance," Lloyd's Register & Ocean Hyway Cluster, PRJ11100256122r1, May 2020.

[14] K. Gjerstad, "Produksjonsanlegg for Hydrogen legges til Mongstad.," *Industri Energi Equinor*, May 13, 2020. https://www.industrienergiequinor.no/2020/05/13/produksjonsanlegg-for-hydrogen-legges-til-mongstad/ (accessed Apr. 15, 2021).

[15] "Åpner for historisk satsing på grønt hydrogen og grønn ammoniakk i Norge | Yara International," *Yara None*, Feb. 18, 2021. https://www.yara.com/corporate-releases/apner-for-historisk-satsing-pa-gront-hydrogen-og-gronn-ammoniakk-i-norge/ (accessed Apr. 17, 2021).

[16] INC Gruppen, "Hydrogenprosjekt," *INC Gruppen*. https://www.incgruppen.no/saga-fjordbase-as/hydrogenprosjekt/ (accessed May 14, 2021).

[17] Ocean Hyway Cluster, "About us," *Arena Ocean Hyway Cluster*. https://www.oceanhywaycluster.no/about-us (accessed Feb. 12, 2021).

[18] M. Purkis, "Inspiring (and inspiration from) the next generation," *Arena Ocean Hyway Cluster*, Feb. 09, 2021. https://www.oceanhywaycluster.no/news/hvlcollaboration (accessed Apr. 13, 2021).

[19] J. Gretz, J. P. Baselt, O. Ullmann, and H. Wendt, "The 100 MW euro-Quebec hydro-hydrogen pilot project," *International Journal of Hydrogen Energy*, vol. 15, no. 6, pp. 419–424, Jan. 1990, doi: 10.1016/0360-3199(90)90199-9.

[20] B. Drolet, J. Gretz, D. Kluyskens, F. Sandmann, and R. Wurster, "The Euro-Quebec Hydro-hydrogen pilot project [EQHHPP]: demonstration phase," *International Journal of Hydrogen Energy*, vol. 21, pp. 305–316, Apr. 1996, doi: 10.1016/0360-3199(95)00083-6.

[21] A. T. Wijayanta, T. Oda, C. W. Purnomo, T. Kashiwagi, and M. Aziz, "Liquid hydrogen, methylcyclohexane, and ammonia as potential hydrogen storage: Comparison review," *International Journal of Hydrogen Energy*, vol. 44, no. 29, pp. 15026–15044, Jun. 2019, doi: 10.1016/j.ijhydene.2019.04.112.

[22] L. V. Hoecke, L. Laffineur, R. Campe, P. Perreault, S. W. Verbruggen, and S. Lenaerts, "Challenges in the use of hydrogen for maritime applications," *Energy Environ. Sci.*, vol. 14, no. 2, pp. 815–843, Feb. 2021, doi: 10.1039/D0EE01545H.

[23] R. Moradi and K. M. Groth, "Hydrogen storage and delivery: Review of the state of the art technologies and risk and reliability analysis," *International Journal of Hydrogen Energy*, vol. 44, no. 23, pp. 12254–12269, May 2019, doi: 10.1016/j.ijhydene.2019.03.041.

[24] T. Helmenstine, "Molecule Atom Colors - CPK Colors," *Science Notes and Projects*, Aug. 28, 2019. https://sciencenotes.org/molecule-atom-colors-cpk-colors/ (accessed Mar. 06, 2021).

[25] Ebbing and Gammon, *General Chemistry*, Eleventh edition. USA: Cengage Learning, 2015.

[26] Y. A. Çengel and M. A. Boles, *Thermodynamics An Engineering Approach*, Eighth edition. New York: McGraw-Hill Education, 2015.

[27] A. Léon, Ed., *Hydrogen technology: mobile and portable applications ; with 50 tables*. Berlin: Springer, 2008.

[28] J. Parnell and N. Blamey, "Global hydrogen reservoirs in basement and basins," *Geochem Trans*, vol. 18, Mar. 2017, doi: 10.1186/s12932-017-0041-4.

[29] "The Future of Hydrogen – Analysis," *IEA*. https://www.iea.org/reports/the-future-of-hydrogen (accessed Apr. 14, 2021).

[30] S. Giovannini, "50 shades of (grey and blue and green) hydrogen," *Energy Cities*, Nov. 13, 2020. https://energy-cities.eu/50-shades-of-grey-and-blue-and-green-hydrogen/ (accessed Apr. 13, 2021).

[31] Blue Move, "The Blue Move for a Green Economy," Blue Move, Norge, Jan. 2017. Accessed: Apr. 16, 2021. [Online]. Available: https://www.regjeringen.no/contentassets/0762c0682ad04e6abd66a9555e7468df/hydrogen-i-norge---synteserapport.pdf

[32] S. M. Holst *et al.*, "Hydrogen verdikjeder og potensial," 5, May 2016.

[33] Britannia, "electrolysis | Definition, Uses, & Facts | Britannica." https://www.britannica.com/science/electrolysis (accessed Apr. 14, 2021).

[34] M. Purkis, "Hydrogen Technology and Supply Chains to the Maritime Sector - B," Norway, B, Dec. 2020. Accessed: Apr. 13, 2021. [Online]. Available:

https://static1.squarespace.com/static/5d1c6c223c9d400001e2f407/t/5fdb362533c6977cf5b32e7f/1608201769287/Endelig+rapport_B.0+Hydrogen+value+chains+2030_V4.pdf

[35] M. Newborough and G. Cooley, "Green hydrogen: The only oxygen and water balanced fuel," *Fuel Cells Bulletin*, p. 4, 2021.

[36] "Hydrocarbon Combustion - an overview | ScienceDirect Topics." https://www.sciencedirect.com/topics/earth-and-planetary-sciences/hydrocarbon-combustion (accessed Apr. 14, 2021).

[37] M. Noussan, P. P. Raimondi, R. Scita, and M. Hafner, "The Role of Green and Blue Hydrogen in the Energy Transition—A Technological and Geopolitical Perspective," *Sustainability*, vol. 13, no. 1, p. 298, Dec. 2020, doi: 10.3390/su13010298.

[38] R. Dickel, *Blue hydrogen as an enabler of green hydrogen the case of Germany*. 2020. Accessed: Apr. 14, 2021. [Online]. Available: https://www.oxfordenergy.org/wpcms/wp-content/uploads/2020/06/Blue-hydrogen-as-an-enabler-of-green-hydrogen-the-case-of-Germany-NG-159.pdf

[39] "Hydrogen Production: Natural Gas Reforming," *Energy.gov*. https://www.energy.gov/eere/fuelcells/hydrogen-production-natural-gas-reforming (accessed Apr. 14, 2021).

[40] F. Farshchi Tabrizi, S. A. H. S. Mousavi, and H. Atashi, "Thermodynamic analysis of steam reforming of methane with statistical approaches," *Energy Conversion and Management*, vol. 103, pp. 1065–1077, Oct. 2015, doi: 10.1016/j.enconman.2015.07.005.

[41] H. Idriss, M. Scott, and V. Subramani, "1 - Introduction to hydrogen and its properties," in *Compendium of Hydrogen Energy*, V. Subramani, A. Basile, and T. N. Veziroğlu, Eds. Oxford: Woodhead Publishing, 2015, pp. 3–19. doi: 10.1016/B978-1-78242-361-4.00001-7.

[42] J.-M. Lavoie, "Review on dry reforming of methane, a potentially more environmentally-friendly approach to the increasing natural gas exploitation," *Front. Chem.*, vol. 2, 2014, doi: 10.3389/fchem.2014.00081.

[43] Fertilizers europe, "How fertilizers are made?," *Fertilizers Europe*. https://www.fertilizerseurope.com/fertilizers-in-europe/how-fertilizers-are-made/ (accessed Apr. 14, 2021).

[44] U. Frøhlke, "Haldor Topsoe to build large-scale SOEC electrolyzer manufacturing facility to meet customer needs for green hydrogen production." https://blog.topsoe.com/haldor-topsoe-to-build-large-scale-soec-electrolyzer-manufacturing-facility-to-meet-customer-needs-for-green-hydrogen-production (accessed Apr. 14, 2021).

[45] Y. Guo, G. Li, J. Zhou, and Y. Liu, "Comparison between hydrogen production by alkaline water electrolysis and hydrogen production by PEM electrolysis," *IOP Conf. Ser.: Earth Environ. Sci.*, vol. 371, p. 042022, Dec. 2019, doi: 10.1088/1755-1315/371/4/042022.

[46] G. Chisholm and L. Cronin, "Hydrogen From Water Electrolysis," in *Storing Energy*, Elsevier, 2016, pp. 315–343. doi: 10.1016/B978-0-12-803440-8.00016-6.

[47] A. Keçebaş, M. Kayfeci, and M. Bayat, "Chapter 9 - Electrochemical hydrogen generation," in *Solar Hydrogen Production*, F. Calise, M. D. D'Accadia, M. Santarelli, A. Lanzini, and D. Ferrero, Eds. Academic Press, 2019, pp. 299–317. doi: 10.1016/B978-0-12-814853-2.00009-6.

[48] G. Chisholm and L. Cronin, "Chapter 16 - Hydrogen From Water Electrolysis," in *Storing Energy*, T. M. Letcher, Ed. Oxford: Elsevier, 2016, pp. 315–343. doi: 10.1016/B978-0-12-803440-8.00016-6.

[49] "Atmospheric Alkaline Electrolyser," *Nel Hydrogen*, May 31, 2018. https://nelhydrogen.com/product/atmospheric-alkaline-electrolyser-a-series/ (accessed Apr. 19, 2021).

[50] "Alkaline Water Electrolysis - an overview | ScienceDirect Topics." https://www.sciencedirect.com/topics/engineering/alkaline-water-electrolysis (accessed Apr. 13, 2021).

[51] "Parts of a Fuel Cell," *Energy.gov*. https://www.energy.gov/eere/fuelcells/parts-fuel-cell (accessed Apr. 14, 2021).

[52] M. Carmo, D. L. Fritz, J. Mergel, and D. Stolten, "A comprehensive review on PEM water electrolysis," *International Journal of Hydrogen Energy*, vol. 38, no. 12, pp. 4901–4934, Apr. 2013, doi: 10.1016/j.ijhydene.2013.01.151.

[53] BASF, "BASF Catalysts - Metal Prices," Apr. 16, 2021. https://apps.catalysts.basf.com/apps/eibprices/mp/ (accessed Apr. 17, 2021).

[54] M. Hall, "The five most expensive metals and where they are mined." https://www.mining-technology.com/features/five-most-expensive-metals-and-where-they-are-mined/ (accessed Apr. 14, 2021).

[55] "Water electrolysers / hydrogen generators," *Nel Hydrogen*. https://nelhydrogen.com/water-electrolysers-hydrogen-generators/ (accessed Apr. 19, 2021).

[56] S. T. Revankar, "Chapter Four - Nuclear Hydrogen Production," in *Storage and Hybridization of Nuclear Energy*, H. Bindra and S. Revankar, Eds. Academic Press, 2019, pp. 49–117. doi: 10.1016/B978-0-12-813975-2.00004-1.

[57] A. Velazquez Abad and P. E. Dodds, "Production of Hydrogen," in *Encyclopedia of Sustainable Technologies*, M. A. Abraham, Ed. Oxford: Elsevier, 2017, pp. 293–304. doi: 10.1016/B978-0-12-409548-9.10117-4.

[58] D. Xu, L. Dong, and J. Ren, "Chapter 2 - Introduction of Hydrogen Routines," in *Hydrogen Economy*, A. Scipioni, A. Manzardo, and J. Ren, Eds. Academic Press, 2017, pp. 35–54. doi: 10.1016/B978-0-12-811132-1.00002-X.

[59] C. C. Vaso and R. B. M. Cervera, "Preparation and Conductivity Measurements of LSM/YSZ Composite Solid Oxide Electrolysis Cell Anode Materials," *International Journal of Materials and Metallurgical Engineering*, vol. 11, no. 1, pp. 23–27, Nov. 2016.

[60] NIST Chemistro WebBook, "Isothermal Properties for Hydrogen," *National Institute of Standards an Technology*. https://webbook.nist.gov/cgi/fluid.cgi?T=20&PLow=0&PHigh=5&PInc=1&Applet=on&Digits=5&ID=C1333740&Action=Load&Type=IsoTherm&TUnit=C&PUnit=bar&DUnit=kg%2Fm3&HUnit=kJ%2Fkg&WUnit=m%2Fs&VisUnit=cP&STUnit=N%2Fm&RefState=DEF (accessed Feb. 01, 2021).

[61] Engineering toolbox, "Fossil and Alternative Fuels Energy Content." https://www.engineeringtoolbox.com/fossil-fuels-energy-content-d_1298.html (accessed Apr. 14, 2021).

[62] "Cryogenics | physics," *Encyclopedia Britannica*. https://www.britannica.com/science/cryogenics (accessed Apr. 19, 2021).

[63] National Institute of Standards and Technology, "Isothermal properties for liquid Hydrogen," *NIST*. https://webbook.nist.gov/cgi/fluid.cgi?T=-253&PLow=0&PHigh=15&PInc=1&Applet=on&Digits=5&ID=C1333740&Action=Load&Type=IsoTherm&TUnit=C&PUnit=bar&DUnit=kg%2Fm3&HUnit=kJ%2Fkg&WUnit=m%2Fs&VisUnit=cP&STUnit=N%2Fm&RefState=DEF (accessed Apr. 16, 2021).

[64] W. Peschka, "Liquid Hydrogen Technology Present State and Future Fuel Application," in *Hydrogen Power: Theoretical and Engineering Solutions*, T. O. Saetre, Ed. Dordrecht: Springer Netherlands, 1998, pp. 517–528. doi: 10.1007/978-94-015-9054-9_69.

[65] NCE Maritime CleanTech, "Norwegian future value chains for liquid hydrogen," Nov. 2016. [Online]. Available: https://maritimecleantech.no/wp-content/uploads/2016/11/Report-liquid-hydrogen.pdf

[66] H. T. Walnum *et al.*, "Principles for the liquefaction of hydrogen with emphasis on precooling processes," *IIR Conference - Dresden*, vol. 12th Cryogenics 2012, no. ID: 080, p. 8, Sep. 2012.

[67] D. O. Berstad, J. H. Stang, and P. Nekså, "Large-scale hydrogen liquefier utilising mixed-refrigerant pre-cooling," *International Journal of Hydrogen Energy*, vol. 35, no. 10, pp. 4512–4523, May 2010, doi: 10.1016/j.ijhydene.2010.02.001.

[68] B. OldWolf, "What Are the Freezing, Melting, and Boiling Points of Solids, Liquids, and Gases?," *Owlcation*, Jan. 28, 2020. https://owlcation.com/stem/Freezing-Melting-and-Boiling-Points-of-Solids-Liquids-and-Gases-in-general-use-today (accessed Apr. 15, 2021).

[69] EnvironmentalChemistry.com, "Periodic Table of Elements: Sorted by Melting Point (EnvironmentalChemistry.com)," *Environmental, Chemistry & Hazardous Materials News, Careers & Resources*. https://environmentalchemistry.com/yogi/periodic/meltingpoint.html (accessed Apr. 15, 2021).

[70] "Hydrogen liquefiers," *Linde Engineering*. https://www.linde-engineering.com/en/process-plants/cryogenic_plants/hydrogen_liquefiers/index.html (accessed Apr. 19, 2021).

[71] L. Yin and Y. Ju, "Review on the design and optimization of hydrogen liquefaction processes," *Front. Energy*, vol. 14, no. 3, pp. 530–544, Sep. 2020, doi: 10.1007/s11708-019-0657-4.

[72] N. Lümmen, "Prosjekt #2157970 - Cryokjøler for flytendegjøring av hydrogen - Cristin," Sep. 15, 2020. https://app.cristin.no/projects/show.jsf?id=2157970 (accessed Apr. 15, 2021).

[73] "Space Applications of Hydrogen and Fuel Cells | NASA." https://www.nasa.gov/content/space-applications-of-hydrogen-and-fuel-cells (accessed Apr. 15, 2021).

[74] N. Bray, "Hydrogen Topic Page," *NASA*, Apr. 15, 2015. http://www.nasa.gov/topics/technology/hydrogen/index.html (accessed Apr. 15, 2021).

[75] M. Kolodziej, "Water Contamination in Hydrogen-Cooled Generators Lurks as Serious Operational Threat," *Power Engineering*, Aug. 01, 2003. https://www.power-eng.com/coal/water-contamination-in-hydrogen-cooled-generators-lurks-as-serious-operational-threat/ (accessed Apr. 15, 2021).

[76] Marco Succi, Giorgio Macchi, and Sarah Riddle Vogt, "High Purity Hydrogen: Guidelines to Select the Most Suitable Purification Technology," *JEE*, vol. 5, no. 5, Sep. 2017, doi: 10.17265/2328-2223/2017.05.005.

[77] M. Ursan, "What is boil-off?" The LNG task force meeting in Brussels, Nov. 03, 2011. Accessed: Apr. 19, 2021. [Online]. Available: https://unece.org/fileadmin/DAM/trans/doc/2011/wp29grpe/LNG_TF-02-06e.pdf

[78] SUSI Partners, "Hydrogen Energy Infrastructure," Paul Scherrer Institute, witzerland, Whitepaper, 2020. Accessed: Apr. 15, 2021. [Online]. Available: https://www.susi-partners.com/news-research/#research

[79] H. Derking, Luuk van der Togt, and Marcel Keezer, "Liquid Hydrogen Storage: Status and Future Persectives," presented at the Cryogenic Heat and Mass Transfer, Enschede, The Netherlands, Nov. 04, 2019. Accessed: Apr. 19, 2021. [Online]. Available: https://www.utwente.nl/en/tnw/ems/research/ats/chmt/m13-hendrie-derking-cryoworld-chmt-2019.pdf

[80] "Cryogenics: Low temperatures, high performance," *CERN*. https://home.cern/science/engineering/cryogenics-low-temperatures-high-performance (accessed Apr. 19, 2021).

[81] L. Decker, "Liquid Hydrogen Distribution Technology," presented at the Hyper Closing Seminar, Brussels, Belgium, Nov. 12, 2019. Accessed: Apr. 19, 2021. [Online]. Available: https://www.sintef.no/globalassets/project/hyper/presentations-day-2/day2_1105_decker_liquid-hydrogen-distribution-technology_linde.pdf

[82] G. Petitpas, "Boil-off losses along LH2 pathway," Lawrence Livermore Natinal Laboratory, Technical report LLNL-TR-750685, Feb. 2018. Accessed: Apr. 19, 2021. [Online]. Available: https://www.osti.gov/servlets/purl/1466121

[83] E. Borgan, "Norge skal satse på hydrogen. Men hva skjer når gassen lekker ut?," Feb. 09, 2021. https://forskning.no/a/1810484 (accessed Apr. 15, 2021).

[84] Cicero, "CICERO skal forske på klimaeffektene av hydrogenutslipp - Cicero." https://cicero.oslo.no/no/posts/prosjekter/cicero-skal-forske-paa-klimaeffektene-av-hydrogenutslipp (accessed Apr. 16, 2021).

[85] M. Aasadnia and M. Mehrpooya, "Large-scale liquid hydrogen production methods and approaches: A review," *Applied Energy*, vol. 212, pp. 57–83, Feb. 2018, doi: 10.1016/j.apenergy.2017.12.033.

[86] M. Ball and M. Weeda, "The hydrogen economy—Vision or reality?," in *Compendium of Hydrogen Energy*, Elsevier, 2016, pp. 237–266. doi: 10.1016/B978-1-78242-364-5.00011-7.

[87] CNH Industrial, "Truck Architecture and Hydrogen Storage," Turin, Oct. 28, 2020. [Online]. Available: https://ec.europa.eu/jrc/sites/jrcsh/files/cnh_20201028_-_truck_architecture_public.pdf

[88] "Physical Hydrogen Storage," *Energy.gov*. https://www.energy.gov/eere/fuelcells/physical-hydrogen-storage (accessed Apr. 15, 2021).

[89] "Manufacturing of ammonia by Haber's process," *worldofchemicals.com*, Feb. 25, 2014. https://www.worldofchemicals.com/442/chemistry-articles/manufacturing-of-ammonia-by-habers-process.html (accessed Apr. 17, 2021).

[90] PubChem, "Ammonia." https://pubchem.ncbi.nlm.nih.gov/compound/222 (accessed Feb. 01, 2021).

[91] V. Hacker and K. Kordesch, "Ammonia crackers," in *Handbook of Fuel Cells*, W. Vielstich, A. Lamm, H. A. Gasteiger, and H. Yokokawa, Eds. Chichester, UK: John Wiley & Sons, Ltd, 2010, p. f302011. doi: 10.1002/9780470974001.f302011.

[92] H. Kobayashi, A. Hayakawa, K. D. K. A. Somarathne, and E. C. Okafor, "Science and technology of ammonia combustion," *Proceedings of the Combustion Institute*, vol. 37, no. 1, pp. 109–133, Jan. 2019, doi: 10.1016/j.proci.2018.09.029.

[93] A. Valera-Medina, H. Xiao, M. Owen-Jones, W. I. F. David, and P. J. Bowen, "Ammonia for power," *Progress in Energy and Combustion Science*, vol. 69, pp. 63–102, Nov. 2018, doi: 10.1016/j.pecs.2018.07.001.

[94] The Royal Society, *Ammonia: zero-carbon fertiliser, fuel and energy store*. 2020.

[95] The Royal Society, "Green ammonia | Royal Society," Feb. 19, 2020. https://royalsociety.org/topics-policy/projects/low-carbon-energy-programme/green-ammonia/ (accessed Mar. 17, 2021).

[96] Alfa Laval, "Ammonfuel - An industrial view of ammonia as a marine fuel," ALFA LAVAL, Aug. 2020. Accessed: Apr. 02, 2021. [Online]. Available: https://hafniabw.com/wp-content/uploads/2020/08/Ammonfuel-Report-an-industrial-view-of-ammonia-as-a-marine-fuel.pdf

[97] K. Mögenburg, "Ammoniakk," *Yara Norge*, Mar. 28, 2018. https://www.yara.no/kjemiske-og-miljomessige-losninger/prosesskjemikalier/ammoniakk/ (accessed Feb. 01, 2021).

[98] "Reducing NOx with SNCR and SCR systems using Ammonia Solution | Yara International," *Yara Norge*, Feb. 28, 2018. https://www.yara.com/chemical-and-environmental-solutions/exhaust-gas-treatment-for-industrial-plants/ammonia-solution/ (accessed Feb. 01, 2021).

[99] T. Brown, "The Future of Ammonia: Improvement of Haber-Bosch … or Electrochemical Synthesis?," Nov. 17, 2017. https://ammoniaindustry.com/the-future-of-ammonia-improvement-of-haber-bosch-or-electrochemical-synthesis/ (accessed Feb. 11, 2021).

[100] Britannica, "Haber-Bosch process | Definition, Conditions, Importance, & Facts," *Encyclopedia Britannica*. https://www.britannica.com/technology/Haber-Bosch-process (accessed Feb. 04, 2021).

[101] S. Chen, S. Perathoner, C. Ampelli, and G. Centi, "Chapter 2 - Electrochemical Dinitrogen Activation: To Find a Sustainable Way to Produce Ammonia," in *Studies in Surface Science and Catalysis*, vol. 178, S. Albonetti, S. Perathoner, and E. A. Quadrelli, Eds. Elsevier, 2019, pp. 31–46. doi: 10.1016/B978-0-444-64127-4.00002-1.

[102] T. Lipman and N. Shah, "Ammonia as an Alternative Energy Storage Medium for Hydrogen Fuel Cells: Scientific and Technical Review for Near-Term Stationary Power Demonstration Projects, Final Report," Nov. 2007, Accessed: Feb. 04, 2021. [Online]. Available: https://escholarship.org/uc/item/7z69v4wp

[103] "Standard state and enthalpy of formation, Gibbs free energy of formation, entropy and heat capacity." https://www.engineeringtoolbox.com/standard-state-enthalpy-formation-definition-value-Gibbs-free-energy-entropy-molar-heat-capacity-d_1978.html (accessed May 02, 2021).

[104] "The Haber Process for the manufacture of ammonia." https://www.chemguide.co.uk/physical/equilibria/haber.html (accessed Feb. 04, 2021).

[105] "Ammonia storage - WIND ENERGY STORAGE." http://www.esru.strath.ac.uk/EandE/Web_sites/17-18/windies/ammonia-storage.html (accessed Apr. 19, 2021).

[106] C. Smith, A. K. Hill, and L. Torrente-Murciano, "Current and future role of Haber–Bosch ammonia in a carbon-free energy landscape," *Energy & Environmental Science*, vol. 13, no. 2, pp. 331–344, 2020, doi: 10.1039/C9EE02873K.

[107] A. Risholm and Amon Maritime, "Ammonia value chains," Ocean Hyway Cluster, Florø, OHC HI B.2, Nov. 2020.

[108] Rusch, Emilie, "Reversible protonic ceramic fuel cells able to store energy," Mar. 18, 2019. https://www.minesnewsroom.com/news/reversible-protonic-ceramic-fuel-cells-able-store-energy (accessed Feb. 15, 2021).

[109] C. Duan *et al.*, "Highly efficient reversible protonic ceramic electrochemical cells for power generation and fuel production," *Nature Energy*, vol. 4, pp. 230–240, Mar. 2019, doi: 10.1038/s41560-019-0333-2.

[110] R. F. ServiceJul. 12, 2018, and 2:00 Pm, "Ammonia—a renewable fuel made from sun, air, and water—could power the globe without carbon," *Science | AAAS*, Jul. 12, 2018. https://www.sciencemag.org/news/2018/07/ammonia-renewable-fuel-made-sun-air-and-water-could-power-globe-without-carbon (accessed Feb. 15, 2021).

[111] "ammonia stress corrosion cracking." https://inspectioneering.com/tag/ammonia+stress+corrosion+cracking (accessed Apr. 19, 2021).

[112] G. Kobrin, *Stainless Steel in Ammonia Production*. Washingtoin, D.C.: American Iron and Steel Institute, 1978. Accessed: Feb. 02, 2021. [Online]. Available: https://nickelinstitute.org/media/1817/stainlesssteelsinammoniaproduction_9013_.pdf

[113] J. Reynolds, "99 Diseases of Pressure Equipment: Ammonia Stress Corrosion Cracking." https://inspectioneering.com/journal/2003-11-01/474/99-diseases-of-pressure-equipm (accessed Feb. 02, 2021).

[114] Emtiaz Ali Brohi, "Ammonia as fuel for internal combustion engines?," Master of Science Thesis, Chalmers University of Technology, Gothenburg, Sweden, 2014. Accessed: Apr. 19, 2021. [Online]. Available: https://publications.lib.chalmers.se/records/fulltext/207145/207145.pdf

[115] "Ammonia Crackers | Exporter of Ammonia Crackers | Ammonia Cracking Units | Ammonia Crackers Manufacturers | India." http://samgasindia.com/ammonia-cracker.html (accessed Apr. 19, 2021).

[116] "Round-trip Efficiency of Ammonia as a Renewable Energy Transportation Media," *Ammonia Energy Association*. https://www.ammoniaenergy.org/articles/round-trip-efficiency-of-ammonia-as-a-renewable-energy-transportation-media/ (accessed Apr. 19, 2021).

[117] N. Garg, A. Sarkar, and B. Sundararaju, "Recent developments on methanol as liquid organic hydrogen carrier in transfer hydrogenation reactions," *Coordination Chemistry Reviews*, vol. 433, p. 213728, Apr. 2021, doi: 10.1016/j.ccr.2020.213728.

[118] "Reactions - Inorganic and Organic, Redox, Synthesis, Decomposition, Dissociation, Single Displacement, Double Displacement, and Combustion." http://chemistry-reference.com/rxnlist.asp?sort=rxn&language=en (accessed Apr. 21, 2021).

[119] L. Yang and X. Ge, "Chapter Three - Biogas and Syngas Upgrading," in *Advances in Bioenergy*, vol. 1, Y. Li and X. Ge, Eds. Elsevier, 2016, pp. 125–188. doi: 10.1016/bs.aibe.2016.09.003.

[120] B. Lee *et al.*, "Renewable methanol synthesis from renewable H2 and captured CO2: How can power-to-liquid technology be economically feasible?," *Applied Energy*, vol. 279, p. 115827, Dec. 2020, doi: 10.1016/j.apenergy.2020.115827.

[121] B. G. Abraham and R. Chetty, "Design and fabrication of a quick-fit architecture air breathing direct methanol fuel cell," *International Journal of Hydrogen Energy*, vol. 46, no. 9, pp. 6845–6856, Feb. 2021, doi: 10.1016/j.ijhydene.2020.11.184.

[122] X. Zhen, X. Li, Y. Wang, D. Liu, and Z. Tian, "Comparative study on combustion and emission characteristics of methanol/hydrogen, ethanol/hydrogen and methane/hydrogen blends in high compression ratio SI engine," *Fuel*, vol. 267, p. 117193, May 2020, doi: 10.1016/j.fuel.2020.117193.

[123] M. Niermann, A. Beckendorff, M. Kaltschmitt, and K. Bonhoff, "Liquid Organic Hydrogen Carrier (LOHC) – Assessment based on chemical and economic properties," *International Journal of Hydrogen Energy*, vol. 44, no. 13, pp. 6631–6654, Mar. 2019, doi: 10.1016/j.ijhydene.2019.01.199.

[124] M. Markiewicz *et al.*, "Environmental and health impact assessment of Liquid Organic Hydrogen Carrier (LOHC) systems – challenges and preliminary results," *Energy Environ. Sci.*, vol. 8, no. 3, pp. 1035–1045, 2015, doi: 10.1039/C4EE03528C.

[125] "Toxic Potential Indicator (TPI) - Fraunhofer IZM," *Fraunhofer Institute for Reliability and Microintegration IZM*. https://www.izm.fraunhofer.de/en/abteilungen/environmental_reliabilityengineering/key_research_areas/environmental_assessmentandeco-design/toxic-potential-indicator--tpi-.html (accessed Mar. 02, 2021).

[126] M. Kerscher *et al.*, "Thermophysical properties of diphenylmethane and dicyclohexylmethane as a reference liquid organic hydrogen carrier system from experiments and molecular simulations," *International Journal of Hydrogen Energy*, vol. 45, no. 53, pp. 28903–28919, Oct. 2020, doi: 10.1016/j.ijhydene.2020.07.261.

[127] D. J. Han *et al.*, "A Novel Eutectic Mixture of Biphenyl and Diphenylmethane as a Potential Liquid Organic Hydrogen Carrier: Catalytic Hydrogenation," *Energy Technol.*, vol. 7, no. 1, pp. 113–121, Jan. 2019, doi: 10.1002/ente.201700694.

[128] K. Müller *et al.*, "Liquid Organic Hydrogen Carriers: Thermophysical and Thermochemical Studies of Benzyl- and Dibenzyl-toluene Derivatives," *Ind. Eng. Chem. Res.*, vol. 54, no. 32, pp. 7967–7976, Aug. 2015, doi: 10.1021/acs.iecr.5b01840.

[129] H. Jorschick, M. Geißelbrecht, M. Eßl, P. Preuster, A. Bösmann, and P. Wasserscheid, "Benzyltoluene/dibenzyltoluene-based mixtures as suitable liquid organic hydrogen carrier systems for low temperature applications," *International Journal of Hydrogen Energy*, vol. 45, no. 29, pp. 14897–14906, May 2020, doi: 10.1016/j.ijhydene.2020.03.210.

[130] P. M. Modisha, J. H. L. Jordaan, A. Bösmann, P. Wasserscheid, and D. Bessarabov, "Analysis of reaction mixtures of perhydro-dibenzyltoluene using two-dimensional gas chromatography and single quadrupole gas chromatography," *International Journal of Hydrogen Energy*, vol. 43, no. 11, pp. 5620–5636, Mar. 2018, doi: 10.1016/j.ijhydene.2018.02.005.

[131] G. Sievi *et al.*, "Towards an efficient liquid organic hydrogen carrier fuel cell concept," *Energy Environ. Sci.*, vol. 12, no. 7, pp. 2305–2314, 2019, doi: 10.1039/C9EE01324E.

[132] "About HySTOC." http://www.hystoc.eu/ (accessed Apr. 21, 2021).

[133] Hydrogenious, "Hydrogen infrastructure solutions." Aug. 2018. Accessed: Apr. 18, 2021. [Online]. Available: https://www.hydrogenious.net/wp-content/uploads/2018/08/Hydrogenious_porduct_booklet_short_final.pdf

[134] HyStoc, "LOHC production cost estimation study," Business development and sustainability D8.4, Jun. 2019. Accessed: Apr. 18, 2021. [Online]. Available: http://www.hystoc.eu/.cm4all/uproc.php/0/Public%20Deliverables/HySTOC-D8.4%20LOHC%20production%20cost%20estimation%20study%20Rev.0%202019-06-28.pdf?cdp=a&_=16fc2e600b8

[135] Equilex Chemicals, "PYGAS (Pyrolysis gasoline)." Equilex Chemicals BV, Feb. 09, 2016. Accessed: Apr. 18, 2021. [Online]. Available: https://www.equilex.com/wp-content/uploads/2016/02/Pygas.pdf

[136] IARC, "Some Organic Solvents, Resin Monomers and Related Compounds, Pigments and Occupational Exposures in Paint Manufacture and Painting.," *IARC Working Group on the Evaluation of Carcinogenic Risks to*, 1989. https://www.ncbi.nlm.nih.gov/books/NBK524840/ (accessed Apr. 04, 2021).

[137] M. Hurskainen and J. Ihonen, "Techno-economic feasibility of road transport of hydrogen using liquid organic hydrogen carriers," *International Journal of Hydrogen Energy*, vol. 45, no. 56, pp. 32098–32112, Nov. 2020, doi: 10.1016/j.ijhydene.2020.08.186.

[138] M. Eypasch *et al.*, "Model-based techno-economic evaluation of an electricity storage system based on Liquid Organic Hydrogen Carriers," *Applied Energy*, vol. 185, pp. 320–330, Jan. 2017, doi: 10.1016/j.apenergy.2016.10.068.

[139] G. Nayik, B. Dar, and V. Nanda, "Rheological behavior of high altitude Indian honey varieties as affected by temperature," *Journal of the Saudi Society of Agricultural Sciences*, vol. 17, Jul. 2016, doi: 10.1016/j.jssas.2016.07.003.

[140] I. Ashqer, A. Bahti, and S. Musameh, "Rheological Properties for Olive Oil in Palestine," 2014.

[141] WHO, "WHO Diesel Toxicity." https://www.who.int/ipcs/emergencies/diesel.pdf (accessed Apr. 21, 2021).

[142] "MARLOTHERM® SH | Chem Group Evansville, IN," *Chem Group*. https://chem-group.com/products/heat-transfer-fluids/marlotherm/marlotherm-sh/ (accessed Apr. 21, 2021).

[143] HyStoc, “Final operational concept of hydrogen supply chain,” Business development and sustainability D8.2, Jun. 2019. Accessed: Apr. 18, 2021. [Online]. Available: http://www.hystoc.eu/.cm4all/uproc.php/0/Public%20Deliverables/HySTOC-D8.2-Final%20operational%20concept%20of%20hydrogen%20supply%20chain-Rev1_2020-01-17.pdf?cdp=a&_=16fc2e604a0

[144] O. US EPA, “Understanding Global Warming Potentials,” *US EPA*, Jan. 12, 2016. https://www.epa.gov/ghgemissions/understanding-global-warming-potentials (accessed Apr. 12, 2021).

[145] A. Wunsch, M. Mohr, and P. Pfeifer, “Intensified LOHC-Dehydrogenation Using Multi-Stage Microstructures and Pd-Based Membranes,” *Membranes*, vol. 8, no. 4, Art. no. 4, Dec. 2018, doi: 10.3390/membranes8040112.

[146] A. Wunsch, T. Berg, and P. Pfeifer, “Hydrogen Production from the LOHC Perhydro-Dibenzyl-Toluene and Purification Using a 5 µm PdAg-Membrane in a Coupled Microstructured System,” *Materials*, vol. 13, no. 2, p. 277, Jan. 2020, doi: 10.3390/ma13020277.

[147] Hydrogenious LOHC Technologies, *Liquid Organic Hydrogen Carrier (LOHC) technology for large-scale hydrogen logistics*, (Apr. 24, 2018). Accessed: Apr. 21, 2021. [Online Video]. Available: https://www.youtube.com/watch?v=DW8UN-H_YwU

[148] M. Geißelbrecht, S. Mrusek, K. Müller, P. Preuster, A. Bösmann, and P. Wasserscheid, “Highly efficient, low-temperature hydrogen release from perhydro-benzyltoluene using reactive distillation,” *Energy Environ. Sci.*, vol. 13, no. 9, pp. 3119–3128, Sep. 2020, doi: 10.1039/D0EE01155J.

[149] “Marine Gasoil (MGO) | Glossary | Marquard & Bahls.” https://www.marquard-bahls.com/en/news-info/glossary/detail/term/marine-gasoil-mgo.html (accessed Apr. 21, 2021).

[150] “ISO 8217:2017(en), Petroleum products — Fuels (class F) — Specifications of marine fuels.” https://www.iso.org/obp/ui/#iso:std:iso:8217:ed-6:v1:en (accessed Apr. 12, 2021).

[151] PubChem, “Hydrogen.” https://pubchem.ncbi.nlm.nih.gov/compound/783 (accessed Apr. 21, 2021).

[152] “Thermophysical Properties of Ammonia -33.” https://webbook.nist.gov/cgi/fluid.cgi?T=-33.33&PLow=0&PHigh=20&PInc=1&Applet=on&Digits=5&ID=C7664417&Action=Load&Type=IsoTherm&TUnit=C&PUnit=bar&DUnit=kg%2Fm3&HUnit=kJ%2Fkg&WUnit=m%2Fs&VisUnit=cP&STUnit=N%2Fm&RefState=DEF (accessed Feb. 02, 2021).

[153] PubChem, “Methanol.” https://pubchem.ncbi.nlm.nih.gov/compound/887 (accessed Apr. 20, 2021).

[154] A. Dicks and D. A. J. Rand, *Fuel cell systems explained*, Third edition. Hoboken, NJ, USA: Wiley, 2018.

[155] N. Lümmen, *Termodynamikk - Kort og godt*, 1st ed. Universitetsforlaget, 2020. [Online]. Available: https://www.universitetsforlaget.no/termodynamikk-kort-og-godt

[156] D. DeFelice, “NASA - Fuel Cells: A Better Energy Source for Earth and Space.” https://www.nasa.gov/centers/glenn/technology/fuel_cells.html (accessed Mar. 01, 2021).

[157] J. Danebergs, F. Aarskog, and IFE, “Future compressed hydrogen infrastructure for the domestic maritime sector,” Institute for Energy Technology, Kjeller, Norway, IFE/E-2020/006, Nov. 2021.

[158] V. Ahuja, “Co2 removal from air for alkaline fuel cells operating with liquid hydrogen,” Ph.D Thesis, University of Catenbury, Christchurch, New Zealand, 1996. Accessed: Apr. 20, 2021. [Online]. Available: https://core.ac.uk/download/pdf/35465756.pdf

[159] T. Tronstad, H. H. Åstrand, G. P. Haugom, and L. Langfeldt, "Study on the use of fuel cells in shipping," European Maritime Safety Agency, Hamburg, Germany, 2017. Accessed: Feb. 03, 2021. [Online]. Available: http://www.emsa.europa.eu/tags/download/4545/2921/23.html

[160] "High Temperature Polymeric Electrolyte Membrane Fuel Cells (HTPEM) | Chalmers." https://www.chalmers.se/en/projects/Pages/High-Temperature-Polymeric-Electrolyte-Membrane-Fuel-Cells-(HTPEM)-.aspx (accessed Apr. 20, 2021).

[161] J. Kang and J. Kim, "Membrane electrode assembly degradation by dry/wet gas on a PEM fuel cell," *International Journal of Hydrogen Energy - INT J HYDROGEN ENERG*, vol. 35, pp. 13125–13130, Dec. 2010, doi: 10.1016/j.ijhydene.2010.04.077.

[162] G. Omdal, "Prototech Awarded Contract to Supply 2MW Zero-Emission Ammonia Fuel Cell Module." https://prototech.no/news/2020/01/23/prototech-awarded-contract-to-supply-2mw-zero-emission-ammonia-fuel-cell-module/ (accessed Mar. 02, 2021).

[163] M. Ni, M. K. H. Leung, and D. Leung, "Ammonia-fed solid oxide fuel cells for power generation—A review," *International Journal of Energy Research*, vol. 33, pp. 943–959, Sep. 2009, doi: 10.1002/er.1588.

[164] "The formation of NOx." https://www.alentecinc.com/papers/NOx/The%20formation%20of%20NOx_files/The%20formation%20of%20NOx.htm (accessed May 14, 2021).

[165] "How is NOx Formed | CleanBoiler.org." http://cleanboiler.org/workshop/how-is-nox-formed/ (accessed May 14, 2021).

[166] M. Bugge, N. E. Haugen, Ø. Skreiberg, T. Løvås, and E. Houshfar, "Numerical simulations of staged biomass grate fired combustion with an emphasis on NOx emissions," Mar. 26, 2014. [Online]. Available: https://www.sintef.no/globalassets/project/cenbio/cenbio_days_2014/cenbiodays2014_bugge.pdf

[167] E. Skjong, E. Rodskar, M. Molinas, T. A. Johansen, and J. Cunningham, "The Marine Vessel's Electrical Power System: From its Birth to Present Day," *Proc. IEEE*, vol. 103, no. 12, pp. 2410–2424, Dec. 2015, doi: 10.1109/JPROC.2015.2496722.

[168] Y. Demirel, *Energy: Production, Conversion, Storage, Conservation, and Coupling*. London: Springer-Verlag, 2012. doi: 10.1007/978-1-4471-2372-9.

[169] "ABB Conversations > ABB reaches 99.05% efficiency, the highest ever recorded for a synchronous motor." https://www.abb-conversations.com/2017/07/abb-motor-sets-world-record-in-energy-efficiency/ (accessed Apr. 18, 2021).

[170] ABB, "Saving energy with VSD systems." https://search.abb.com/library/Download.aspx?DocumentID=9AKK107492A2928&LanguageCode=en&DocumentPartId=&Action=Launch (accessed Apr. 18, 2021).

[171] D. Laskay, "BLDC Motor Controllers...for Maximum Performance & Efficiency," p. 12.

[172] "ABB synchronous motors, ABB motors, ABB supplier, ABB catalogues." https://www.globalindustrialsupplies.eu/abb_catalogues/abb_synchronous_motors/abb_synchronous_motors_3.html (accessed Apr. 20, 2021).

[173] DNV GL, "Study on Electrical Energy Storage for Ships." http://www.emsa.europa.eu/publications/item/3895-study-on-electrical-energy-storage-for-ships.html (accessed Apr. 18, 2021).

[174] R. Staff, "Tesla's Musk hints of battery capacity jump ahead of industry event," *Reuters*, Aug. 25, 2020. Accessed: Apr. 18, 2021. [Online]. Available: https://www.reuters.com/article/us-tesla-batteries-idUSKBN25L0MC

[175] "The Evoy Configurator." https://config.evoy.no/ (accessed Apr. 20, 2021).

[176] A. Valera-Medina *et al.*, "Premixed ammonia/hydrogen swirl combustion under rich fuel conditions for gas turbines operation," *International Journal of Hydrogen Energy*, vol. 44, no. 16, pp. 8615–8626, Mar. 2019, doi: 10.1016/j.ijhydene.2019.02.041.

[177] P. Dimitriou and R. Javaid, "A review of ammonia as a compression ignition engine fuel," *International Journal of Hydrogen Energy*, vol. 45, no. 11, pp. 7098–7118, Feb. 2020, doi: 10.1016/j.ijhydene.2019.12.209.

[178] D. H. Porter, *The life and times of Sir Goldsworthy Gurney: gentleman scientist and inventor, 1793-1875*. Bethlehem: Lehigh University Press, 1998.

[179] "Ford AA 1930-1931 mod. Innstallasjon for amm. forsøk." https://digitaltmuseum.no/011013004244/ford-aa-1930-1931-mod-innstallasjon-for-amm-forsok (accessed Apr. 20, 2021).

[180] G. Walmsley, *The Shell Book of how Cars Work: An Introduction to the Motor-car, Its Fuel and Lubricants*. J. Baker, 1977. [Online]. Available: https://books.google.no/books?id=M6eRAAAACAAJ

[181] Motordynasty, "How diesel two-phase motors work and their stroke cycle," *motordynasty*, Oct. 21, 2020. https://motordynasty.com/2020/10/22/how-diesel-two-phase-motors-work-and-their-stroke-cycle/ (accessed Mar. 03, 2021).

[182] "Mazda: Skyactiv-X | We are Engineers." https://www.mazda.com/en/innovation/mazda-stories/engineers/skyactiv-x/ (accessed Apr. 13, 2021).

[183] "Wärtsilä and MAN Energy Solutions race to build ammonia engine," Aug. 21, 2020. https://shippingwatch.com/suppliers/article12359286.ece (accessed Apr. 13, 2021).

[184] MAN energy solutions, "Engineering the future two-stroke green-ammonia engine," MAN Energy Solutions, Copenhagen, Denmark, Nov. 2019. Accessed: Mar. 03, 2021. [Online]. Available: https://fathom.world/wp-content/uploads/2020/05/engineeringthefuturetwostrokegreenammoniaengine1589339239488.pdf

[185] MAN Energy Solutions, "Future-proof your investments," *MAN Energy Solutions*. https://www.man-es.com/marine/products/lgip (accessed Mar. 03, 2021).

[186] A. Gruber, M. R. Bothien, A. Ciani, K. Aditya, J. H. Chen, and F. A. Williams, "Direct Numerical Simulation of hydrogen combustion at auto-ignitive conditions: Ignition, stability and turbulent reaction-front velocity," *Combustion and Flame*, vol. 229, p. 111385, Jul. 2021, doi: 10.1016/j.combustflame.2021.02.031.

[187] "MAN ES Hydrogen," *MAN Energy Solutions*. https://www.man-es.com/marine/strategic-expertise/future-fuels/hydrogen (accessed Apr. 16, 2021).

[188] "Wärtsilä gas engines to burn 100% hydrogen," *Wartsila.com*. https://www.wartsila.com/media/news/05-05-2020-wartsila-gas-engines-to-burn-100-hydrogen-2700995 (accessed Apr. 16, 2021).

[189] "MHIET Conducts Combustion Test for Hydrogen Engine with Pure Hydrogen," *Mitsubishi Heavy Industries, Ltd.* https://www.mhi.com/news/210121.html (accessed Apr. 16, 2021).

[190] "Scania and Westport Fuel Systems will cooperate in hydrogen research project," *Scania Group*. /group/en/home/newsroom/news/2021/Scania-and-Westport-Fuel-System-will-cooperate-in-hydrogen-research-project.html (accessed Apr. 16, 2021).

[191] "Today BeHydro launches the first hydrogen-powered dual-fuel engine with a capacity of 1 megawatt (MW)," Sep. 17, 2020. https://www.cmb.be/en/new/today-behydro-launches-the-first-hydrogen-powered-dual-fuel-engine-with-a-capacity-of-1-megawatt-mw (accessed Apr. 16, 2021).

[192] R. Babayev, A. Andersson, A. S. Dalmau, H. G. Im, and B. Johansson, "Computational characterization of hydrogen direct injection and nonpremixed combustion in a compression-ignition engine," *International Journal of Hydrogen Energy*, Apr. 2021, doi: 10.1016/j.ijhydene.2021.02.223.

[193] Y. Wang, X. Zhou, and L. Liu, "Theoretical investigation of the combustion performance of ammonia/hydrogen mixtures on a marine diesel engine," *International Journal of Hydrogen Energy*, vol. 46, no. 27, pp. 14805–14812, Apr. 2021, doi: 10.1016/j.ijhydene.2021.01.233.

[194] D. K. Myrseth, "HISC i duplex korrosjonsbestandige stål og optimalisering av super duplex rørkomponenter," *HISC in duplex stainless steels and optimization of super duplex pipe components*, 2019, Accessed: Apr. 22, 2021. [Online]. Available: https://nmbu.brage.unit.no/nmbu-xmlui/handle/11250/2619212

[195] J. Øverli, *Termiske maskiner*, 2nd ed., vol. 3, 3 vols. Tapir Forlag.

[196] H. O. Kristenen, "Energy demand and exhaust gas emissions of marine engines," Technical University of Denmark, Denmark, Work Package 2.3 Report no. 03, Sep. 2015. Accessed: Feb. 05, 2021. [Online]. Available: file:///C:/Users/ander/Downloads/energy-demand-and-emissions-of-marine-engines-september-2015.pdf

[197] Rolls Royce, "MTU Turbocharging | Cutaway of turbocharger with rotating im… | Flickr." https://www.flickr.com/photos/115828059@N03/12234184576 (accessed Apr. 21, 2021).

[198] Rolls Royce, "Gas Turbines." https://www.rolls-royce.com/products-and-services/defence/naval/gas-turbines.aspx (accessed Apr. 22, 2021).

[199] "Gas turbine - Energy Education." https://energyeducation.ca/encyclopedia/Gas_turbine (accessed May 14, 2021).

[200] S. K. Ayaz, O. Altuntas, and H. Caliskan, "Effect of ammonia fuel fraction on the exergetic performance of a gas turbine," *Energy Procedia*, vol. 144, pp. 150–156, Jul. 2018, doi: 10.1016/j.egypro.2018.06.020.

[201] SINTEF, "Hydrogen-firing of gas turbines," *Hydrogen-firing of gas turbines*. https://www.sintef.no/projectweb/nccs/annual-report-2019/nccs-2019-case-c-hydrogen-firing-of-gas-turbines-task-5/ (accessed Apr. 17, 2021).

[202] S. Patel, "Siemens' Roadmap to 100% Hydrogen Gas Turbines," *POWER Magazine*, Jul. 01, 2020. https://www.powermag.com/siemens-roadmap-to-100-hydrogen-gas-turbines/ (accessed Apr. 17, 2021).

[203] M. Ditaranto, T. Heggset, and D. Berstad, "Concept of hydrogen fired gas turbine cycle with exhaust gas recirculation: Assessment of process performance," *Energy*, vol. 192, p. 116646, Feb. 2020, doi: 10.1016/j.energy.2019.116646.

[204] "Wayback Machine," Aug. 13, 2011. https://web.archive.org/web/20110813030259/http://www.energy.siemens.com/us/pool/hq/power-generation/gas-turbines/downloads/SGT5-8000H_benefits.pdf (accessed May 02, 2021).

[205] "LM6000 Aeroderivative Gas Turbine | GE Gas Power," *gepower-v2*. https://www.ge.com/gas-power/products/gas-turbines/lm6000 (accessed May 02, 2021).

[206] A. Matamis *et al.*, "Optical characterization of methanol compression-ignition combustion in a heavy-duty engine," *Proceedings of the Combustion Institute*, vol. 38, no. 4, pp. 5509–5517, Jan. 2021, doi: 10.1016/j.proci.2020.06.024.

[207] A. N. Hayhurst and A. D. Lawrence, "Emissions of nitrous oxide from combustion sources," *Progress in Energy and Combustion Science*, vol. 18, no. 6, pp. 529–552, Jan. 1992, doi: 10.1016/0360-1285(92)90038-3.

[208] A. Colorado, V. McDonell, and S. Samuelsen, "Direct emissions of nitrous oxide from combustion of gaseous fuels," *International Journal of Hydrogen Energy*, vol. 42, no. 1, pp. 711–719, Jan. 2017, doi: 10.1016/j.ijhydene.2016.09.202.

[209] Frøy, "forside," *froygruppen.no*. https://froygruppen.no/ (accessed Apr. 09, 2021).

[210] "MV Rubin," *ntsasa.no*. http://ntsshipping.ntsasa.no/wp-content/uploads/sites/9/2018/07/rubin2018_factsheet2018.pdf (accessed Mar. 17, 2021).

[211] K. I. Giske, "Rubin (10/2014) - Maritimt.com," *Maritimt Magasin*, Oct. 24, 2014. https://maritimt.com/nb/batomtaler/rubin-102014 (accessed Apr. 09, 2021).

[212] Frøy, "Rubin," *froygruppen.no*. https://froygruppen.no/portfolio/rubin/ (accessed Mar. 07, 2021).

[213] Heidi Hansen, *Petter Solberg english - the Girboks*, (Apr. 07, 2011). Accessed: Apr. 20, 2021. [Online Video]. Available: https://www.youtube.com/watch?v=DcmAUwPA-5o

[214] "What is Deadweight Tonnage (DWT): Meaning & its Usage in Shipping Industry." https://www.cogoport.com/shipping-terms/deadweight-tonnage-dwt-2 (accessed Apr. 20, 2021).

[215] "Wärtsilä 20 - Diesel engine," *Wartsila.com*. https://www.wartsila.com/marine/build/engines-and-generating-sets/diesel-engines/wartsila-20 (accessed Mar. 16, 2021).

[216] Leroy Somer, "Alternators LSA 49.1 - 4 Pole." Leroy Somer. Accessed: Sep. 04, 2021. [Online]. Available: http://www.qaswaa-albararry.com/uploads/leroy%20somer/660-910%20kva.pdf

[217] Brunvoll, "Brunvoll FU 63 1750." Accessed: Sep. 04, 2021. [Online]. Available: https://www.si-benelux.nl/schiff/produkte/brunvoll/pdf/brunvoll-product-range.pdf

[218] Stamford, "Stamford HCM434F." Accessed: Sep. 04, 2021. [Online]. Available: https://muldermotoren.nl/volvopentadvd/marine_genset_asp/data_sources/techdata_generator/td_hcm434f.gb_10.06_05_gb.pdf

[219] Baudouin, "12 M262 Marine Engine," *Baudouin*. https://baudouin.com/portfolio/12-m262-marine-engine-baudouin/ (accessed Apr. 06, 2021).

[220] K. Egelert, "How to Use AIS," *Boating Safety*, Oct. 23, 2012. https://www.boatingsafetymag.com/boatingsafety/how-use-ais (accessed Mar. 06, 2021).

[221] "MarineTraffic: Global Ship Tracking Intelligence | AIS Marine Traffic." https://www.marinetraffic.com/en/ais/home/centerx:5.5/centery:60.2/zoom:11 (accessed Feb. 25, 2021).

[222] "Overview of the LNG industry | OwnerTeamConsultation." https://www.ownerteamconsult.com/overview-of-the-lng-industry/ (accessed Apr. 22, 2021).

[223] "Fuel Oil Storage Tanks." https://www.engineeringtoolbox.com/fuel-oil-storage-tanks-dimensions-d_1585.html (accessed Apr. 21, 2021).

[224] Miljødirektoratet, "Klimakur 2030," *Miljødirektoratet/Norwegian Environment Agency*. https://www.miljodirektoratet.no/ansvarsomrader/klima/klimatiltak/klimakur/ (accessed Apr. 23, 2021).

[225] S. F. Kostøl, "Liquid hydrogen infrastructure for the maritime sector in 2030," Ocean Hyway Cluster, Florø, Value chain B.1.1, Nov. 2020.

[226] S. Larsson, "Weight and dimensions of heavy commercial vehicles as established by Directive 96/53/EC and the European Modular System (EMS)," p. 31.

[227] A. Kulikowska - Wielgus, "60-tonne, 24-metre-long trucks approved in Norway," *Trans.INFO*. https://trans.info/en/60-tonne-24-metre-long-trucks-approved-in-norway-171524 (accessed Apr. 23, 2021).

[228] "Nikola Two," *Nikola Motor Company*. https://www.nikolamotor.com/two (accessed Apr. 23, 2021).

[229] Statens Vegvesen, "Kjøre- og hviletid," *Statens vegvesen*. https://www.vegvesen.no/kjoretoy/yrkestransport/kjore-og-hviletid/kjore-og-hviletid (accessed Apr. 25, 2021).

[230] USDRIVE, "Hydrogen Delivery Roadmap," Jun. 2013. [Online]. Available: https://www.energy.gov/sites/prod/files/2014/02/f8/hdtt_roadmap_june2013.pdf

[231] M. van der Hoeven, "Technology Roadmap Hydrogen and Fuel Cells," IEA Energy Technology Policy Division, Paris, France, Roadmap, Jun. 2015. Accessed: Jan. 03, 2021. [Online]. Available: https://www.iea.org/reports/technology-roadmap-hydrogen-and-fuel-cells

[232] L. Bertuccioli, A. Chan, D. Hart, F. Lehner, B. Madden, and E. Standen, "Development of Water Electrolysis in the European Union," E4Tech, Switzerland, Final, Jul. 2014. Accessed: Sep. 24, 2021. [Online]. Available: https://www.fch.europa.eu/sites/default/files/study%20electrolyser_0-Logos_0_0.pdf

[233] T. Smolinka *et al.*, *Studie IndWEDe: Industrialisierung der Wasserelektrolyse in Deutschland: Chancen und Herausforderungen für nachhaltigen Wasserstoff für Verkehr, Strom und Wärme*. 2018.

[234] "Valutakurser." https://www.norges-bank.no/tema/Statistikk/Valutakurser/?tab=currency&id=EUR (accessed Apr. 23, 2021).

[235] G. Bartnes, J. S. Amundsen, and I. B. Holm, "Kraftmarkedsanalyse 2018 - 2030," NVE, Oslo, Norway, Market analysis Nr 84/2018, Oct. 2018. Accessed: Apr. 24, 2021. [Online]. Available: http://publikasjoner.nve.no/rapport/2018/rapport2018_84.pdf

[236] "Utkoblbart forbruk - NVE." https://www.nve.no/reguleringsmyndigheten/nettjenester/nettleie/nettleie-for-forbruk/utkoblbart-forbruk/ (accessed Apr. 23, 2021).

[237] "Global average levelised cost of hydrogen production by energy source and technology, 2019 and 2050 – Charts – Data & Statistics," *IEA*. https://www.iea.org/data-and-statistics/charts/global-average-levelised-cost-of-hydrogen-production-by-energy-source-and-technology-2019-and-2050 (accessed Apr. 30, 2021).

[238] S. Bruce, M. Temminghoff, E. Scmidt, D. Palfreyman, and P. Harley, "National Hydrogen Roadmap," CSIRO, 2018. Accessed: Apr. 24, 2021. [Online]. Available: https://www.csiro.au/-/media/Do-Business/Files/Futures/18-00314_EN_NationalHydrogenRoadmap_WEB_180823.pdf

[239] M. Rivarolo, G. Riveros-Godoy, L. Magistri, and A. F. Massardo, "Clean Hydrogen and Ammonia Synthesis in Paraguay from the Itaipu 14 GW Hydroelectric Plant," *ChemEngineering*, vol. 3, no. 4, Art. no. 4, Dec. 2019, doi: 10.3390/chemengineering3040087.

[240] C. A. Fernandez and M. C. Hatzell, "Editors' Choice—Economic Considerations for Low-Temperature Electrochemical Ammonia Production: Achieving Haber-Bosch Parity," *J. Electrochem. Soc.*, vol. 167, no. 14, p. 143504, Nov. 2020, doi: 10.1149/1945-7111/abc35b.

[241] "1 USD to EUR | Convert US Dollars to Euros | Xe." https://www.xe.com/currencyconverter/convert/?Amount=1&From=USD&To=EUR (accessed Apr. 24, 2021).

[242] L. Collins, "'World's first international hydrogen supply chain' realised between Brunei and Japan | Recharge," *Recharge | Latest renewable energy news*, Apr. 27, 2020. https://www.rechargenews.com/transition/-world-s-first-international-hydrogen-supply-chain-realised-between-brunei-and-japan/2-1-798398 (accessed Apr. 29, 2021).

[243] R. Pedersen, "Ansattkostnad," *Smarte Penger*, Jun. 13, 2016. https://www.smartepenger.no/kalkulatorer/2734-ansattkostnad (accessed Apr. 26, 2021).

[244] "Drivstoffpriser | Circle K." https://www.circlek.no/bedrift/drivstoff/drivstoffpriser (accessed Apr. 26, 2021).

[245] Advanced Research Projects Agency, "Renewable Energy to Fuels Through Utilization of Energy-Dense Liquids (REFUEL)," U.S. Department of Energy, USA, Funding report CFDA Number 81.135, Apr. 2016. Accessed: Apr. 25, 2021. [Online]. Available: https://arpa-e.energy.gov/sites/default/files/documents/files/REFUEL_Project_Descriptions_Final.pdf

[246] "2022 Polar 10600 265 PSI Industrial Gas Tank Trailer For Sale | Kansas City, KS | KTC 9423," *MyLittleSalesman.com*. https://www.mylittlesalesman.com/2018-polar-10600-265-psi-available-for-lease-or-purchase-industrial-gas-tank-trailer-9223001 (accessed Apr. 25, 2021).

[247] "Lindner & Fischer TSA 60 SD 4-axle Fuel Tank Trailer," *Autoline*. https://autoline.info/-/sale/fuel-tank-trailers/LINDNER-FISCHER-TSA-60-SD-4-axle-Fuel-Tank-Trailer-NEW-2-Units--17121413330436656200 (accessed Apr. 25, 2021).

[248] "Strømforbruk i Norge har lavt klimagassutslipp - NVE." https://www.nve.no/nytt-fra-nve/nyheter-energi/stromforbruk-i-norge-har-lavt-klimagassutslipp/ (accessed Apr. 26, 2021).

[249] DNV GL, "LNG as Ship Fuel," DNG GL, Hamburg, Germany, 01 2014, 2014. Accessed: Apr. 26, 2021. [Online]. Available: https://www.dnv.com/Images/LNG_report_2015-01_web_tcm8-13833.pdf

[250] P. Sun, B. Young, and A. Elgowainy, "Criteria Air Pollutants and Greenhouse Gas Emmisions from Hydrogen Production in U.S. Steam Methane Reforming Facilitites," Argonne Natinal Laboratory, MA. USA, 2018. Accessed: May 05, 2021. [Online]. Available: https://www.osti.gov/pages/servlets/purl/1546962

[251] P. Sun and A. Elgowainy, "Updates of Hydrogen Production from SMR Process in GREET® 2019," Argonne Natinal Laboratory, Sep. 2019. Accessed: May 05, 2021. [Online]. Available: https://greet.es.anl.gov/files/smr_h2_2019

[252] PricewaterhouseCoopers, "IMO 2020 Regulation," *PwC*. https://www.pwc.com/ng/en/publications/imo-2020-regulation.html (accessed Feb. 24, 2021).

[253] SOLAS, "SOLAS." https://www.imo.org/en/KnowledgeCentre/ConferencesMeetings/Pages/SOLAS.aspx (accessed Apr. 13, 2021).

[254] "International Convention for the Safety of Life at Sea (SOLAS), 1974." https://www.imo.org/en/About/Conventions/Pages/International-Convention-for-the-Safety-of-Life-at-Sea-(SOLAS),-1974.aspx (accessed Apr. 26, 2021).

[255] A. Risholm, "Ammonia fuel infrastructure for the maritime sector in 2030," Ocean Hyway Cluster, Scenario study OHC HI B.2, Nov. 2020.

[256] "ISO 20519:2017," *ISO*. https://www.iso.org/cms/render/live/en/sites/isoorg/contents/data/standard/06/82/68227.html (accessed Apr. 14, 2021).

[257] O. R. Hansen and G. O. Myhr, "Sikkerhet og regelverk - Lloyd's Register," Høgskulen på Vestlandet, Oct. 24, 2019.

[258] B. Scholz, "Alternative low flashpoint fuels - challenges and perspectives," DNV-GL, Høvik, Norway, 2016. Accessed: Apr. 17, 2021. [Online]. Available: https://www.propulsionconference.com/__data/assets/pdf_file/0022/70528/Low-flashpoint-fuels.pdf

[259] C. C. for O. H. and S. Government of Canada, "Flammable & Combustible Liquids - Hazards : OSH Answers," Apr. 27, 2021. https://www.ccohs.ca/ (accessed Apr. 27, 2021).

[260] "Difference Between Flammable & Combustible | Fire Safety," *The Hub | High Speed Training*, Jan. 28, 2019. https://www.highspeedtraining.co.uk/hub/difference-between-flammable-and-combustible/ (accessed Apr. 27, 2021).

[261] O. R. Hansen, "Liquid hydrogen releases show dense gas behavior," *International Journal of Hydrogen Energy*, vol. 45, no. 2, pp. 1343–1358, Jan. 2020, doi: 10.1016/j.ijhydene.2019.09.060.

[262] R. Moradi and K. M. Groth, "Hydrogen storage and delivery: Review of the state of the art technologies and risk and reliability analysis," *International Journal of Hydrogen Energy*, vol. 44, no. 23, pp. 12254–12269, May 2019, doi: 10.1016/j.ijhydene.2019.03.041.

[263] J. Kokarakis, "The case of ammonia as a marine fuel," *SAFETY4SEA*, Apr. 09, 2020. https://safety4sea.com/cm-the-case-of-ammonia-as-a-marine-fuel/ (accessed Mar. 01, 2021).

[264] Hydro Instruments, "Ammonia Handling Manual," Hydro Instruments, Telford, PA, Manual NH3-001, Feb. 2013. Accessed: Dec. 02, 2021. [Online]. Available: http://www.hydroinstruments.com/files/Ammonia%20Handling%20Manual.pdf

[265] Public Health England, "Compendium of Chemical Hazards: Ammonia," Public Health England, England, 2014790, Aug. 2019. Accessed: Jun. 02, 2021. [Online]. Available: https://assets.publishing.service.gov.uk/government/uploads/system/uploads/attachment_data/file/825191/Ammonia_IM_PHE_140819__1_.pdf

[266] C. on A. E. G. Levels, C. on Toxicology, and N. R. Council, *Acute Exposure Guideline Levels for Selected Airborne Chemicals*, vol. Volume 6. Washingtoin, D.C.: National Academy Press, 2007. Accessed: Feb. 16, 2021. [Online]. Available: https://www.epa.gov/sites/production/files/2014-11/documents/ammonia_final_volume6_2007.pdf

[267] Hydrogenious, *LOHC - safe and efficient hydrogen storage*, (Jul. 23, 2019). Accessed: Apr. 26, 2021. [Online Video]. Available: https://www.youtube.com/watch?v=9LnrNiHC_34

[268] J. L. Chen, C. M. Chen, S.-B. Yen, J. Y. R. Chiou, S. F. Yeh, and C.-Y. Liu, "Toxic Potential Indicator (TPI) for Material Assessment in Automobile Industry," in *2005 4th International Symposium on Environmentally Conscious Design and Inverse Manufacturing*, Dec. 2005, pp. 244–245. doi: 10.1109/ECODIM.2005.1619212.

[269] "Toxic Potential Indicator (TPI) - Fraunhofer IZM," *Fraunhofer Institute for Reliability and Microintegration IZM*. https://www.izm.fraunhofer.de/en/abteilungen/environmental_reliabilityengineering/key_research_areas/environmental_assessmentandeco-design/toxic-potential-indicator--tpi-.html (accessed Apr. 26, 2021).

[270] Y.-Q. Zhang *et al.*, "Mobility and adsorption of liquid organic hydrogen carriers (LOHCs) in soils – environmental hazard perspective," *Green Chem.*, vol. 22, no. 19, pp. 6519–6530, 2020, doi: 10.1039/D0GC02603D.

[271] M. Markiewicz *et al.*, "Hazard assessment of quinaldine-, alkylcarbazole-, benzene- and toluene-based liquid organic hydrogen carrier (LOHCs) systems," *Energy Environ. Sci.*, vol. 12, no. 1, pp. 366–383, 2019, doi: 10.1039/C8EE01696H.

[272] L. Vandebroek and J. Berghmans, "Safety Aspects of the use of LNG for Marine Propulsion," *Procedia Engineering*, vol. 45, pp. 21–26, 2012, doi: 10.1016/j.proeng.2012.08.114.

[273] "Hydrogen Incident Examples - Select Summaries of Hydrogen Incidents from the H2tools.org Lessons Learned Database," PNNL-29731, Mar. 2020.

[274] A. B. Jensen, "Nel setter av 35 millioner kroner for å rydde opp etter hydrogen-eksplosjon," *Tu.no*, Aug. 28, 2019. https://www.tu.no/artikler/nel-setter-av-35-millioner-kroner-for-a-rydde-opp-etter-hydrogen-eksplosjon/472633 (accessed Apr. 26, 2021).

[275] N. / Redaksjonen, "Kundene raser, og skylder på myndighetene," *elbil24.no*, Feb. 07, 2020. https://www.elbil24.no/nyheter/kundene-raser-og-skylder-pa-myndighetene/72114681 (accessed Apr. 26, 2021).

[276] "Ammonia leak at Alberni Valley Multiplex," *Technical Safety BC*. https://www.technicalsafetybc.ca/alerts/ammonia-leak-alberni-valley-multiplex (accessed Apr. 26, 2021).

[277] D. A. Drago, "Gasoline-related injuries and fatalities in the United States, 1995-2014," *International Journal of Injury Control and Safety Promotion*, vol. 25, no. 4, pp. 393–400, Oct. 2018, doi: 10.1080/17457300.2018.1431947.

[278] "Ammonia Leak on Tanker Kills One and Injures Three off Malaysia," *The Maritime Executive*. https://www.maritime-executive.com/article/ammonia-leak-on-tanker-kills-one-and-injures-three-off-malaysia (accessed Apr. 26, 2021).

[279] "Ammonia leak kills seafarer onboard gas carrier off Malaysia," *SAFETY4SEA*, Apr. 08, 2021. https://safety4sea.com/ammonia-leak-kills-seafarer-onboard-gas-carrier-off-malaysia/ (accessed Apr. 26, 2021).

[280] J. W. McConnell *et al.*, *Functions, Statistics, and Trigonometry SE*. University of Chicago, 2015. [Online]. Available: https://books.google.no/books?id=n5n2jgEACAAJ

[281] "Spherical law of cosines," *Wikipedia*. Apr. 22, 2021. Accessed: May 18, 2021. [Online]. Available: https://en.wikipedia.org/w/index.php?title=Spherical_law_of_cosines&oldid=1019368890

[282] "What is latitude and longitude? - Definition from WhatIs.com," *WhatIs.com*. https://whatis.techtarget.com/definition/latitude-and-longitude (accessed Mar. 07, 2021).

[283] R. A. Adams and C. Essex, *Calculus: a Complete Course*. Ontario: Prentice Canada, 2018.

[284] NASA, "Imagine the Universe!" https://imagine.gsfc.nasa.gov/features/cosmic/earth_info.html (accessed Mar. 07, 2021).

[285] "Latitude and Longitude in Excel: Calculate Distance, Convert Degrees, and Geocode Addresses – BatchGeo Blog." https://blog.batchgeo.com/manipulating-coordinates-in-excel/ (accessed Mar. 07, 2021).

[286] "Google Maps," *Google Maps*. https://www.google.com/maps (accessed Mar. 06, 2021).

[287] Anish, "What is Marine Electricity And How It is Generated?," *Marine Insight*, Mar. 17, 2021. https://www.marineinsight.com/marine-electrical/what-is-marine-electricity/ (accessed Apr. 09, 2021).

[288] "Wärtsilä Shaft Generator - economical electrical power generation," *Wartsila.com*. https://www.wartsila.com/marine/build/electrical-and-power-systems/shaft-generator-systems/shaft-generator (accessed Apr. 29, 2021).

[289] CRIST, "CRIST S.A." https://www.crist.com.pl/general-cargo-carrier,80,en.html (accessed Apr. 12, 2021).

[290] "Svovelinnhold i marint drivstoff," *Regjeringen.no*, Jan. 22, 2013. https://www.regjeringen.no/no/sub/eos-notatbasen/notatene/2013/jan/svovelinnhold-i-marint-drivstoff/id2433131/ (accessed Apr. 04, 2021).

[291] E. Lindstad, G. S. Eskeland, A. Rialland, and A. Valland, "Decarbonizing Maritime Transport: The Importance of Engine Technology and Regulations for LNG to Serve as a Transition Fuel," *Sustainability*, vol. 12, no. 21, p. 8793, Oct. 2020, doi: 10.3390/su12218793.

[292] "Kart, veibeskrivelse og kjørerute - map/maps | 1881." https://kart.1881.no/?direction={60.8005431|5.0061575|Mongstad%2C%20Mongstad}{61.6109983327101|5.07581868524423|Fjord%20Base%2C%20Flor%C3%B8%20(Fabrikk)} (accessed Apr. 29, 2021).

[293] "Viking Energy to be retrofit for ammonia fuel in 2024," *Ammonia Energy Association*. https://www.ammoniaenergy.org/articles/viking-energy-to-be-retrofit-for-ammonia-fuel-in-2024/ (accessed Apr. 29, 2021).

[294] "Kart, veibeskrivelse og kjørerute - map/maps | 1881." https://kart.1881.no/?direction={61.612377166748|5.07635498046875|Fjord%20Base%20AS%2C%20Botnaneset%2C%20Flor%C3%B8}{59.12040153324467|9.62875444130234|Her%C3%B8ya%20industripark} (accessed Apr. 30, 2021).

[295] "Ramp up nuclear power to beat climate change, says UN nuclear chief," *UN News*, Oct. 07, 2019. https://news.un.org/en/story/2019/10/1048732 (accessed May 02, 2021).

[296] "Nuclear power and climate change," Apr. 13, 2016. https://www.iaea.org/topics/nuclear-power-and-climate-change (accessed May 02, 2021).

[297] "2 things we believe: Chernobyl was catastrophic, and we need nuclear power more than ever," *USA TODAY*. https://www.usatoday.com/story/opinion/2019/06/17/hbo-chernobyl-tragic-nuclear-power-safe-clean-vital-column/1409096001/ (accessed May 02, 2021).

[298] R. AT.no, "Pumpeeffekten er et problem med 9 aksler i vårløsningen," Apr. 28, 2021. https://www.at.no/transport/pumpeeffekten-er-et-problem-med-9-aksler-i-varlosningen/571984 (accessed May 02, 2021).

[299] "Northern Lights CCS - transport og lagring av CO2 - equinor.com." https://www.equinor.com/no/what-we-do/northern-lights.html (accessed May 02, 2021).

[300] "Nikolaus Otto | German engineer," *Encyclopedia Britannica*. https://www.britannica.com/biography/Nikolaus-Otto (accessed May 02, 2021).

[301] "Zero Emissions," *Hydrogen Dual Fuel for Transport | ULEMCo Ltd*. https://ulemco.com/zero-emissions/ (accessed May 02, 2021).

[302] Amnesty, "South Africa: Mining gathering must confront human rights violations." https://www.amnesty.org/en/latest/news/2020/02/south-africa-mining-gathering-must-confront-human-rights-violations/ (accessed May 02, 2021).

[303] B. J. Glaister and G. M. Mudd, "The environmental costs of platinum–PGM mining and sustainability: Is the glass half-full or half-empty?," *Minerals Engineering*, vol. 23, no. 5, pp. 438–450, Apr. 2010, doi: 10.1016/j.mineng.2009.12.007.

[304] M. Posner, "How Tesla Should Combat Child Labor In The Democratic Republic Of The Congo," *Forbes*. https://www.forbes.com/sites/michaelposner/2020/10/07/how-tesla-should-combat-child-labor-in-the-democratic-republic-of-the-congo/ (accessed May 02, 2021).

[305] "Langvarig stress svekker immunforsvaret," *SINTEF*. https://www.sintef.no/siste-nytt/2016/langvarig-stress-svekker-immunforsvaret/ (accessed May 02, 2021).

[306] A. Holt, "Review of the Progress of Steam Shipping during the last Quarter of a Century," Mar. 12, 2008. https://web.archive.org/web/20080312052959/http://listserv.linguistlist.org/cgi-bin/wa?A2=ind0710B&L=ADS-L&P=R432&I=-3 (accessed May 02, 2021).

[307] "NumPy." https://numpy.org/ (accessed May 02, 2021).

[308] G. Van Brummelen, *Heavenly Mathematics: The Forgotten Art of Spherical Trigonometry*. Princeton University Press, 2012. [Online]. Available: https://books.google.no/books?id=mYz7QIt3vQoC

[309] K. Gade, "A Non-singular Horizontal Position Representation," *J. Navigation*, vol. 63, no. 3, pp. 395–417, Jul. 2010, doi: 10.1017/S0373463309990415.

[310] F. Aarskog, J. Danebergs, T. Strømgren, and Ø. Ulleberg, "Energy and cost analysis of a hydrogen driven high speed passenger ferry," *International Shipbuilding Progress*, vol. 67, pp. 1–27, Jun. 2020, doi: 10.3233/ISP-190273.

List of equations

(1) *Volumetric energy density* 3

(2) *Gibbs free energy* 3

(3) *Efficiency, thermodynamic* 28

(4) *Efficiency, ICE* 38

(5) *Volumetric energy density, DBT+tank* 46

(6) *Gravimetric energy density, DBT+tank* 47

(7) *Efficiency, system #1* 50

(8) *Efficiency, system #2* 50

(9) *Annual hydrogen-need, 5 MV Rubin-equivalents* 53

(10) *Annual expenditure* 54

(11) *Installed power rating, HBP* 55

(12) *Cost hydrogenation, pronominal* 55

(13) *Installed power rating, DBT* 55

(14) *Number of daily deliveries of fuel* 56

(15) *Number of trips per day, per truck* 57

(16) *Number of delivery trucks* 57

(17) *Specific weight ratio, general* 58

(18) *Amount of CO_2 emission per trip* 59

(19) *Spherical Law of Cosine* 69

(20) *Cosine Rule with Latitudes* 69

(21) *Gravimetric energy density for MGO* 72

(22) *Average work done* 73

(23) *Efficiency, liquefaction* 75

(24) *Available waste heat* 76

(25) *Distance with regard to velocity and time* 115

(26) *Haversine formula* 115

List of figures

Figure 1: Molecular model (ball and stick) of hydrogen. 4

Figure 2: Hydrogen worldwide production and consumption by source and application [7], [31], [32] 5

Figure 3: Basic principle of an alkaline electrolyser cell, inspired by Keçebaş [47] 7

Figure 4: Basic principle of a PEM electrolyser cell. 8

Figure 5: Basic principle of a solid oxide electrolyser cell. 9

Figure 6: Extremely simplified liquification diagram. 11

Figure 7: Molecular model (ball and stick) of ammonia. 13

Figure 8: Haber-Bosch process, inspired by esru.strath.ac.uk [105] 15

Figure 9: Concept illustration of direct ammonia electrolyser [110] 16

Figure 10: Active cooling system for liquid ammonia storage. 16

Figure 11: Synthetic fuel and LOHC supply chains. 18

Figure 12: Molecular model (ball and stick) of methanol. 19

Figure 13: Hydrogenation/dehydrogenation cycle of toluene. 20

Figure 14: Chemical structure of three different DBT isomers. 22

Figure 15: Hydrogenation process, inspired by Eypasch et al. [138] 24

Figure 16: Basic principle of an alkaline fuel cell, inspired by Keçebaş [47] 29

Figure 17: Simplified diagram of an AFC fuelled by liquid hydrogen [131] 29

Figure 18: Basic principle of a PEM fuel cell. 30

Figure 19: Basic principle of a solid oxide fuel cell. 32

Figure 20: A variety of motor sizes from ABB [172]. © ABB. 33

Figure 21: Early hydrogen-car, with permission from Norsk Industriarbeidermuseum [179]. 34

Figure 22: Four stroke Diesel cycle, inspired by Motordynasty.com [181]. 35

Figure 23: MAN ME-LGIP, the base for the ammonia engine [185]. Yes, those are stairways. © MAN ES 36

Figure 24: Cutaway illustration of a turbocharger [197]. CC license, © Rolls Royce Power Systems AG. 38

Figure 25: Working principle of a gas turbine [26]. 39

Figure 26: A jet engine, i.e., a gas turbine optimised for exhaust gas pressure [199]. CC license. 39

Figure 27: MV Rubin unloading fish food at a fish farm [210]. 41

Figure 28: MV Rubin shipping route for February 2021 [221] 43

Figure 29: Comparison of energy densities of different fuels. 45

Figure 30: Comparison of energy densities of different fuels, including storage. 47

Figure 31: Sankey diagram of liquid hydrogen supply chain. 50

Figure 32: Sankey diagram of ammonia supply chain. 50

Figure 33: Sankey diagram of dibenzyltoluene supply chain. 50

Figure 34: Generalised supply chains of liquid hydrogen, ammonia and dibenzyltoluene. 51

Figure 35: Estimated cost of green hydrogen produced in Norway. 54

Figure 36: Added cost of hydrogen carriers. 56

Figure 37: Total cost of hydrogen carrier, lowest and highest scenario 58

Figure 38: Process of regulatory framework, diagram is inspired by Lloyd's [257]. 62

Figure 39: An illustration of the arc lengths [281] (modified from Public Domain figure). 69

Figure 40: A possible power schematic diagram for MV Rubin [287] 71

Figure 41: Propulsion system for MV Rubin with liquid hydrogen and alkaline fuel cells. 74

Figure 42: Liquefaction efficiency. 75

Figure 43: Sankey-diagram illustrating the supply chain of liquid hydrogen for MV Rubin. 75

Figure 44: Propulsion system for MV Rubin with ammonia and Solid oxide fuel cells 76

Figure 45: Sankey-diagram illustrating the supply chain of ammonia for MV Rubin. 77

Figure 46: Propulsion system for MV Rubin using DBT and SOFC, created in Illustrator. 78

Figure 47: Sankey-diagram illustrating the supply chain of dibenzyltoluene for MV Rubin. 79

List of tables

Table 1: Colours of hydrogen [30] 4

Table 2: Comparison of different hydrogen production technologies 9

Table 3: Gravimetric- and volumetric density comparison – hydrogen and diesel [27], [60], [61] 10

Table 4: Energy density and hydrogen content of ammonia [92], [93] 14

Table 5: A comparison of reusable LOHC molecules [123], [126]–[128] 21

Table 6: Hydrogenious StorageBOX and ReleaseBOX base module properties [133] 23

Table 7: Viscosities of common fluids and DBT [128], [139], [140] 25

Table 8: By-products created from hydrogenation on Ni-based catalyst [130] 26

Table 9: Thermophysical properties of select fuels and hydrogen carriers. 27

Table 10: Comparison of different fuel cell technologies. 32

Table 11: Engine speeds and efficiencies for large maritime ICEs [196] 38

Table 12: MV Rubin, Technical information [211], [212]. 41

Table 13: Power output and specific fuel consumption – machinery MV Rubin 42

Table 14: Operating profile of MV Rubin 43

Table 15: Comparison of hydrogen storage solutions [27], [34] 48

Table 16: Truck requirements for transporting 3 tons of hydrogen. 48

Table 17: CAPEX for AEC from multiple analysis 52

Table 18: CAPEX for PEMEC from multiple analysis 52

Table 19: CAPEX for SOEC from multiple analysis 53

Table 20: CAPEX and OPEX for transportation of hydrogen carriers 57

Table 21: Total cost of hydrogen carrier, low and high scenario 59

Table 22: CO_2 emission of the different hydrogen carriers 60

Table 23: EPA Acute Exposure Guideline Levels [265], [266] 64

Table 24: Safety related properties, bullet points [13] 65

Table 25: Safety related data on liquid hydrogen, ammonia, dibenzyltoluene and liquid natural gas 66

Table 26: MV Rubin's shipping route for February, see **Attachment 1.** 70

Table 27: Total average work done by MV Rubin on its longest journey between Jan. & Feb. 2020. 73

List of reaction equations

(i) $CH_4\ (g) + H_2O\ (g) \rightleftharpoons CO\ (g) + 3H_2\ (g)$ 5

(ii) $CO\ (g) + H_2O\ (g) \rightleftharpoons CO_2\ (g) + H_2\ (g)$ 5

(iii) $CH_4\ (g) + CO_2\ (g) \rightleftharpoons 2CO\ (g) + H_2\ (g)$ 5

(iv) $Anode: 4OH^-\ (aq) \rightarrow O_2\ (g) + 2H_2O\ (l) + 4e^-$ 6

(v) $Cathode: 4H_2O\ (l) + 4e^- \rightarrow 2H_2\ (g) + 4OH^-\ (aq)$ 6

(vi) $Overall: 2H_2O\ (l) \rightarrow 2H_2\ (g) + O_2\ (g)$ 6

(vii) $Anode: 2H_2O\ (l) \rightarrow O_2\ (g) + 2H^+\ (g) + 4e^-$ 7

(viii) $Cathode: 4H^+\ (g) + 4e^- \rightarrow 2H_2\ (g)$ 7

(ix) $Overall: 2H_2O\ (l) \rightarrow 2H_2\ (g) + O_2\ (g)$ 7

(x) $Anode: 2O^{2-}\ (g) \rightarrow O_2\ (g) + 4e^-$ 8

(xi) $Cathode: 2H_2O\ (g) + 4e^- \rightarrow 2H_2\ (g) + 2O^{2-}\ (g)$ 8

(xii) $Overall: 2H_2O\ (g) \rightarrow 2H_2\ (g) + O_2\ (g)$ 8

(xiii) $N_2\ (g) + 3H_2\ (g) \rightleftharpoons 2NH_3\ (g)$ 14

(xiv) $2NH_3\ (g) \rightleftharpoons N_2\ (g) + 3H_2\ (g)$ 17

(xv) $CO_2\ (g) + 3H_2(g) \rightarrow CH_3OH\ (l) + H_2O\ (l)$ 18

(xvi) $CO_2\ (g) + H_2\ (g) \rightarrow CO\ (g) + H_2O\ (l)$ 18

(xvii) $CO\ (g) + 2H_2\ (g) \rightarrow CH_3OH\ (l)$ 18

(xviii) $Anode: 2H_2(g) + 4OH^-(aq) \rightarrow 4H_2O(l) + 4e^-$ 28

(xix) $Cathode: O_2(g) + 4e^- + 2H_2O(l) \rightarrow 4OH^-(aq)$ 28

(xx) $Overall: O_2(g) + 2H_2(g) \rightarrow 2H_2O(l)$ 28

(xxi) $CO_2(g) + 2OH^-\ (aq) \rightarrow CO_3{}^{2-}\ (aq) + H_2O\ (l)$ 29

(xxii) $CO_3{}^{2-}\ (aq) + 2K^-\ (aq) \rightarrow K_2CO_3\ (s)$ 29

(xxiii) $Anode: 2H_2(g) \rightarrow 4H^+(aq) + 4e^-$ 30

(xxiv) $Cathode: O_2(g) + 4e^- + 4H^+(aq) \rightarrow 2H_2O(l)$ 30

(xxv) $Overall: 2H_2(g) + O_2\ (g) \rightarrow 2H_2O(l)$ 30

(xxvi) $Anode: 2H_2(g) + 2O^{2-}(aq) \rightarrow 2H_2O(l) + 4e^-$ 31

(xxvii) $Cathode: O_2(g) + 4e^- \rightarrow 2O^{2-}(aq)$ 31

(xxviii) $Overall: 2H_2(g) + O_2\ (g) \rightarrow 2H_2O(l)$ 31

(xxix) $4NH_3\ (g) + 3O_2\ (g)\ \rightarrow 2N_2\ (g) + 6H_2O\ (l)$ 36

(xxx) $4NO\ (g) + 4NH_3\ (g) + O_2\ (g) \rightarrow 4N_2\ (g) + 6H_2O\ (l)$ 37

(xxxi) $6NO_2\ (g) + 8NH_3\ (g) \rightarrow 7N_2\ (g) + 12H_2O\ (l)$ 37

Attachments

Attachment 1. **Calculations**

Submitted as separate file. Energycalculations.xlsx

Attachment 2. **E-mail correspondence with MV Rubin**

Submitted as separate file. Attachment 2 - MV Rubin.eml

Attachment 3. **E-mail correspondence with Prototech**

Submitted as separate file. Attachment 3 - Prototech.eml

Attachment 4. **AIS - Automated calculations**

For large and cumbersome datasets, an automated approach to distance calculations is desired. A small script was written in Python and configured to read standard AIS data. The distance was calculated using two different methods, and the code is available in its entirety in **Attachment 5.** Note that the *numpy* library is required for the second method [307].

The first method is the simplest: Timestamp and speed data is extracted and converted to total seconds passed since 00:00. It is assumed that the speed given for one event is constant until the next event. Stops and dockings are filtered out with a speed threshold of 1 knot. The speed at a given point is multiplied by the duration of time between the current point and the next one, as described by…

$$Dist_{12} = v * 0.514 * t \tag{25}$$

…where v is the speed in knots, 0.514 is the conversion ratio between m/s and knots, and t is time. The resulting distance in meters is simply added for every step. Using this method on the unedited dataset, a total travelled distance of 5222 km was calculated.

The second method uses a variant of the aforementioned spherical law of cosines, namely the *haversine formula*. First tabulated in 1805, this relationship allows for simple and accurate calculations of distances based on coordinate positions, and was favoured by seamen for a long time [308]. For use in modern computers, however, the formula is written on a slightly more complex form using simpler trigonometric functions…

$$Dist_{12} = 2\,r\,\sin^{-1}\left(\sqrt{sin^2\left(\frac{\lambda_2-\lambda_1}{2}\right) + cos(\lambda_2)\,cos(\lambda_1)\,sin^2\left(\frac{L_2-L_1}{2}\right)}\right) \tag{26}$$

…as described by Gade (2010), but with the same symbols as the previous formulas [280], [309]. Indexes 1 and 2 are the first and second coordinate points and r is the Earth's radius. Assumptions about the planet's sphericity still apply. However, this particular expression is sufficiently accurate even for small angles in the sin^{-1} argument, as opposed to traditional formulations using cos^{-1}. Note that the argument under the square root needs to have values between 0 and 1, otherwise the sin^{-1} function will return a *floating-point error* because of solutions with imaginary numbers. These cannot, after all, be described as mere decimals. To avoid such errors, the script checks this condition in advance.

Using this method on the unedited dataset, a total travelled distance of 5349 km was calculated, whereas the *corrected* dataset yielded 6306 km. The latter lies very close to the manual calculations that were done with a simpler formula. Although the automated result may be closer to reality, energy requirement calculations are best erred on the side of caution. A desired range of 6500 km/month is therefore defined.

The accuracy can be improved by increasing the event ping frequency of the AIS data, but very small distances / angles will lead to inaccuracies in the arcsin function, in which case the simpler method using speed and distance is probably better. A limit could be defined for switching between the two but is not deemed necessary for this case. Energy calculations can be based on the desired range per month, but a more precise method

would be to connect the AIS data to a speed-power function. If the ping frequency is sufficiently high, like in the report by Aarskog, et.al. (2020), then the energy requirement can be very accurately determined [310]. Further developments of the script could include simpler user inputs and comparisons of several ships at once, among other things.

Attachment 5. **Python script**

Submitted as separate file. Attachment 5 – Boat_dist_v.0.2.py

Attachment 6. **AIS CSV-file for use with python script**

Submitted as separate file. Attachment 6– Rubin_sortert.csv